**อนุภาคขนาดนาโนเมตรของลาเท็กซ์พอลิเมทิลเมทาคริเลตและพอลิเมทิลเมทาคริเลตที่มี
หมู่ฟังก์ชันไกลซิดิลผ่านการเกิดพอลิเมอร์แบบดิฟเฟอเรนเชียลไมโครอิมัลชัน**

นายชัยวัฒน์ นรกานต์กร
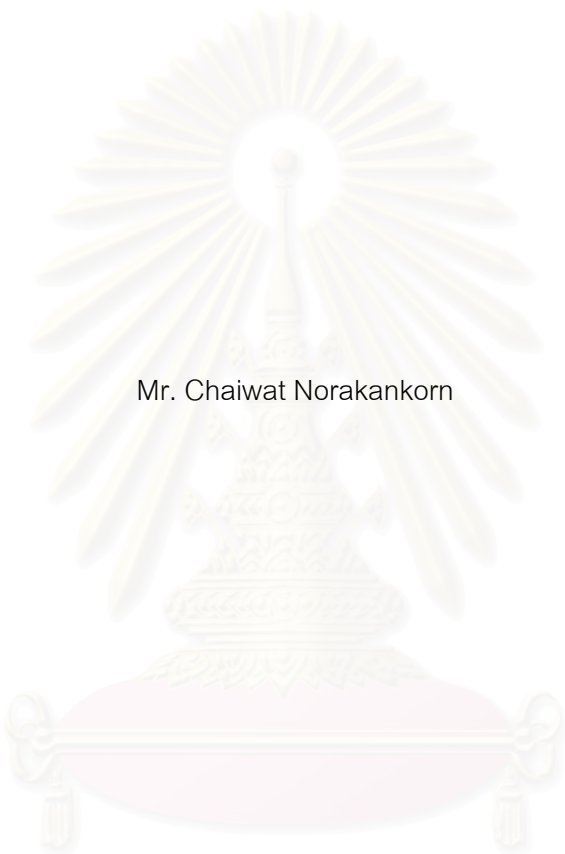
POLY(METHYL METHACRYLATE) AND GLYCIDYL-FUNCTIONALIZED POLY(METHYL

METHACRYLATE) NANO-SIZE LATEX PARTICLES VIA DIFFERENTIAL MICROEMULSION

POLYMERIZATION

Mr. Chaiwat Norakankorn

A Dissertation Submitted in Partial Fulfillment of the Requirements

for the Degree of Doctor of Philosophy Program in Materials Science

Department of Materials Science

Faculty of Science

Chulalongkorn University

Academic Year 2007

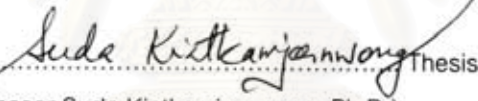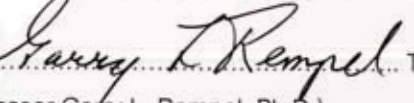| Thesis Title | POLY(METHYL METHACRYLATE) AND GLYCIDYL-FUNCTIONALIZED |
	POLY(METHYL METHACRYLATE) NANO-SIZE LATEX PARTICLES VIA
	DIFFERENTIAL MICROEMULSION POLYMERIZATION
By	Chaiwat Norakankorn
Field of Study	Materials Science
Thesis Advisor	Professor Suda Kiatkamjornwong, Ph.D.
Thesis Co-advisor	Professor Garry L. Rempel, Ph.D.

Accepted by the Faculty of Science, Chulalongkorn University in Partial Fulfillment of the Requirements for the Doctoral Degree
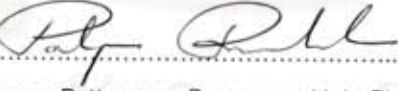
.... Dean of the Faculty of Science

(Professor Supot Hannongbua, Ph.D.)

THESIS COMMITTEE

.... Chairman

(Associate Professor Weerasak Udomkichdecha, Ph.D.)

.... Thesis Advisor

(Professor Suda Kiatkamjornwong, Ph.D.)

.... Thesis Co-advisor

(Professor Garry L. Rempel, Ph.D.)

.... Member

(Professor Pattarapan Prasassarakich, Ph.D.)

.... Member

(Associate Professor Khemchai Hemachandra, Ph.D.)

.... Member

(Siriwan Phattanarudee, Ph.D.)

.... External Member

(Nopporn Pramojaney, Ph.D.)

นายชัยวัฒน์ นรกานต์กร อนุภาคขนาดนาโนเมตรของลาเท็กซ์พอลิเมทิลเมทาคริเลตและพอลิเมทิลเม
ทาคริเลตที่มีหมู่ฟังก์ชันไกลซิดิลผ่านการเกิดพอลิเมอร์แบบดิฟเฟอเรนเชียลไมโครอิมัลชันอ. ที่ปรึกษา :
ศ. ดร. สุดา เกียรติกำจรวงศ์, อ.ที่ปรึกษาร่วม : Prof. Garry L. Rempel, Ph.D., 140 หน้า.

ได้นำเทคนิคการเกิดพอลิเมอร์แบบดิฟเฟอเรนเชียลไมโครอิมัลชันชนิดสองกระบวนการมาใช้ในการ
สังเคราะห์อนุภาคขนาดนาโนเมตรของพอลิเมทิลเมทาคริเลต (PMMA) ที่มีหมู่ฟังก์ชันไกลซิดิล ในปฏิกิริยาใช้ปริมาณ
สารลดแรงตึงผิวโซเดียมโดเดคซิลซัลเฟต (SDS) เพียง 1/217 ของน้ำหนักมอนอเมอร์ทั้งหมด และอัตราส่วนของสารลด
แรงตึงผิวต่อน้ำสามารถลดลงเหลือเพียง 1/600 กระบวนการแรกเป็นการสังเคราะห์อนุภาคขนาดนาโนเมตรของ PMMA
ซึ่งมีน้ำหนักโมเลกุลสูงอยู่ในช่วง 10^6 กรัมต่อโมล เพื่อทำหน้าที่เป็นแกนกลางของอนุภาค โดยใช้ AIBN ซึ่งเป็นสาร
ริเริ่มปฏิกิริยาแบบละลายในน้ำมัน และทำปฏิกิริยาที่อุณหภูมิ 70 องศาเซลเซียส ใช้เวลาในการหยดมอนอเมอร์นาน 90
นาที อนุภาคขนาดนาโนเมตรของลาเท็กซ์ PMMA ที่มีน้ำหนักโมเลกุลสูงจะมีปริมาณโครงแบบซินดิโอแทคทิค
(syndiotactic) สูง (ร้อยละ 53-57) อัตราการเกิดพอลิเมอร์เพิ่มขึ้นเมื่อความเข้มข้นของสารลดแรงตึงผิว SDS เพิ่มขึ้น
การเปลี่ยนแปลงเป็นพอลิเมอร์เกิดขึ้นสูงสุดเมื่อเวลาของการการเกิดพอลิเมอร์ผ่านไป 3600 วินาที ค่าการกระจายตัวของ
น้ำหนักโมเลกุล (PDI) เกือบคงตัวตลอดช่วงเวลาของการเกิดพอลิเมอร์ แสดงให้เห็นถึงนัยของการเกิดอนุภาคด้วยกลไก
การเกิดอนุภาคแบบไม่เป็นเนื้อเดียวกัน อนุภาคขนาดนาโนเมตรของ PMMA ที่มีน้ำหนักโมเลกุลสูงมีลักษณะเป็นทรง
กลมและมีค่าอุณหภูมิการเปลี่ยนสถานภาพแก้ว (T_g) 125 องศาเซลเซียส สำหรับกระบวนการที่สองเป็นการเติมไกลซิดิล
เมทาคริเลตลงในลาเท็กซ์ PMMA ในลักษณะเดียวกันกับกระบวนการแรกเพื่อทำให้เกิดเป็นอนุภาคขนาดนาโนเมตรของ
PMMA ที่มีหมู่ฟังก์ชันไกลซิดิล โครงสร้างเป็นเปลือก core/shell ของอนุภาคขนาดนาโนเมตรของ PMMA ที่มีหมู่
ฟังก์ชันไกลซิดิล ประกอบด้วยอนุภาคขนาดนาโนเมตรของ PMMA ที่มีน้ำหนักโมเลกุลสูงทำหน้าที่เป็นแกนกลางและมี
โคพอลิเมอร์แบบสุ่มของพอลิเมทิลเมทาคริเลต-ไกลซิดิลเมทาคริเลตทำหน้าที่เป็นชั้นเปลือกอยู่บนพื้นผิวของอนุภาค
PMMA ที่เป็นแกนกลาง อนุภาคขนาดนาโนเมตรของ PMMA ที่มีหมู่ฟังก์ชันไกลซิดิลมีขนาดอนุภาคประมาณ 50 นาโน
เมตร และมีน้ำหนักโมเลกุลอยู่ในช่วง 1×10^6 ถึง 3×10^6 กรัมต่อโมล หมู่ฟังก์ชันไกลซิดิลที่ตรวจพบด้วยวิธีการไทเทรตมี
ค่าประมาณร้อยละ 1-2 โดยน้ำหนัก PMMA ที่มีหมู่ฟังก์ชันไกลซิดิลมีค่า T_g สองช่วงคือ ที่ 90 และ 125 องศาเซลเซียส
ซึ่งบ่งชี้ว่าเป็นพอลิเมทิลเมทาคริเลต-ไกลซิดิลเมทาคริเลต และ PMMA ตามลำดับ สิ่งที่น่าสนใจมากของงานวิจัยนี้คือ
การเปลี่ยนแปลงเป็นพอลิเมอร์เกิดขึ้นมากสุดในช่วงเวลาสั้นๆ ของการเกิดปฏิกิริยาโดยใช้สารลดแรงตึงผิวน้อยและไม่
ต้องใช้สารร่วมลดแรงตึงผิว (co-surfactant) ช่วย รวมทั้งอัตราส่วนของมอนอเมอร์ต่อน้ำมีค่าสูงด้วย.

ภาควิชา	วัสดุศาสตร์	ลายมือชื่อนิสิต	ชัยวัฒน์ นรกานต์กร
สาขาวิชา	วัสดุศาสตร์	ลายมือชื่ออาจารย์ที่ปรึกษา	
ปีการศึกษา	2550	ลายมือชื่ออาจารย์ทีปรึกษาร่วม	Garry L. Rempel

4573860023: MAJOR MATERIALS SCIENCE

KEY WORD: NANOPARTICLES / POLY[(METHYL METHACRYLATE)-*RAN*-(GLYCIDYL METHACRYLATE)] / CORE/SHELL STRUCTURE / FUNCTIONAL POLYMER NANOPARTICLE / GLYCIDYL-FUNCTIONALIZED PMMA NANOPARTICLE

CHAIWAT NORAKANKORN: POLY(METHYL METHACRYLATE) AND GLYCIDYL-FUNCTIONALIZED POLY(METHYL METHACRYLATE) NANO-SIZE LATEX PARTICLES VIA DIFFERENTIAL MICROEMULSION POLYMERIZATION.   THESIS ADVISOR: PROF. SUDA KIATKAMJORNWONG, PH.D. THESIS COADVISOR : PROF. GARRY L. REMPEL, PH.D., 140 PP.

The differential microemulsion polymerization technique was used to synthesize nanoparticles of glycidyl-functionalized poly(methyl methacrylate), PMMA, via a two-step process, by which the amount of sodium dodecyl sulfate (SDS) surfactant required was 1/217 of the monomer amount by weight and the surfactant/water ratio could be as low as to 1/600. The first step was to synthesize the core PMMA nanoparticles having high molecular weight of 10^6 g mol^{-1} using the AIBN oil soluble initiator at 70°C for 90 min by drop-wise addition of the monomer. The high molecular weight PMMA latex nanoparticles (~ 20 nm in size) have a rich syndiotactic configuration (53-57 % *rr* triads). The rate of polymerization increased with an increase in the concentration of the SDS surfactant. The maximum conversion of polymerization was observed at a polymerization time of 3600 s. The nearly constant value of PDI over the whole range of the polymerization time could be attributed to the significance of particle nucleation occurring via a heterogeneous nucleation mechanism. The high molecular weight PMMA nanoparticles have spherical shape with a T_g of about 125°C. The second step was to add glycidyl methacrylate in the PMMA latex via a similar manner to obtain the glycidyl-functionalized PMMA nanoparticles. A core/shell structure of the glycidyl-functionalized PMMA latex nanoparticles observed are composed of a high molecular weight PMMA core with the random copolymer of poly[(methyl methacrylate)-*ran*-(glycidyl methacrylate)] as a shell layer on the surface. Particle sizes of about 50 nm were achieved and the molecular weight of glycidyl-functionalized PMMA was in the range of about 1x10^6 to 3x10^6 g mol^{-1}. Approximately 1-2 wt% of glycidyl functional groups were determined using a titration method. The low content detected was due to precipitation and a drying effect. The glycidyl-functionalized PMMA has two regions of T_g at 90 $^\circ$C and 125°C, which were referred to as poly[(methyl methacrylate)-*ran*-(glycidyl methacrylate)] and PMMA, respectively. It is very interesting to note that the polymerization conversion reaches a maximum, within a short reaction time in the presence of less surfactant and without the need of a co-surfactant along with a high monomer-to-water ratio.

Department	Materials Science	Student's signature ...Chaiwat N....
Field of study	Materials Science	Advisor's signature ...Suda Kiatkamjornwong...
Academic year	2007	Co-advisor's signature ...Garry L. Rempel...

ACKNOWLEDGEMENTS

CONTENTS

LIST OF TABLES

LIST OF FIGURES

CHAPTER 1

INTRODUCTION

Nanoscience and nanotechnology deal with nanomaterials with sizes of less than 100 nm. Polymer nanoparticles are interesting nanomaterials for many branches of nanoscience and nanotechnology. Polymer nanoparticles may be applied in biomedical applications, nanobiotechnology, textile finishing, catalysis applications, semiconductors, and nanostructure engineering. In addition, polymer nanoparticles have large specific surface areas, so surface modification of polymer nanoparticles is a very interesting issue to explore. Functional polymer nanoparticles with core/shell structure are one of the interesting substrates resulting from the modification of the surface of the core polymer nanoparticles because the high performance functional polymer nanoparticle with core/shell structure can be obtained even though a lower amount of functional monomer is incorporated. The functional polymer nanoparticle with core/shell structure is an interesting nanomaterial for biomedical applications (especially drug delivery systems) and biotechnology applications, since many biological molecules are compatible with many reactive functional groups. Latex technology is an important green technology to produce functional polymer nanoparticles with core/shell structure, since the latex process (or emulsion polymerization process) is a solvent-free polymerization technique.

1.1 Historical and important concepts

For many years, well-defined polymer particles, especially those of a submicron-size range are useful as suitable colloidal supports in a large number of biotechnological,

pharmaceutical and medical applications such as in bioseparations, drug delivery systems (DDS) and targeting, etc. For these purposes, a considerable amount of research has been dedicated to the design and preparation of colloidal polymers with appropriate properties for interacting with biologically active macromolecules. Latex particles for drug delivery systems should fulfill many requirements: particle size and size distribution, surface charge density, polarity of the particle interface, presence of (bio) reactive groups (when covalent grafting is desired), biodegradability, bioresorbability, and nontoxicity.

Kawaguchi [1] has provided a review about functional particles prepared directly by heterogeneous polymerization, e.g. emulsion polymerization and dispersion polymerization. Modification of existing particles is another method to prepare functional particles. Medical and biochemical applications of particles, including absorbents, latex diagnostics, affinity bioseparators, drug and enzyme carriers, are the most practical ones at present. Surface-functionalized latex for biotechnological application has been reviewed by Pichot [2], and he mentioned that latex particles for biotechnological applications should fulfill many requirements which could become important for some specific applications: particle size (which controls the available surface area) and size distribution (monodispersity is often required for sake of reproducibility); surface charge density; polarity of the particle interface; presence of (bio)reactive groups (when covalent grafting is desired); biodegradability, bioresorbability and nontoxicity in the case of particles used in DDS.

Table 1.1 gives an overview of the main functionalities revealing the huge possibilities which are offered. It should be underlined that several functionalities may be

imparted to the same particles such as bioreactivity, thermal sensitivity, biodegradability, targeting, etc.

Table 1.1 Various available functionalities and related properties which can be functionalized to latex particles. [2]

Functionality	Property
Charged groups. ($-OSO_3^-$, $-SO_3^-$, $-COO^-$, $-PO_3^-$, etc.)	Colloidal stability, electrostatic interactions (adsorption of polyelectrolytes, biomolecules).
Reactive groups. ($-CHO$, $-CH_2Cl$, $-OH$, $-NH_2$, $-SH$, epoxide, activated ester, etc.)	Covalent immobilization on plain supports (silica wafers); grafting of biomolecules; chemical modification of performed particles.
Hydrophilicity, (polyacrylamide, poly(acrylic acid), etc.)	Steric stabilization, depletion of biomolecules.
Sensitivity to stimulus. (temperature, pH, light, electric, stress, etc.)	Shape, swelling behavior (microgel); reaction rate; ionic charge.
Dye label. (color, fluorescence)	Detection of a molecular interaction.
Conductive polymers. (pyrrole, aniline)	Conductivity, optical absorbance.
Complexation (poly(methacrylic acid), metal chelates, etc.)	Protein purification, oriented immobilization (protein etc.)
Ligand.(oligosaccharide, lipid, peptide, nucleic acid, antibody, protein)	Recognition of antigen, specific cells, DNA, RNA, protein, etc.

Surface functionalization with bioreactive groups has motivated many efforts aimed at controlling the nature, location, distribution and surface density of a given chemical group in the produced particles to be used for in-vitro and in-vivo applications. The presence of these bioreactive groups should allow the immobilization of biomolecules by physical adsorption (through hydrophobic, hydrogen bonding, and electrostatic interactions) but preferentially via covalent coupling or chelation. Many types of chemical functionalization are indeed available in biomolecules especially amine, thiol, carboxyl, hydroxyl, guanidine, and imidazole groups.

Many polymerization techniques are presently appropriate for preparing latex particles which can fulfill most or all of the above-mentioned requirements such as emulsion polymerization, dispersion polymerization, and precipitation polymerization. It is worth mentioning that other processes such as microemulsion polymerizations provide small-size particles (down to 20-30 nm). All these heterogeneous polymerization techniques were found to produce latex particles with a broad diversity of internal and surface morphologies depending on the formulation recipe and type of process (batch, semi-batch, core-shell, shot growth, etc.).

Microemulsion polymerization is a technique that provides colloidal polymer particles with diameters usually smaller than 50 nm dispersed in a continuous aqueous phase [3]. Nevertheless, batch microemulsion polymerization has two great drawbacks which limit its broad application, i.e., (1) low monomer/surfactant weight ratios, usually < 1, and (2) low polymer content, usually less than 10 wt%.

One approach for overcoming these drawbacks is to carry out the polymerization using a differential monomer feeding technique [4-5]. Differential microemulsion

polymerization includes three steps: (i) an initial period in which a mixture of initiator and surfactant in the recipe is heated in the reactor; (ii) an addition period over which the total monomer is added to the reactor; and (iii) an aging period to allow for complete polymerization of unreacted monomer. He et al. [4] were the first group to report on the differential microemulsion polymerization technique. The reports on differential microemulsion polymerization indicate that this operation leads to an increase in the polymer/surfactant ratio, keeping particle size in the range of 15 nm, and homogeneous nucleation was claimed [5-6]. Nevertheless, to minimize particle size and surfactant in this type of homogeneous polymerization, it is necessary to operate under the so-called monomer-starved conditions during the addition period. However high concentrated polymer nanoparticle emulsions with particle size of 15 nm or less were not successfully achieved because of the extension of particle size by the aggregation of oligomers during propagation in the aqueous phase [4]. So the utilization of oil soluble initiator instead of a water soluble initiator will probable recover the aggregation of oligomers during polymerization since heterogeneous nucleation will possibly predominate throughout the reaction and a highly concentrated polymer nanoparticle emulsion can probably be obtained. Additionally, the differential microemulsion polymerization via a two-step process was used to give the polymer nanoparticles of poly(methyl methacrylate)/polystyrene (PMMA/PS) [7].

The dispersion copolymerization between methyl methacrylate (MMA) and glycidyl methacrylate (GMA) has been studied [8]. The nonporous microparticles of methyl methacrylate (MMA) copolymerized with glycidyl methacrylate (GMA) were prepared by dispersion polymerization [8]. The particle size was found to decrease from

4.2 to 2.1 mm with an increasing mass ratio of GMA/MMA but an increase in the GMA/MMA ratio also led to a decrease in glycidyl functional group density on the particle surface [8]. The higher reactivity of the GMA monomer over that of the MMA monomer caused the GMA/MMA to firstly be copolymerized inside the core particle [8]. As a result low epoxy group density on the surface of the GMA/MMA copolymer particle was obtained. The increments of the glycidyl functional group density on the surface of the polymer particle could possibly be achieved by the reduction of the particle from the micro scale to the nanosized range since the nanoparticle has a higher specific surface area than the microparticle. Otherwise, a two-step process could inhibit the initial copolymerization of GMA with the MMA monomer inside the core particle. So a lower amount of glycidyl functional group was hidden inside the polymer particles.

From the literature reviewed above, the glycidyl-functionalized PMMA latex nanoparticle could possibly be synthesized by the differential microemulsion polymerization via a two-step process. AIBN oil-soluble initiator was the chosen initiator to initiate the polymerization in this research since the depletion of the glycidyl functional group was low [9]. The PMMA latex nanoparticles prepared by the differential microemulsion polymerization with an oil-soluble initiator were the nuclei for the GMA polymerization. The glycidyl-functionalized PMMA latex nanoparticles were likely poly(methyl methacrylate)/poly[(methyl methacrylate)-(glycidyl methacrylate)] core/shell latex nanoparticles since the GMA monomer polymerization involved continuous feeding after the end of MMA monomer feeding. So the unreacted MMA monomer was possibly copolymerized with the GMA monomer when it was fed. Furthermore, the core/shell structure of the glycidyl-functionalized PMMA latex

nanoparticle was an interesting issue to be explored in this research since the previous work reported by He and Pan [7] did not investigated the core/shell structure of the PS/PMMA latex particle although the differential microemulsion polymerization via a two-step process was applied. Otherwise, the amounts of glycidyl functional group on the surface of the glycidyl-functionalized PMMA instead of the glycidyl-functionalized PMMA latex nanoparticle were investigated since the titration method of the glycidyl functional group on the surface [8] was limited with the solid polymer particle. Then the effect of the polymer latex coagulation during separation of the glycidyl-functionalized PMMA from the glycidyl-functionalized PMMA latex nanoparticles on the amounts of the surviving glycidyl functional group was also studied.

1.2 Attractive force

Functional polymer latex nanoparticles with core/shell structure are important nanomaterials for many advanced applications of nanotechnology. They can be used as a carrier for many biological molecules and innovative pharmaceutical agents, since the many kinds of functional group on the surface of polymer nanoparticle is dependent on the type of functional polymer or copolymer within the particle surface. The glycidyl-functionalized PMMA latex nanoparticle was a selected functionalized polymer latex nanoparticle to study since the MMA microemulsion polymerization and the differential microemulsion polymerization of MMA were widely researched [10-19]. In addition, the preparation of glycidyl-functionalized PMMA microparticle was also studied by dispersion copolymerization [8]. So the important effects during the synthesis of the glycidyl-functionalized PMMA latex nanoparticles with the differential microemulsion

polymerization via a two-step process will be clearly observed. In addition, the core/shell structure of the glycidyl-functionalized PMMA latex nanoparticles will be investigated. In addition, the coagulation effect on the amounts of glycidyl functional group of the glycidyl-functionalized PMMA will be studied

1.3 Objectives

The research aimed to find a suitable operating condition to synthesize the core/shell structure of glycidyl-functionalized PMMA nanoparticles with a high surface functionality by differential microemulsion polymerization via a two-step process. As for making the glycidyl-functionalized PMMA nanoparticle which has a core/shell structure, AIBN oil-soluble initiator was used. Then it is important to develop suitable conditions to synthesize the PMMA nanoparticle via differential microemulsion polymerization technique using AIBN oil-soluble initiator and this is the first objective of the research. Afterward, operating conditions of the differential microemulsion polymerization via a two-step process will be investigated in order to obtain optimal parameters for making glycidyl-functionalized PMMA nanoparticles which have a core/shell structure and this forms the second objective. The rest of the glycidyl functional groups on the surface of glycidyl-functionalized PMMA and the impact of the coagulation on the functionality are the last objective of the research

This work also investigates the structure, characteristics, and possible nucleation mechanism of both PMMA nanoparticle formation and glycidyl-functionalized PMMA nanoparticle formation.

1.4 Outline

This dissertation is composed of the 5 chapters. The content of each chapter is outlined as below.

Chapter 1 contains the historical background and important concepts, objective, and outline of research.

Chapter 2 reviews the literature of the related theoretical background for the preparation of functional polymer nanoparticle emulsions.

Chapter 3 describes how the high molecular weight PMMA nanoparticle and the core/shell nanoparticles are synthesized via differential microemulsion using an oil-soluble initiator.

Chapter 4 reports on the results and discussion of synthesis of core/shell structure of glycidyl-functionalized PMMA latex nanoparticles via differential microemulsion polymerization.

Chapter 5 provides a summary of the Conclusions from the present research and Recomendations for further research.

CHAPTER 2

THEORETICAL BACKGROUND
AND
LITERATURE SURVEY

The aim of this chapter is to report on the necessary theoretical background and progress in the field of emulsion and microemulsion polymerizations and functionalization methodologies leading to reactive polymer colloids with the core/shell structure. The features of emulsion and microemulsion polymerizations will be briefly summarized and the synthesis methodology for functional latexes will be reviewed. Special attention will be focused on elaborating on functionalized latex nanoparticles with a core/shell structure by differential microemulsion polymerization via a two-step process.

2.1 Introduction

In life science, the immobilization of biologically active molecules like proteins, enzymes, and antibodies on latex particles is useful for enabling detection, quantification, or targeted delivery. Most of the latter applications involve polymer particles bearing functional groups that permit the covalent binding of biomolecules. Functional polymer particles have also been widely used as catalysts and reactant supports since they provide high surface area and can be prepared in a variety of sizes and compositions. The activity of latex-supported catalysts depends on the accessibility of the active sites and the

reaction rates are usually limited by diffusion. Consequently, surface functional polymer particles have been widely studied.

Although much progress has been documented in recent years [20-25], the development of new selective materials with improved functionality and reagent accessibility as well as a good colloidal stability and suitable solubility properties continues to be a challenging endeavor. In addition, the chemical and physical properties of the chosen functional carrier (monomer, surfactant, and initiator) should be considered in order to target the desired localization of the functional compounds (particle surface or inside the polymer matrix). The core/shell structure of the functional polymer particle presents an interesting morphology for high surface functional polymer particles since most of the functional group was located on the surface of the polymer particle [20-25]. Additionally, the nanosized range of the surface functional polymer particles can increase the amount of the functional group on the surface of the functional polymer particle since a high specific surface area was obtained [26-29]. Thus, functionalized polymer nanoparticles with the core/shell structure are widely researched [30-33].

The technique of microemulsion polymerization [26-29] offers new opportunities since it allows one to produce stable suspensions of ultrafine polymer particles in the nanosized range (i.e., with diameters smaller than 60 nm), which exhibit a very large specific surface area and high surface functionality. Moreover, owing to the huge surface per volume ratio in nanoparticles, surface becomes prominent over volume so that, when functionalized particles are considered, the functional residues can be located at the surface, thus ensuring a very high accessibility. However, most of the functional groups can be located at the surface if the core/shell structure of functional polymer

nanoparticles was developed by the microemulsion polymerization technique via a two-step process [32-33]. Otherwise, the high amounts of surfactant and the low solid content of the polymer are still the major two drawbacks of the microemulsion polymerization. Differential microemulsion polymerization [4-6] via a two-step process [7] is a very attractive method to prepare the core/shell structure of functional polymer latex nanoparticles due to the well controllable particle size and high-density surface functionalization of the nanoparticles inherent in its core/shell structure. It is especially suitable to prepare the nanoparticles with diameters in the range of 20–50 nm. Moreover low amounts of the surfactant were required and the high solid content of polymer was obtained.

Poly(glycidyl methacrylate) (PGMA) and copolymer of GMA with MMA have been prepared using a batch dispersion polymerization [8-9]. In addition, GMA copolymers have been synthesized using a semi-batch dispersion by adding GMA monomer into the polymerization reaction after the first monomer has been polymerized [34]. From those techniques, GMA copolymer obtained had the core-shell morphology in that GMA becomes an important component of the shell layer. Thus, the glycidyl-functional PMMA latex nanoparticles shall be studied and extensively surveyed [8-9, 34].

2.2 Functional polymer particle

Functional polymer particles have been prepared directly by heterogeneous polymerization, e.g. emulsion polymerization and dispersion polymerization. Modification of existing particles is another method to prepare functional particles. The features of nano- or microparticles such as a large specific surface area, high mobility, easy recovery from the dispersion and reversible dispersibility, etc., are utilized for the

exhibition of functions. Medical and biochemical applications of particles, including absorbents, latex diagnostics, affinity bioseparators, drug and enzyme carriers, are the most practical ones at present. Table 2.1 shows a brief summary about the biomedical applications of polymer microspheres.

Table 2.1 Biomedical applications of functional polymer microspheres [1]

2.3 Polymer particle preparation

Microsphere particles having a suitable size, surface structure and morphology can be applied in many biomedical fields. Polymer particles can be prepared by two routes as shown in Figure 2.1.
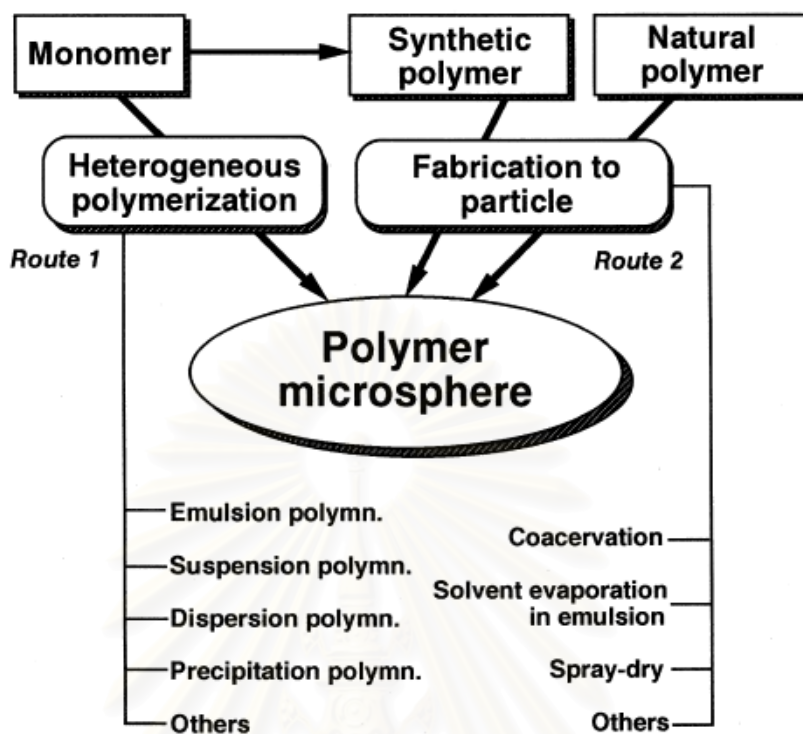
Figure 2.1 Preparative routes to polymer particles [1]

In route 1, each polymerization forms particles having different size ranges as shown in Table 2.2. The feature of microspheres prepared by emulsion polymerization is controlled not only by the monomers used, but also by surfactants and initiators.

Table 2.2 Particle-forming polymerizations and size of resulting particles [1]
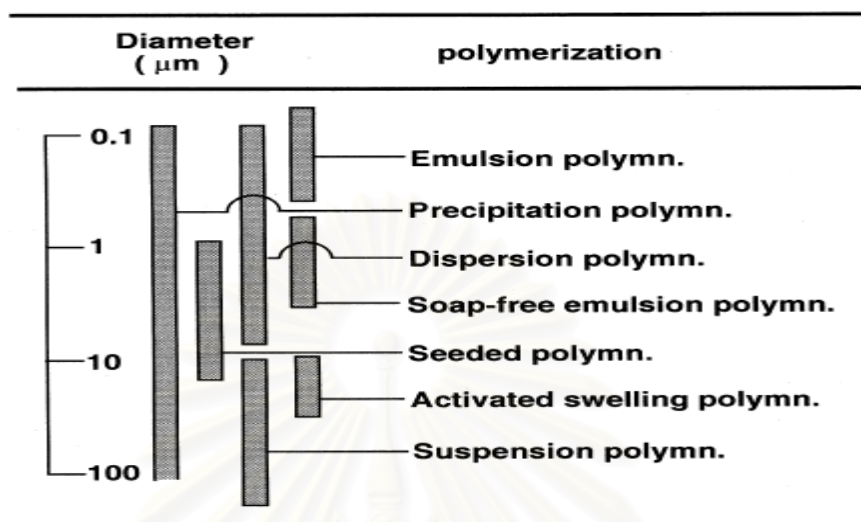
2.4 Surface modification of polymer particles

Seeded polymerizations are performed for three purposes: (1) enlargement of particle size; (2) formation of skin layer to introduce new functions; and (3) formation of nonspherical or uneven particles caused by phase separation during the polymerization. The formation of skin layer on existing particles has been often tried. A shell growth mechanism observed in a seeded polymerization may support the validity of this strategy [35]. The technology for shell growth sometimes named shot-growth polymerization, two-shot polymerization or stage feed polymerization although the meaning of each term is not exactly the same [36]. When a significant phase separation occurs during seeded polymerization, uneven-shaped particles are formed [37]. This is the case if the seed particles are crosslinked because the elastic network is apart to send forth the once-adsorbed monomers when a high temperature polymerization starts [37]. Particles having various shapes have been prepared on the basis of this principle.

Surface modifications might be performed after the polymerizations, using chemical reactions other than polymerization. Post-reaction carried out under different conditions gives a series of particles having the same size but different surfaces. Poly(glycidyl methacrylate) particles are reactive, especially with amines. Therefore, they are suitable as a carrier for biofunctional compounds [38]. Concentrated poly(glycidyl methacrylate) particles were easily crosslinked using diamine to form strong films [38]. Contrary to our expectation, they are not susceptible to protein adsorption [39]. This is another reason why poly(glycidyl methacrylate) latex is used for biomedical applications [40]. Particles carrying different amounts of an aldehyde group were prepared by treating polystyrene particles with dialdehyde [41]. Many kinds of biocompounds are immobilized via suitable reactions between a surface group on the particles and a group on the biocompound which should not affect their biofunctions [42].

2.5 Functionalization of polymer latex

Heterogeneous polymerization, especially emulsion polymerization, occupies an important place in the production of polymer materials because it permits the production of colloidal dispersions of polymer or latex particles by free-radical reaction [43]. The nature of the process (very considerable subdivision of reaction sites) results in latex polymers with high solids content. Commonly used in industry to synthesize widely available polymers (synthetic elastomers, binders for paints, films for paper, textile finishing, adhesives, and so forth), this method is also used to produce increasingly more technical materials (supports for biological compounds, colored and magnetic latexes, measurement scales, etc.). Thanks to the major advances in identifying the mechanisms of polymerization in heterogeneous media and in characterizing colloid properties, it is

now possible to better adapt latex to predefined final uses. A large number of processes have been developed during the last decade, permitting the synthesis of latexes with specific properties. There are the so called structured latexes [in which a heterogeneous distribution of two (or more) polymers of different natures within the particles is developed], and there are the functional latexes (in which the incorporation of a low-content chemical function is concentrated either at the surface or, more rarely, inside the particles) [20–25]. For practical reasons, these latexes are very often copolymers; hence the possibility arises, on the basic level, of preparing a large number of types of latex for use in process correlation studies of colloidal and/or weight properties/structure/syntheses.

Although the general methods of synthesizing these latexes are now well known, the control of their structural and colloidal properties remains somewhat uncertain due to the effects of various but poorly understood phenomena: emulsion copolymerization mechanisms (particle nucleation), especially in the presence of a water soluble monomers, distribution of the functional monomer in the different latex phases, organization of the polymer inside the particles, and so forth. The use of modern analysis methods permits better knowledge of the internal and superficial morphologies of these latex particles and better understanding of their colloidal behavior and the properties of the films derived from them. At present, it is possible to obtain various functional particle morphologies, from the relatively simple smooth and core-shell structure, a most studied one, to much more complex structures (hollow, microgel, etc.) (Figure 2.2), sometime leading to irregular and unstable forms.
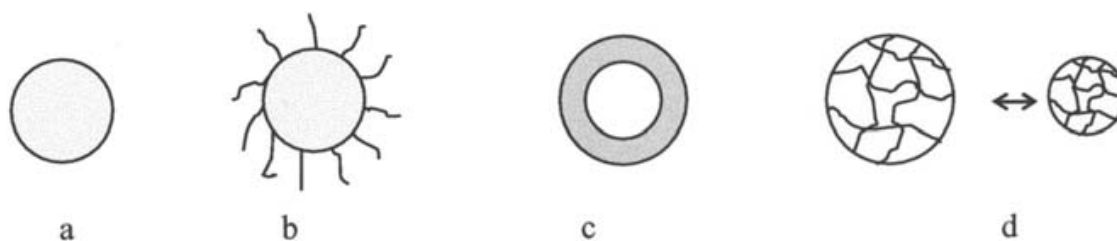
Figure 2.2 Main morphology of functionalized particles: (a) plain particle, (b) hairy

particle, (c) core/shell particle, (d) microgel [2]

2.6 Emulsion polymerization

Free-radical polymerization is a widely utilized technology to prepare synthetic polymers in an aqueous colloidal dispersion form. It is by far the most commonly used process in industry; manufacturers find that it has a large number of technical advantages (i.e., conventional reaction vessels, easy-to-run operations, high molar mass polymers, and a wide variety of potential products) and economic advantages (i.e., good productivity, inexpensive reagents, relatively low investments). Figure 2.3 represents the synopsis of the emulsion polymerization process in a production plant. Large quantities of inexpensive commodity polymers are manufactured in this way: they may be thermoplastics, such as certain poly(vinyl chloride) (PVC) grades, or elastomers, such as styrene-butadiene rubbers (SBR) or polychloroprene rubbers.
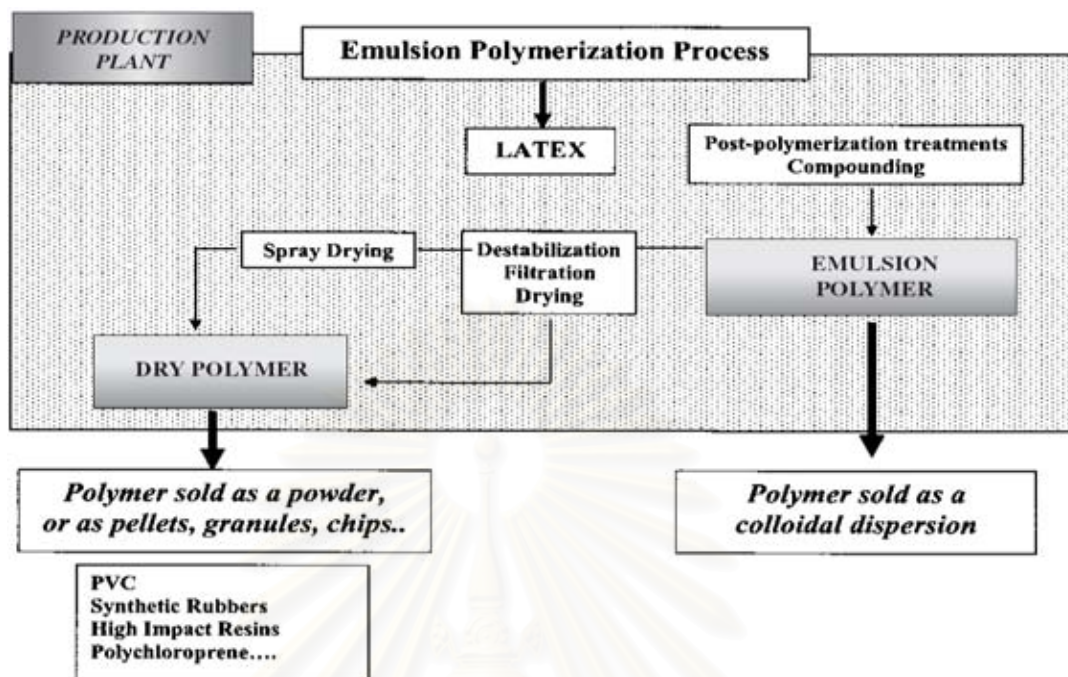
Figure 2.3 Emulsion polymerization process: synopsis of a production plant [44]

There are four main types of liquid-phase heterogeneous free-radical polymerization processes; microemulsion polymerization, emulsion polymerization, miniemulsion polymerization and dispersion polymerization, all of which can produce nano- to micron-sized polymeric particles. Emulsion polymerization is sometimes called macroemulsion polymerization. In recent years, these heterophase polymerization reactions have become more and more important technologically and commercially, not only as methods for producing high performance polymeric materials, but also from an environmental point of view. It is well known that microemulsion, miniemulsion and dispersion polymerizations bear many similarities to emulsion polymerization in the kinetics of particle nucleation and growth and in polymer structure development. Therefore, for optimal design and operation of these heterophase free radical

polymerizations, it is important to have detailed knowledge of the kinetics and mechanisms of emulsion polymerization.

To gain a fundamental understanding of polymerization mechanisms and kinetics is a must in designing quality products. Emulsion polymerization is a rather complex process because nucleation, growth and stabilization of polymer particles are controlled by the free radical polymerization mechanisms in combination with various colloidal phenomena. Perhaps, the most striking feature of emulsion polymerization is the segregation of free radicals among the discrete monomer-swollen polymer particles. This will greatly reduce the probability of bimolecular termination of free radicals and, thereby, result in a faster polymerization rate and polymer with a higher molecular weight. This advantageous characteristic of emulsion polymerization cannot be achieved simultaneously in bulk or solution polymerization. Although the nucleation period is quite short, generation of particle nuclei during the early stage of the polymerization plays a crucial role in determining the final latex particle size and particle size distribution and it has also a significant influence on the quality of latex products.

A typical emulsion polymerization formulation comprises monomer (e.g. butadiene, styrene, acrylonitrile, acrylate ester and methacrylate ester monomers, vinyl acetate, and vinyl chloride), water, surfactant and a water-soluble initiator (e.g. sodium persulfate (NaPS)) or an oil-soluble initiator (e.g. 2,2'-azobisisobutyronitrile (AIBN)) [45–46]. Surfactants are known to play a very important role in emulsion polymerization. To appreciate the role of a surfactant, we must understand the physicochemical properties of surfactant solutions. When a surfactant is dissolved in water, several physical properties of the solution (e.g., osmotic pressure, conductivity, relative viscosity, and

surface tension) change. Figure 2.4 shows these changes as a function of the molar concentration of the emulsifier. Beyond a particular level of concentration, there is a sudden change in the slope of these physicochemical properties, as shown in the figure. This concentration is called the critical micelle concentration (CMC).
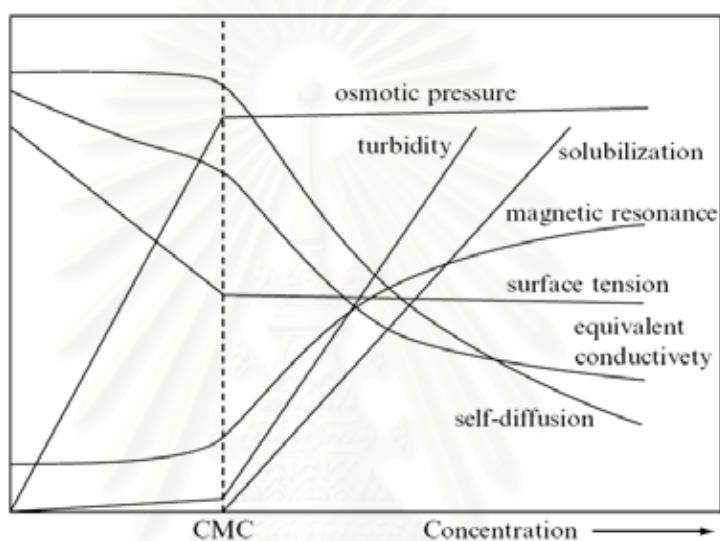
Figure 2.4 Changes in physical properties of water as a function of the concentration

of the sodium dodecyl sulfate surfactant [47]

A surfactant molecule consists of a long hydrocarbon chain, which is hydrophobic in nature, and a small hydrophilic end, as shown in Figure 2.5a.

(a) An emulsifier molecule

(b) Lammellar micelles in water and monomer solution

(c) Spherical micelles in water and monomer solution
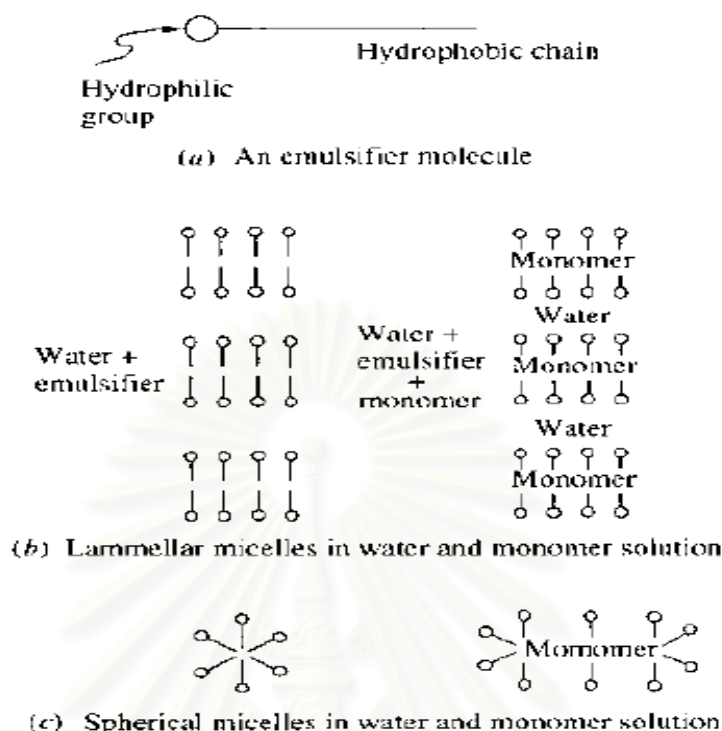
Figure 2.5 Representation of micelle formation in emulsion polymerization [48]

For very small concentrations of the surfactant, molecules of the latter arrange themselves on the free surface of water such that the hydrophobic ends point outward and the hydrophilic ends are buried in the water. In this way, the total free energy of the system is minimized. When more molecules of the surfactants are present than necessary to form a monolayer on the free surface, they tend to form aggregates, called micelles, so as to minimize the energy of interaction. This aggregate formation starts when the surfactant concentration increases above the CMC. The idealized lamellae and spherical aggregates are shown in Figure 2.5b and 2.5c. Beyond the CMC, the surfactant molecules stay primarily in micellar form. These micelles are responsible for the changes in the physical properties that can be observed in Figure 2.4. When a surfactant is added to water and a sparingly soluble monomer is dissolved, the solubility of the monomers is

found to increase. The apparently higher solubility is attributed to the presence of micelles, which really become a kind of reservoir for the excess monomer, as shown in Figures 2.5b and 2.5c. At the beginning of the emulsion polymerization, therefore, a surfactant acts as the solubilizer of the monomer, thus giving a higher rate of emulsion polymerization. Simplified representation of an emulsion polymerization system is shown in Figure 2.6.
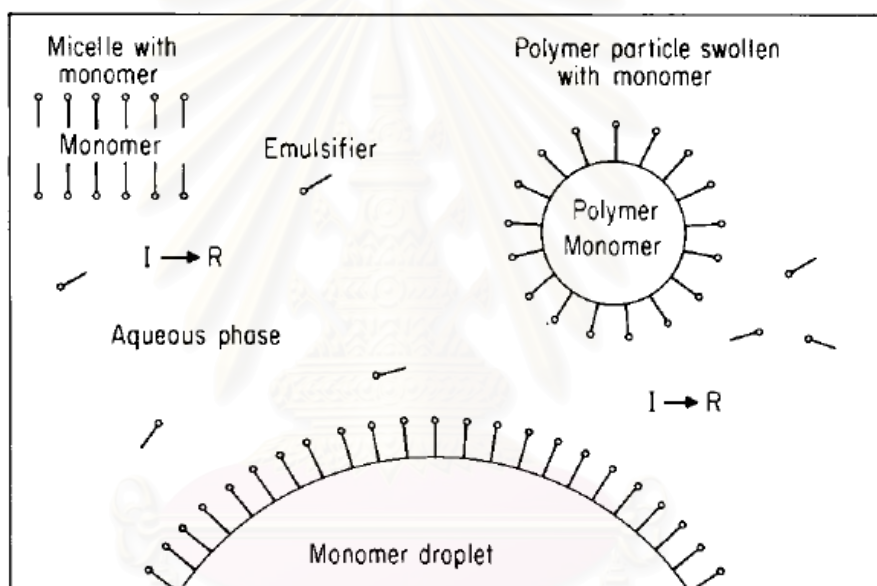
Figure 2.6 Simplified representation of an emulsion polymerization system [49]

The reaction system is characterized by the emulsified monomer droplets dispersed in the continuous aqueous phase with the aid of an oil-in-water surfactant at the very beginning of polymerization. Monomer-swollen micelles may also exist in the reaction system provided that the concentration of surfactant in the aqueous phase is above its critical micelle concentration. Only a small fraction of the relatively hydrophobic monomer is present in the micelles (if present) or dissolved in the aqueous

phase. Most of the monomer molecules dwell in the large monomer reservoirs (i.e. monomer droplets). The polymerization is initiated by the addition of initiator, submicron latex particles are generated via the capture of free radicals by micelles, which exhibit an extremely large oil–water interfacial area. In general, monomer droplets are not effective in competing with micelles in capturing free radicals generated in the aqueous phase due to their relatively small surface area. However, monomer droplets may become the predominant particle nucleation loci if the droplet size is reduced to the submicron range. Figure 2.7 depicts the generally accepted three major mechanisms for particle formation which has been proposed to date.
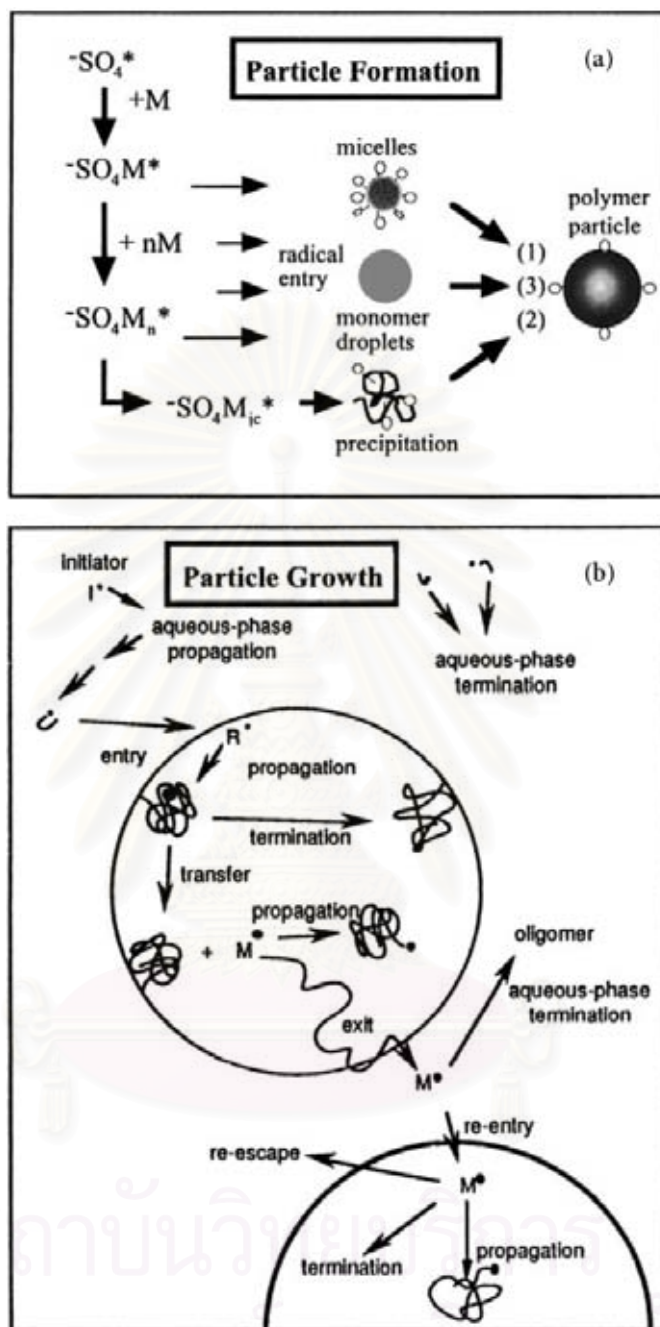
Fig. 2.7 (a) Three major mechanisms of particle formation, and (b) mechanism of particle

growth in an emulsion polymerization [50]

Figure 2.7a shows the proposed scheme for particle formation in emulsion polymerization initiated by water-soluble initiators. Particle formation is considered to take place when either: (1) a free radical in the aqueous phase enters a monomer-swollen emulsifier micelle and propagation proceeds therein (heterogeneous nucleation); (2) the chain length of a free radical growing in the aqueous phase exceeds its solubility limit and precipitates to form a particle nucleus (homogeneous nucleation), or; (3) a free radical growing in the aqueous phase enters a monomer droplet and propagation proceeds therein (droplet nucleation). However, if the resultant polymer particles are not stable enough, the final number of polymer particles produced, regardless of the mechanism of particle formation, is determined by coagulation between the existing particles (coagulative nucleation). In the process of particle growth, various chemical and physical events occur in both the aqueous and particle phases, as illustrated in Figure 2.7b [50].

2.7 Functional polymer particle via emulsion polymerization

Functionalization of latex has become a common method for modifying its superficial and colloidal properties. In the first case, the advantage is chemical and mechanical stability. This permits increasing the interaction of the particles with different organic (cellulose and textile fibers), mineral (pigments), or metal substrates. In the second case, the desired improvement concerns the enhancement and control of the immobilization of biomolecules such as proteins, antibodies, and nucleic acids for biomedical purposes. This functionalization is implemented by incorporating reactive chemical groups contributed by the radical initiator (potassium persulfate, nitrosulfonated, carboxylated, cationic derivatives) or by an emulsifier (anionic, cationic,

zwitterionic, nonionic) or, lastly, by a functional monomer. The latter method is the most used due to the availability and the variety of functional monomers (i.e., acrylic acid, methacrylic acid, aminoethyl methacrylate). Furthermore, it gives several advantages in comparison to surfactants: incorporation of the monomer by covalent linking, control of particle size and charge density, low foaming effect.

Although widespread, the use of these functional monomers raises certain problems, some of which are far from being solved or even well understood [21–25]. These are:

1. The hydrophilic properties of these monomers (except for specific cases), which favors their distribution in the aqueous phase but which can also depend on the pH of the medium, especially for charged monomers such as (aminoethyl methacrylate, acrylic acid, etc.).

2. Localization of the functional monomer at the end of polymerization. At the water–polymer interface or inside the particles or in the aqueous phase. The functional monomer distribution depends on several parameters among which are hydrophilic properties, the neutralization rate in the case of charged monomers (i.e., carboxylic, amine), reactivity in (co)polymerization, pH of the aqueous phase, and method of adding the functional monomer in the reactive system.

3. The optimization of functionalization processes in terms of favoring the concentration of the functional monomer on the surface of the particles. This implies good control of the first two aspects.

According to the numerous functionalization processes, the chemical and physical properties of the chosen functional carrier (monomer, surfactant, and initiator) should be considered in order to target the desired localization of the functional compounds (particle surface or inside the polymer matrix). The parameters to consider are as follows:

- The nature of the functional monomer is of great importance (partition coefficient, reactivity, pH effect, etc.)

- The nature and concentration of the functional emulsifier (possible interactions with the ionic monomer and its polymers)

- Functional initiator (transfer reaction, decomposition rate)

Following the choice of functional compound and the chemical carrier (monomer, initiator, or surfactant), the following main operating methods and distinctions can be made (here consider the monomer only):

1. Batch polymerization, in which all of the reactants are introduced at the beginning in one step. This method, apart from certain exceptions, is of little interest because a large part of the functional monomer is consumed, providing substantial quantities of water-soluble polymers affecting the nucleation process, the polymerization reaction, and the final properties of the particles (i.e., colloidal stabilization, surface charge density, size and size distribution, surface polarity, and in some cases morphology).

2. Semicontinuous addition, which is very useful for performing copolymerizations requiring well-controlled chain structure and particle composition. The functionalization efficiency is based on the reactivity of the functional monomer and its introduction in the polymerization medium at a

suitable conversion, favoring their incorporation at the surface or its distribution in the vicinity of the interface. When the functional monomer is added at high conversion during the polymerization, the process is also called shot polymerization.

3. Multistage polymerization (seed polymerization), among which can be mentioned the deferred addition of an ionic comonomer (constituting the basic latex), favoring a highly efficient surface functionalization.

Generally, the batch process does not allow sufficient incorporation at the surface, since the penetration of the charged monomer (amine or carboxylic groups) predominates if the charged compound is not neutralized. On the contrary, polymerization in the aqueous phase is preferred if it is completely neutralized ($-NH_2$, or -COOH) [51]. Then in a process, most of the functional monomer is wasted (buried in the particles or as water-soluble polymers). The water-soluble polymer content depends on the water solubility of the monomer, and the percentage is found to be higher for acrylic acid, which is more water soluble than methacrylic acid. The more solubility in the particle of the functional monomer is (e.g., methacrylic acid in comparison to acrylic acid), the more buried it will be. With the shot process, when the internal viscosity of the particles is high, the functional monomer (i.e., methacrylic acid) favors better surface incorporation, and localization is optimized by adding a mixture of main monomer and functional comonomer.

To favor the immobilization of biomolecules on the particles, functional groups should be present at the surface of the particles. The monomer addition method (shot process) was successfully carried out with carboxylate, butyl acrylate–methyl

methacrylate emulsion copolymers using either acrylic acid or methyacrylic acid [52]. When adding the carboxylic acid in the presence of the more hydrophobic comonomer (butyl acrylate), surface carboxyl group yield of the order of 70–80% was reached.

Seed polymerization is a good process to obtain functional particles, and many functional spheres (such as carboxyl, hydroxyl, chloromethyl, amino, etc.) have been prepared [53-55]. In some applications (model colloids in biomedical fields), it is necessary to eliminate the influence of the emulsifier; this requires the use of polymerization methods without surfactant which permits the production of monodispersed latexes. Surfactant-free emulsion polymerization is a good choice for the elaboration of surface-clean polymer colloids [51, 56]. Although the introduction of a functional monomer permits varying the particle size over a wider range and produces more concentrated polymers (40% instead of 20% in their absence), the formation of water-soluble polymers is nonetheless substantial and surface localization remains low (from 15% to 30% as a function of the functional monomer).

2.8 Preparation of functional core/shell particles by a two-stage seeded emulsion polymerization

The core-shell particle is a very important type of functional particle. A number of polymerization-based methods have been employed to produce particles that consist of solid cores coated with a shell of polymeric materials [57]. These include monomer adsorption onto particles followed by a subsequent polymerization [58–60], heterocoagulation polymerization [61], or emulsion polymerization [57, 62]. A two-stage seeded emulsion polymerization is the first general method developed to prepare latex

particles result in a core-shell structure. The first stage, or core latex preparation, is carried out either separately or *in situ*, and the mode of polymerization for the second stage is usually a seeded swelling batch or a semi-batch process.

2.9 Microemulsion

Microemulsions are thermodynamically stable, isotropic, and optically transparent dispersions of two immiscible liquids, oil and water, obtained in the presence of a surfactant (or with a co-surfactant). In the water- or oil-rich regions, oil-in-water (o/w) micelle or water-in-oil (w/o), microemulsions consist of small microdroplets (diameter < 10 nm) surrounded by a surfactant monolayer (Figure 2.8). The small size of the droplets accounts for the transparency, which is commonly used as a criterion for the preparation of microemulsions. The thermodynamic stability of the microemulsions arises from the very low interfacial tension and the entropic gain resulting from the reduced droplet size.
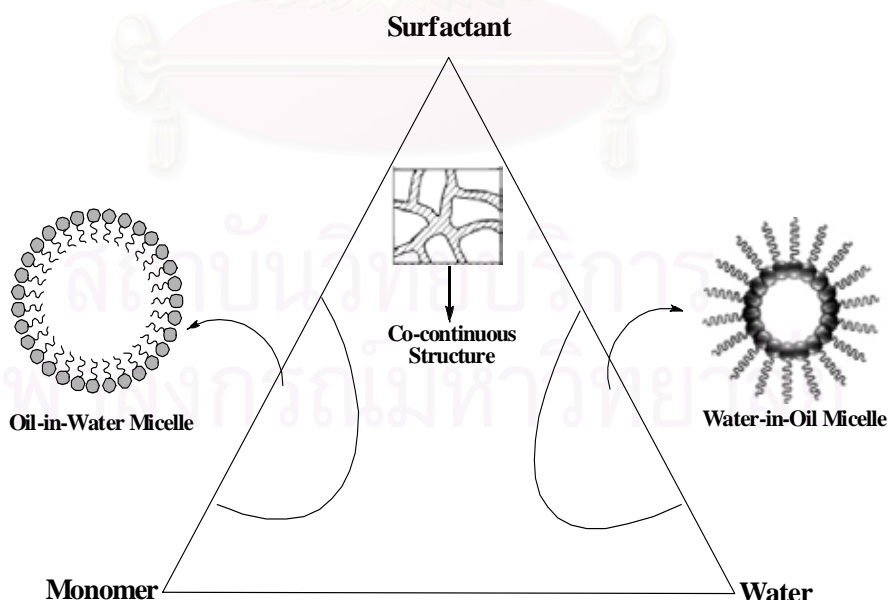
Figure 2.8 Isotropic microemulsion domains in the phase diagram [44].

2.10 Microemulsion polymerization techniques

Research interests in microemulsion polymerization techniques have grown rapidly since the 1980s because of their potential applications in the preparation of fine latex particles, ultrahigh molecular weight water-soluble polymers (flocculants), novel porous materials, polymeric supports for binding metal ions, conducting polymers, colloidal particles containing various functional groups for the biomedical field, and transparent colloidal systems for photochemical and other chemical reactions [3, 10-16].

Microemulsion polymerization involves the propagation reaction of free radicals with a vinyl monomer in very fine oil (or water) droplets dispersed in the continuous aqueous (or oily) phase. Unlike the classical emulsion, the transparent or translucent reaction system comprising microemulsion droplets is thermodynamically stable in nature and these tiny droplets (1–10 nm in diameter) exhibits an extremely large oil–water interfacial area ($\sim 10^5$ m^2 dm^{-3}). Relatively stable polymer particles ($\sim$10-50 nm in diameter) consisting of only a few polymer chains per particle are produced and, therefore, the resultant polymer molecular weight is very high ($10^6 - 10^7$ g mol^{-1}) [3, 10-16]. Two major drawbacks have limited its broad application, i.e., (1) low monomer/surfactant weight ratios, usually < 1, and (2) low polymer content, usually less than 10 wt% [3, 10-16]. Therefore, in order to make microemulsion polymerization more practical and attractive, it is desirable to minimize the surfactant amount used and maximize polymer content. A modified microemulsion polymerization [17] has been successfully employed to prepare a high-solid content nanosized polymeric microemulsion, in which monomer was gradually added into the polymerizing microemulsion without disturbing its stability; this method is broadly applicable for

various monomers [18]. The polymerization of an o/w microemulsion [3, 10-19] gives stable transparent bluish latexes. The molecular weights of the polymers are often high, and the number of chains per particle is generally a few chains per particle [3, 10-19]. The comparison between the particle size and the dimension of the linear polymers indicates that the chains are highly compressed within the particles [18-19], such that the orientation of the polymer is increased.

In microemulsion polymerization [10-11], the water-soluble initiator (e.g. potassium persulfate and ammonium persulfate) is found to have a short induction time while the oil-soluble initiator has a long induction time. The reason may be that the thermal decomposition of initiator molecules produced pairs of radicals which are very likely to recombine when produced within a small volume of micelles. But if one radical escapes to the aqueous phase, a single radical is left in an isolated locus which is the prerequisite for microemulsion polymerization. Consequently, it is probable that the minor proportion of an oil-soluble initiator which is partitioned into the aqueous phase is responsible for the major part of the initiation by entry of a single radical from the water in the same way as for that of a water-soluble initiator [15]. It still seems that this is most probable reason why the thermal polymerization of microemulsion polymerization systems with oil-soluble initiators have long induction times. Despite being inefficient, the use of an oil-soluble initiator could be advantageous if it were desirable to avoid the presence of ionic end-groups in the polymer. Since the oil-in-water microemulsion polymerization was believed to have particle nucleation within the micelle, the inside micelle is composed of a small volume of free space and an aggregation of the hydrophobic part of surfactant. So the hydrophobic chain end of the polymeric free

radical initiated by oil-soluble initiators is convenient to further polymerization more than the ionic chain end of polymeric free radical initiated by the water-soluble initiator. The resulting polymer shall have a high conversion and probably a high molecular weight as well. Thus, oil-soluble initiators were possible as efficient initiators for the microemulsion polymerization technique as reviewed. Likewise, oil-soluble initiator (e.g. benzoyl peroxide and 2,2'-azobisisobutyronitrile) is the versatile initiator for free-radical polymerization of the functional polymer particles since the oil-soluble free radical was known to selectively attack the methacrylic double bonds [8-9, 20-25]. In such a system, the side reactions of the free radicals with the functional groups are possibly not observed.

Microemulsion copolymerization techniques were developed to overcome the two major drawbacks of the microemulsion polymerization [26-29]. Most of the studies have been devoted to the copolymerization of 2-ethylhexyl acrylate and acrylonitrile monomers [26], copolymer between methyl methacrylate and acrylonitrile monomers [27-28]. In most cases, the introduction of a second monomer was found to modify the microemulsion domains, the size of the resulting particles, as well as the stability of the final copolymer latex nanoparticles. The partitioning of the comonomer between oil droplets, the interface, and water as well as the chemical modification of the particle surface was proposed to account for the experimental results. In addition, the microemulsion copolymerizations were carried out inside the microemulsion droplets and provided a continuous process in the same manner as for microemulsion polymerization. The modified microemulsion copolymerization was developed to produce the high solid content of polymer latex nanoparticles. Xu et al. [29] has introduced the

copolymerization of acrylate monomers in a modified microemulsion process in which the particle size of the copolymer microlatex did not change distinctly with the monomer composition. The estimation of emulsifier coverage on the microlatex particles indicated that the process switched from a traditional microemulsion to a normal seeded emulsion polymerization very soon after drop addition of monomer began. Therefore, a longer dropping time is needed to produce microlatex with narrow dispersed particle size. Besides, in the modified microemulsion polymerization, a lower amount of the emulsifier is needed to produce the stable microlatex. This behavior is related to the mechanism of normal seeded emulsion polymerization during drop addition of monomer. However, the surfactant/monomer weight ratio was still constant at 1:10, the same as with the modified microemulsion polymerization process. In addition, only residual functional groups were located on the surface of the copolymer latex nanoparticle since almost all the functional comonomers were initialy copolymerized inside the particle [26-28]. Although a two-step process of the modified microemulsion polymerization can inhibit the copolymerization inside the core particle, the amounts of surfactant were not significantly decreased.

The depletion of the functional groups during polymerization of the functional polymer latex nanoparticles could improve the core/shell structure of the functional polymer nanoparticles since most of the functional groups were located on the surface of the particle. The core/shell structure of functional polymer nanoparticles was developed from a two-step process of the modified microemulsion polymerization [33]. The major concern in these methods is that they usually require a high amount of surfactant and it is difficult to decrease the particle size to less than 60 nm.

From the literature reviewed above, a two-step process of the modified microemulsion polymerization techniques provided a suitable polymerization process to prepare the core/shell structure of functional polymer latex particles since the nanosized range of the functional polymer particles with the core/shell structure were obtained. However the amounts of surfactant to stabilize the smaller polymer latex nanoparticle were not much reduced.

2.11 Differential microemulsion polymerization techniques

As mentioned above the microemulsion polymerization method for making polymer nanoparticles requires a large amount of surfactants, which raises concerns with respect to the additional cost of the surfactants and post-treatment to remove the surfactants after polymerization. It is therefore very desirable to improve microemulsion polymerization so that a much smaller amount of surfactant is required. The differential microemulsion polymerization techniques [4-7] present an attempt to significantly reduce the amount of surfactants in microemulsion polymerization for the preparation of further smaller polymer nanoparticles. The differential microemulsion polymerization includes three steps: (i) an initial period in which a mixture of initiator and surfactant in the recipe is heated in the reactor; (ii) a suitable addition period in which the total monomer is added to the reactor; and (iii) an aging period to allow for a complete polymerization of unreacted monomer. The key characteristic of the polymerization operations described above is that the probability of monomer droplets surviving in the reaction system is minimized because of the style of monomer addition, which is different from a conventional emulsion polymerization operation.

He, et al. [4] reported on an innovative development in which PMMA nanosized particles were synthesized by a differential microemulsion polymerization technique. Sodium dodecylsulfate and ammonium persulfate were used as the surfactant and initiator, respectively. The effects of reaction conditions on the particle size have been investigated. A particle size of less than 20 nm in diameter has been achieved with surfactant/monomer and surfactant/water weight ratios of 1:18 and 1:20, respectively; a much milder condition than those previously reported in the literature has been obtained. The homogeneous nucleation mechanism was proposed as the dominant nucleation mechanism for the PMMA nanosized particles synthesized by a differential microemulsion polymerization [5] as shown in the Figure 2.9.
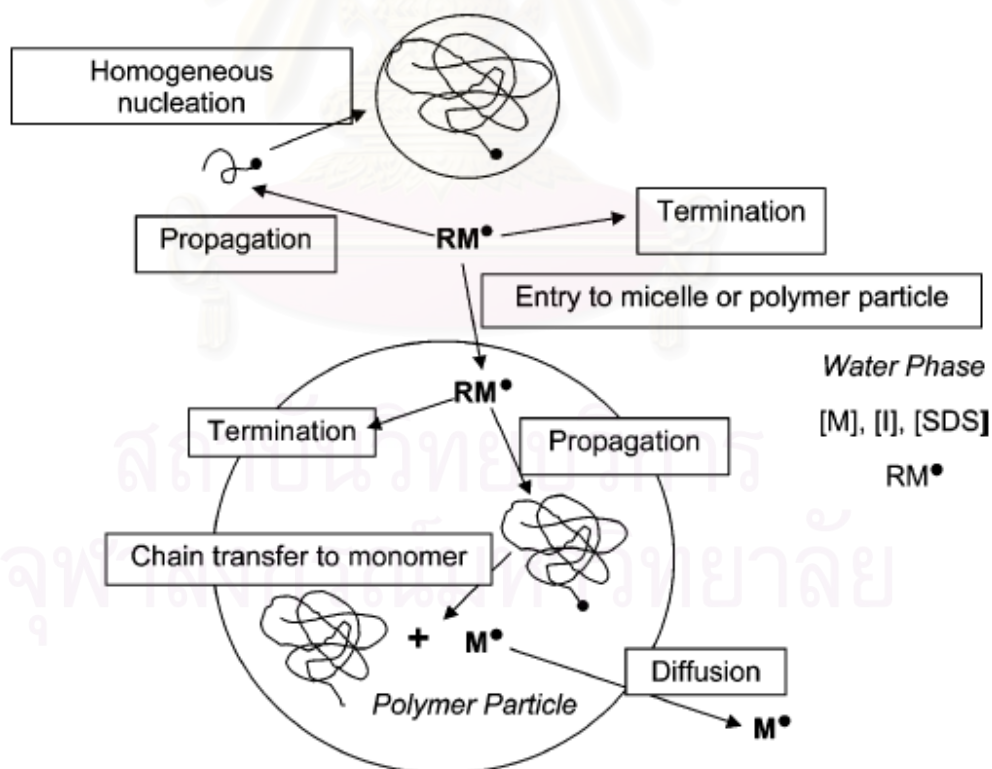
Figure 2.9 A proposed mechanism for a differential microemulsion polymerization [5].

Polystyrene nanosized particles have also been synthesized by a differential microemulsion polymerization via a two-step process [6] involving the use of a small amount of poly(methyl methacrylate)(PMMA) as the seed. Sodium dodecyl sulfate (SDS) and ammonium persulfate (APS) were used as the surfactant and initiator, respectively. The differential microemulsion polymerization is more effective not only in decreasing the particle size of polystyrene but also in decreasing the amount of surfactant required. The size of the polystyrene particles was significantly decreased and particles smaller than 20 nm were achieved at an SDS / (styrene + MMA) weight ratio of 0.043. For the styrene system [7], the nucleation both in the aqueous phase and in the micelles should be taken into consideration, whereas the contribution from the homogeneous nucleation in the water phase is not as important as in the heterogeneous nucleation in the micelles. A heterogeneous nucleation refers to the mechanism in which the particles are generated from the micelles.

2.12 Summary

Inputs of tireless effort in research and applications over the last 20 years have led to fast developments in preparation techniques of structured particles. At present, it is possible to obtain a wide variety of particle morphologies, from a relatively simple structure to a most frequently studied core-shell structure to much more complex structures (multilayer, with spherical and cellular inclusions, etc.). In some cases, the structures can be irregular and unstable forms, and evolve into spherical forms. Under the conventional procedure, i.e., a classical polymerization process, it is very difficult to monitor both the core size and the thickness of the shell. In recent years, a technique for microemulsion polymerization has been introduced for the preparation of a very narrow

distribution of nanoparticles by a group of active researchers led by Rempel and Pan [4-7]. Further, a heterogeneous initiation with the technique of microemulsion polymerization has been developed [32-33] via a two step process of polymerization to produce nanosized core/shell particles. In addition, with this technique, it is easier to decrease the particle size and improve surface functionality properties.

In this research, with merits of the differential microemulsion polymerization via a two-step process technique, a core/shell structure of glycidyl-functionalized PMMA nanoparticles shall be prepared and characterized.
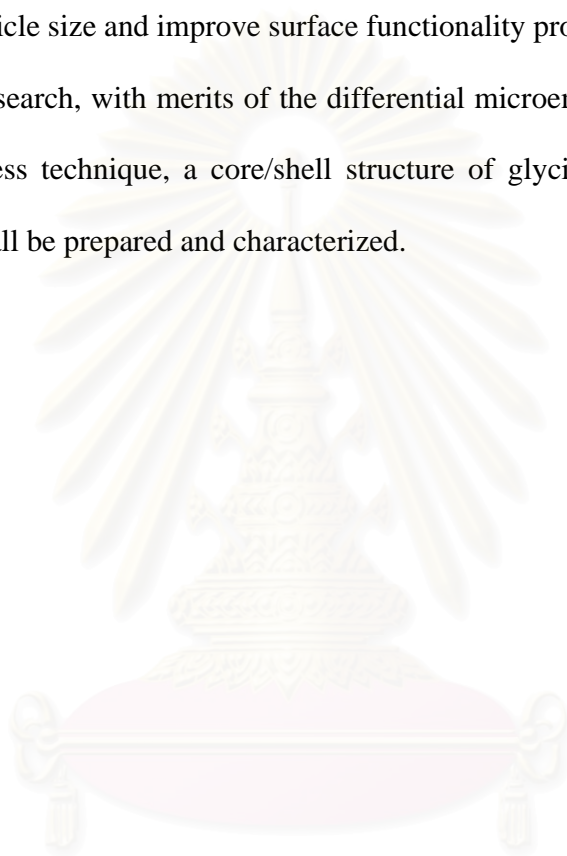
CHAPTER 3

SYNTHESIS OF POLY(METHYL METHACRYLATE) NANOPARTICLES INITIATED BY AZOBISISOBUTYRONITRILE USING DIFFERENTIAL MICROEMULSION POLYMERIZATION

3.1 Introduction

In the previous chapter, AIBN oil soluble initiator was proposed to be a selected initiator for synthesis the poly(methyl methacrylate) nanoparticle via differential microemulsion polymerization. However an AIBN oil soluble initiator has never been used in the differential microemulsion polymerization [4-7]. In addition, the methyl methacrylate monomer is one of the widely used monomers in industry and it has been synthesized with the differential microemulsion polymerization using a water-soluble initiator [4-5]. So it will be convenient to observe the interesting effects by using the previous studies [4-5] as a guideline for the research.

This chapter presents a detailed investigation regarding the application of the differential microemulsion polymerization method for the synthesis of PMMA nanoparticles with an oil soluble initiator, AIBN, in which the particle nucleation is believed to happen in micelles and follow a heterogeneous nucleation mechanism, rather than to occur in the aqueous phase and follow a homogeneous nucleation mechanism. The effect of surfactant concentration on particle size, and conversion as well as on molecular weight is investigated. In addition, the effect of surfactant concentration on the amount of polymer nanoparticles, and the effects of water-to-monomer ratio and

surfactant concentration on the tacticity of PMMA latex nanoparticles, as well as the influences of surfactant concentration, water-to-monomer ratio and polymerization time on conversion, molecular weight, tacticity, and glass transition temperature of PMMA latex nanoparticles.

3.2 Experimental

3.2.1 Materials

Methyl methacrylate (MMA) containing 10 part per million (ppm) of an inhibitor (AR grade from Aldrich, USA), sodium dodecyl sulphate (SDS) powder (97% purity from Aldrich, USA), 2, 2'-azobisisobutyrinitrile (AIBN) (AR grade from Polysciences, USA), hydroquinone (AR grade from Polysciences, USA), methanol (practical grade) and cyclohexane (AR grade from Aldrich, USA) were used as received. De-ionized (DI) water was used as obtained from the Department of Chemical Engineering at the University of Waterloo, Ontario, Canada.

3.2.2 Preparation of PMMA microemulsion

Nanoparticles of PMMA were prepared by differential microemulsion polymerization using an oil-soluble initiator AIBN. The polymerization recipes are provided in Table 3.1

Table 3.1 Polymerization recipes

Water (cm^3)	MMA (cm^3)	AIBN (g)	SDS (mM)
60	14	0.08	4.9-80.9
84	14	0.08	3.5-57.8

The initiator and surfactant were mixed in a specified amount of water in a 500 cm^3 Pyrex glass reactor (Aldrich, Ontario, Canada), which was equipped with a double-jacket condenser and a dropping funnel for addition of monomer feeding. The system was subsequently subjected to heating up to 70ºC under constant agitation (200 rpm) provided by a magnetic stirrer bar using a stirring/temperature controlled digital hotplate system with a constant nitrogen feed to the reaction vessel through a gas inlet tube.

The monomer was fed very slowly under continuous dropping of monomer droplets for a designated time (around 1.5 h) after the temperature of the system had reached 70ºC. After the monomer feeding was completed, the reaction system was kept at 70ºC with constant agitation for another hour (aging time) in order to obtain a higher conversion of the polymer.

In order to quench the reaction, the polymerization system was cooled down by placing the reactor in a bath of cold water at about 10°C for 10 min. Then the product at ambient temperature was mixed with 5 cm^3 of a 3% solution of hydroquinone (HQ) in DI water to fully terminate the reaction.

3.2.3 Separation of polymer samples for characterization

The resultant polymer was precipitated using an excess amount of methanol and it was separated by a vacuum-filtration technique, and the surfactant and initiator were washed with a sufficient amount of warm de-ionized water and methanol. The unreacted monomer was removed by extraction using cyclohexane at 37–40ºC for 24 h. The mixture between PMMA and cyclohexane was filled in a glass bottle before being placed in an automatic temperature-controlled water bath for heating.

3.2.4 Characterization of the nanosized PMMA

3.2.4.1 Particle size and particle size distribution

After the polymerization was completed, the number-average diameter (D_n) and the intensity-average diameter (D_z) of the polymer particles were measured by dynamic light scattering technique on a Nanotrac®150 (Microtrac, Montgomeryville, USA).

3.2.4.2 Polymerization conversion

To avoid the effect of periodic sampling on the reaction system during the reaction, sampling was done only at the end of the reaction, i.e. no sampling was done before the reaction was terminated. Thus, for each single reaction operation with a reaction time t, one conversion X_m was obtained. The polymerization conversion (X_m) is defined as follows and obtained by gravimetric analysis:

$$X_m = \frac{\left(\%\text{wt of cleaned PMMA particles}\right)_t}{\left(\%\text{wt of MMA feed}\right)_t} \times 100\% \qquad (3.1)$$

3.2.4.3 Concentration of latex particles (N_p) and micelles (N_m)

The concentration of latex particles (N_p) and micelles (N_m) were calculated according to the following equations:

$$N_p = \frac{6M_o X_m}{\pi \rho (D_n)^3} \qquad (3.2)$$

$$N_m = \frac{([S] - CMC)}{m} \qquad (3.3)$$

where Mo is the initial concentration of monomer, g dm^{-1}, X_n is the fraction of the polymerization conversion, ρ is the density of PMMA (1.18 g cm^{-3} at 25 °C), D_n is the particle size, nm, [S] is the concentration of surfactant, mM, CMC is the critical micelle concentration of SDS, mM, and "m" is the number of SDS molecules present in a micelle (i.e. an aggregation number). The value of m is 71 based on the spherical micelle formation [72] and CMC is 8.2 mM at 25 ºC [72] as determined via an electrical conductivity measurement.

3.2.4.4 Molecular weight and its polydispersity index (PDI)

The average-molecular weight ($\overline{M}_n$ and $\overline{M}_w$) and polydispersity index (PDI, equivalent with $\overline{M}_w / \overline{M}_n$) were determined by gel permeation chromatography using a multi-angled laser light scattering setup (GPC-MALLS, Wyatt Technology Corporation, California, USA) equipped with an RI detector (Water 150-CV refractive index detector) and MALLS detector (DAWN$^{®}$DSP-F laser Photomer). A PL-Gel$^{®}$ column set up was employed consisting of three 300×8 mm columns.

3.2.4.5 Tacticity measurement

A Bruker Biospin DPX-300 NMR spectrometer was used for ^{1}H-NMR analyses at 300 MHz with CDCl$_3$ solutions at room temperature. The tacticities of the samples were characterized from the integrated ratios of the syndiotactic (*rr*), isotactic

(*mm*), and heterotactic (*mr*) triad signals of α-methyl protons which occur at 0.81, 0.99, and 1.18 ppm, respectively [19, 71].

3.2.4.6 Glass transition temperature (T_g)

The T_g values of the polymer were measured using a NETZSCH DSC-204 F1 differential scanning calorimeter; a 10-mg sample was used at a scanning rate of 10ºC min^{-1} from 25 to 180ºC followed by rapid cooling and heating again at the same rate of 10ºC min^{-1}. Mercury (mp = -38.8ºC), bi-benzene compound (mp = 69.2ºC), indium (mp = 156.6ºC), tin (mp = 231.9ºC), and bismuth (mp = 271.4ºC) were used to calibrate the instrument. The T_g values from the second heating operation were recorded to ensure that the system had reached its thermal steady state during T_g analysis. The T_g was determined using a midpoint method.

3.3 Results and Discussions

The PMMA latex nanoparticles are presented in Figures 3.1 to 3.2. The transparency of the PMMA latex nanoparticles increased with an increasing concentration of SDS present. This implied that the high concentrations of SDS can provide smaller PMMA nanoparticles. This implication will be further discussed later.
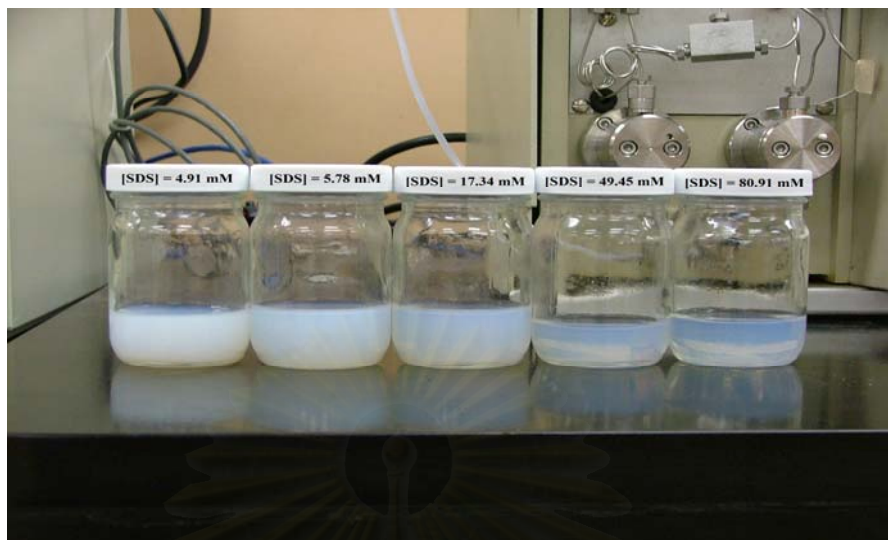
Figure 3.1 PMMA latex nanoparticles at DI water of 60 cm^3 and concentrations of SDS

increased from left to right.
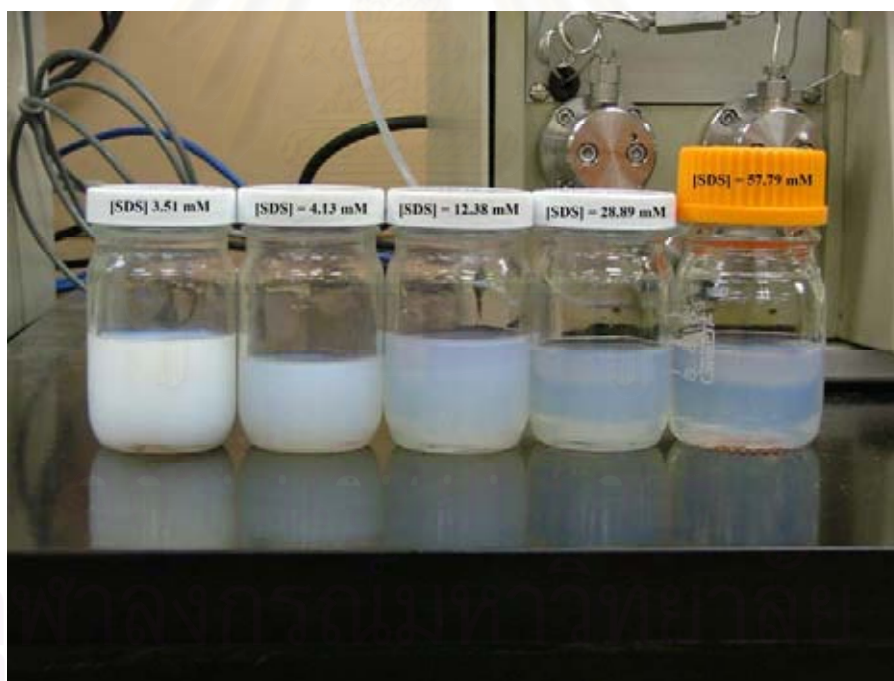
Figure 3.2 PMMA latex nanoparticles at DI water of 84 cm^3 and concentrations of SDS

increased from left to right.

To facilitate the discussion, the curves are defined in terms of three regions, i.e. region 1 (R1): $D_n > 30$ nm, region 2 (R2): 20 nm $< D_n \leq 30$ nm and region 3 (R3): $D_n \leq 20$ nm. The particle size of R1 can be achieved by common emulsion polymerization; the particle size of R2 can be realized by microemulsion polymerization, which usually requires a higher surfactant amount; the particle size of R3 is not so easily achieved by conventional emulsion or microemulsion polymerization methods.

3.3.1 Particle size of PMMA latex nanoparticles

The effects of SDS concentration and water/monomer ratio on particle size have been investigated. Figure 3.3 shows the effect of SDS concentration at the two levels of water/monomer ratio on particle size of the resultant PMMA.
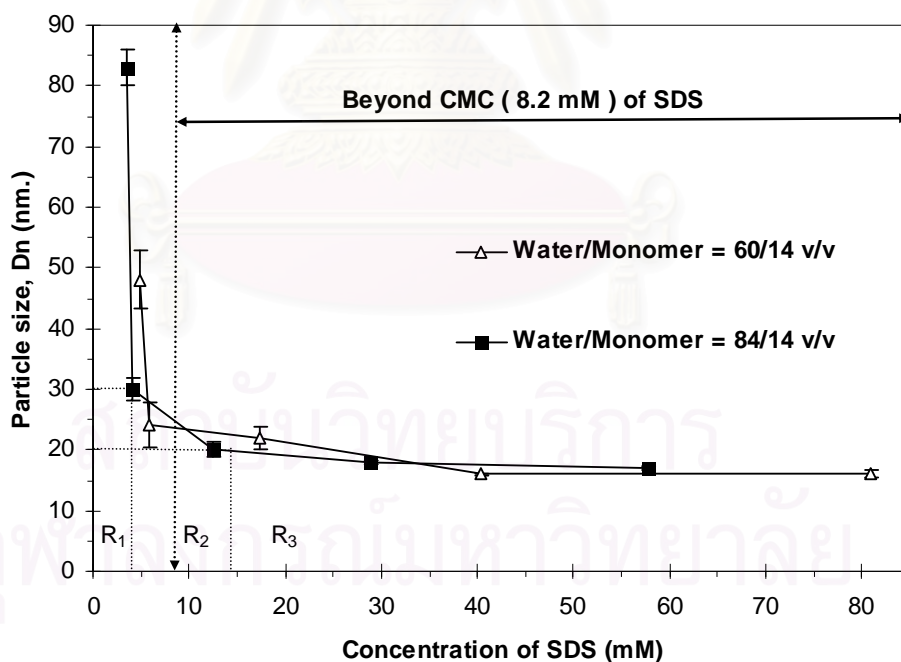
Figure 3.3 Dependence of PMMA particles size produced via differential microemulsion
  polymerization on [SDS]

To avoid too many notations on the figure, only one curve in Figure 3.3 has been noted with R1, R2 and R3 regions, as an example. The results in Figure 3.3 demonstrate that using the differential microemulsion polymerization method, the particle size could span from regions R1 to R3, depending on the SDS concentration. The particle size in the R1 region decreases rapidly with an increase in SDS concentration, and it does not significantly change when it is in the R3 region. The R2 region can be referred to as a transition region, which is located in the vicinity of the CMC. The curves shown in Figure 3.3 indicate that the changes in the size of particles obtained from the present work and from the previous work [4-5] with respect to SDS concentration have similar trends. However, the transition region happens much earlier than the system investigated by He et al. [4-5] although the latter could reach a lower level of the particle size in the R3 region. This implies that if the particle size located in the transition region is acceptable, the system investigated in the present work would be much more economical than the system investigated by He et al. [4-5] as the surfactant required would be much lower for the system investigated in the present work. Another characteristic of R2 is that the particle size can be well adjusted to be within the 20-30 nm range by SDS concentration according to the requirement in a real application.

Figure 3.3 also demonstrates that the water/monomer ratio does not greatly affect the particle size of PMMA in the system investigated in the present work in the R3 region. This phenomenon is different from that observed when a water-soluble initiator was used previously [4-5], where the ratio of water/monomer was found to have a definite effect on the particle size of PMMA although the reaction operation procedure was almost the same. In the present work, a hydrophobic initiator was used; therefore, it

is believed that the nucleation most likely occurred within the micelles rather than in the water phase and thus the ratio of water/monomer may not affect significantly the conditions inside micelles in the R3 region where the surfactant concentration does not have a significant effect on particle size, i.e., the surfactant amount is sufficient to stabilize the particles.

3.3.2 The percentage of conversion

The results with respect to the effect of SDS concentration on the conversion are shown in Figure 3.4.
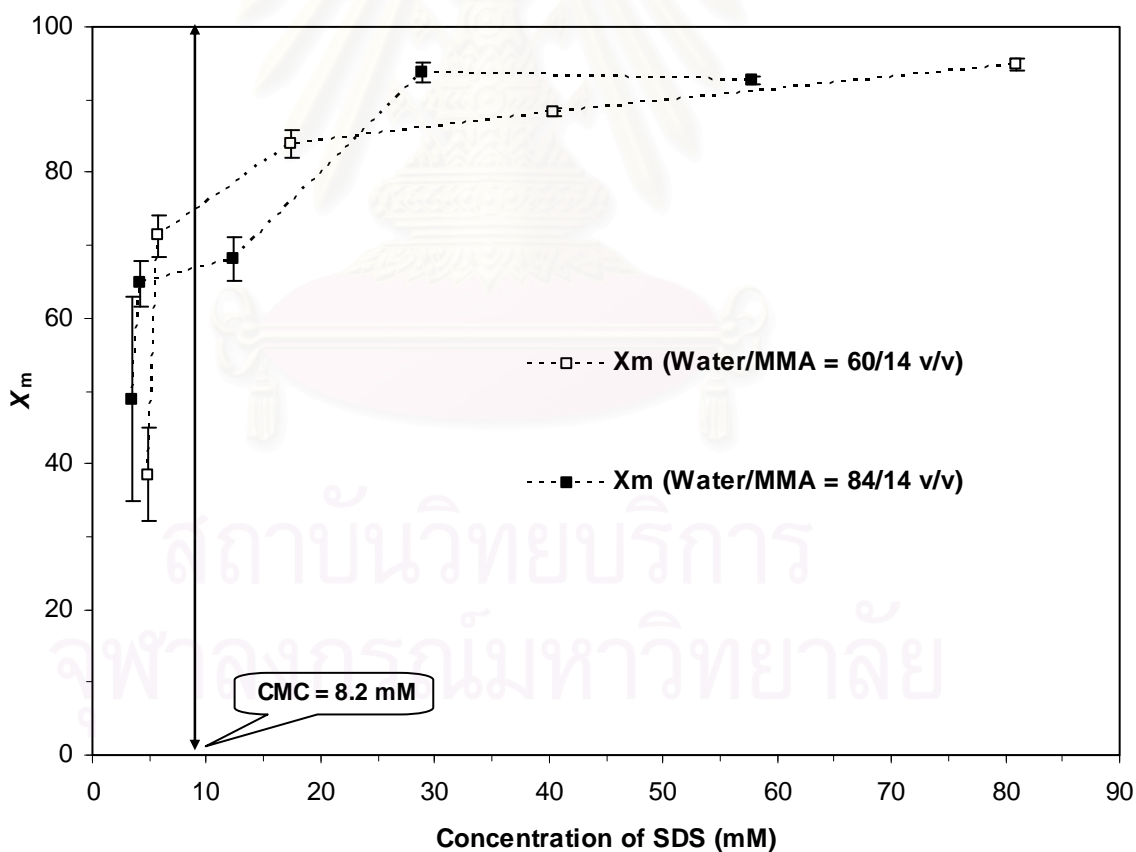
Figure 3.4 Dependence of Conversion of PMMA on SDS concentration

It is seen in Figure 3.4 that with an increase in the SDS concentration, the conversion increases and that in the range of [SDS] = 17.34 to 80.91 mM, which is in the region after the CMC, the difference between the two MMA/water levels is not so significant. There are more micelles at high SDS concentration, which provide more "nano-reactors" in the system; and thus, at a given MMA/water ratio, high SDS concentration results in a higher conversion. At a given SDS concentration, after the SDS concentration exceeds the CMC, the monomer in the aqueous phase can be negligible and there were no monomer droplets in the reaction system [4-5]; thus the reaction mainly occurs in the micelles ("nano-reactors") and the reaction conditions in each micelle should be almost the same in the two systems with the two different MMA/water levels investigated, which may be the reason for the similar conversions in the two systems as shown in Figure 3.4.

3.3.3 Molecular weight and their PDI of PMMA latex nanoparticles

The molecular weights of the PMMA particles produced via the differential microemulsion polymerization have been measured and they are shown in Figure 3.5.
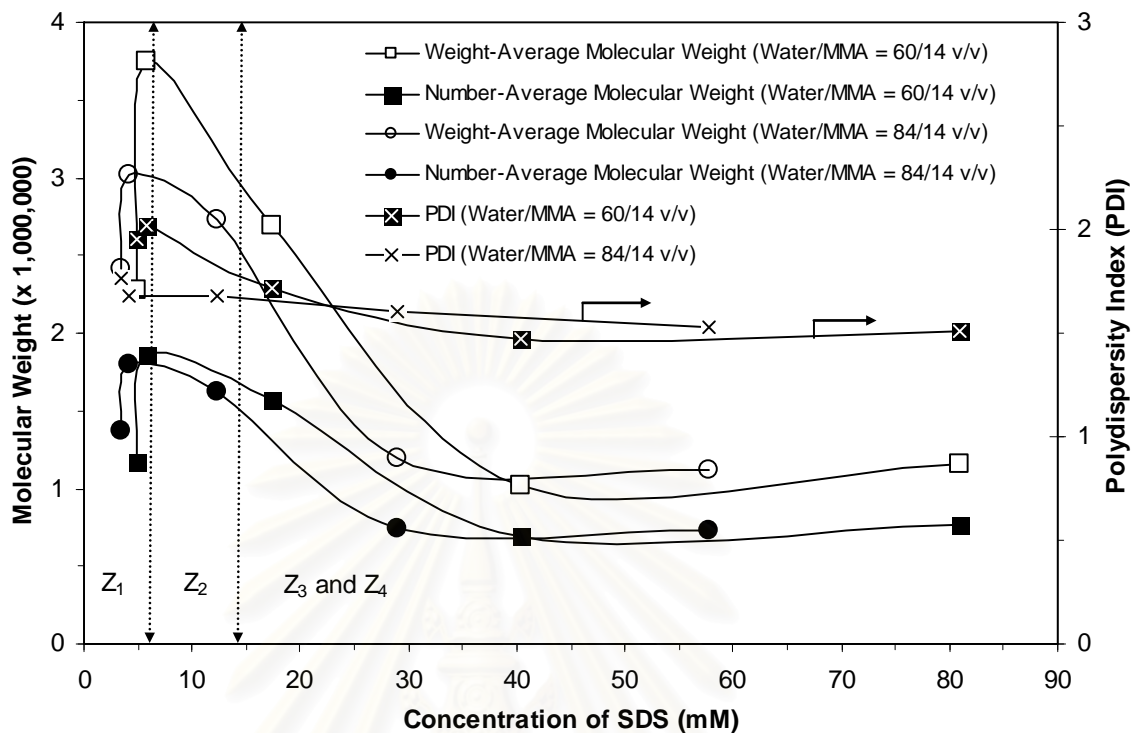
Figure 3.5 Dependence of PMMA Molecular Weight on SDS concentration.

Figure 3.5 indicates an interesting dependence of the molecular weight on the SDS concentration. For all the curves in Figure 3.5, with an increase of the SDS concentration, the molecular weight initially increases over a short SDS range, and then remains at a relatively constant level for a certain SDS range, before it quickly decreases and then finally remains at another relatively constant level, which is around 10^6 (a little over 10^6 for $\overline{M}_w$ and a little bit below 10^6 g mol^{-1} for $\overline{M}_n$). To facilitate discussion below, the four zones will be referred as Z1, Z2, Z3 and Z4 respectively. The Z1 and Z2 zone here correspond to the R1 and R2 region, respectively, discussed above with respect to the SDS concentration. The Z3 and Z4 zones are located in the R3 region. In the Z2 region, the molecular weight reaches the highest value and the difference between $\overline{M}_w$ and $\overline{M}_n$ is also the highest. While in the Z4 zone where the particle size is less than 18

nm, the molecular weight is the lowest. This implies that by adjusting the SDS concentration, the molecular weight of PMMA can be fairly well controlled. It is also interesting that in the R3 region (Z3 and Z4), the dependence of the molecular weight of PMMA (Figure 3.5) on the SDS concentration has a similar trend to the dependence of the particle size of PMMA (Figure 3.3). This implies that the polymer chain number in the particles may not change significantly with the change in SDS concentration although the particle size changes and the polymer chain length changes. As predicted in the previous section, the molecular weight in the reaction system with MMA/water = 14/60 (volume ratio) is slightly higher than that in the system with MMA/water = 14/84 (volume ratio), as shown in Figure 3.5.

3.3.4 Number of PMMA chains per particle

The number of PMMA chains per particle was calculated [4] using equation (3.4);

$$N = \frac{4}{3}\pi(\frac{D_Z}{2})^3\rho\left(\frac{N_A}{M_W}\right)$$

(3.4)

where D_z is a hydrodynamic diameter of the particles, and ρ is the density of the PMMA particles, assuming that all monomers in the particles were polymerized. The density of PMMA is 1.18 g cm^{-3}, N_A is 6.02 x 10^{23} g mol^{-1} and the weight-average molecular weight was obtained from measurements using GPC-MALLS.

Table 3.2 Number of polymer chain per particle (N) of PMMA latex nanoparticles. (MMA 14 cm^3, in the presence of AIBN 0.08 g, DI water, and SDS surfactant was polymerized at 70ºC for 2.5 h.)

Water/MMA	[SDS] (mM)	M_w x 10^{-6}	M_n x 10^{-6}	MWD	D_n (nm)	D_z (nm)	N (chain)
60/14	4.91	2.28	1.17	1.95	65	73	21
60/14	5.78	3.75	1.86	2.02	30	51	4
60/14	17.34	2.69	1.57	1.71	28	43	3
60/14	40.45	1.02	0.69	1.47	22	37	5
60/14	80.91	1.15	0.76	1.51	19	30	2
84/14	3.51	2.41	1.37	1.76	88	100	45
84/14	4.13	3.02	1.80	1.68	40	68	11
84/14	12.38	2.73	1.62	1.68	31	44	3
84/14	28.89	1.19	0.74	1.61	19	37	4
84/14	57.79	1.12	0.73	1.53	18	31	3

In Table 3.2, the PMMA produced by differential microemulsion polymerization using an oil-soluble initiator had few polymer chains per particles when [SDS] was beyond the CMC. Calculation indicates that the average polymer chain number is within 3-4 in the Z3 zone and 1-2 in the Z4 zone, in which the SDS changes from 17.34 mM to 80.91 mM. This may imply that using this method, nanoparticles with relatively uniform chain numbers in the particles can be synthesized. Thus, in the Z4 zone, the nanoparticles would become "molecular bricks" as they were composed by only 1-2 polymer chains. The small chain numbers in the PMMA nanoparticles indicated that a heterogeneous nucleation mechanism was the predominate particle nucleation mechanism throughout the reaction.

3.3.5 Dependence of polymer particle population on concentration of surfactant

The relationship between the concentration of polymer particles (N_p), micelles (N_m) and surfactant, and the fraction between the amount of polymer particles and micelles (N_p/N_m) is presented in Figure 3.6.
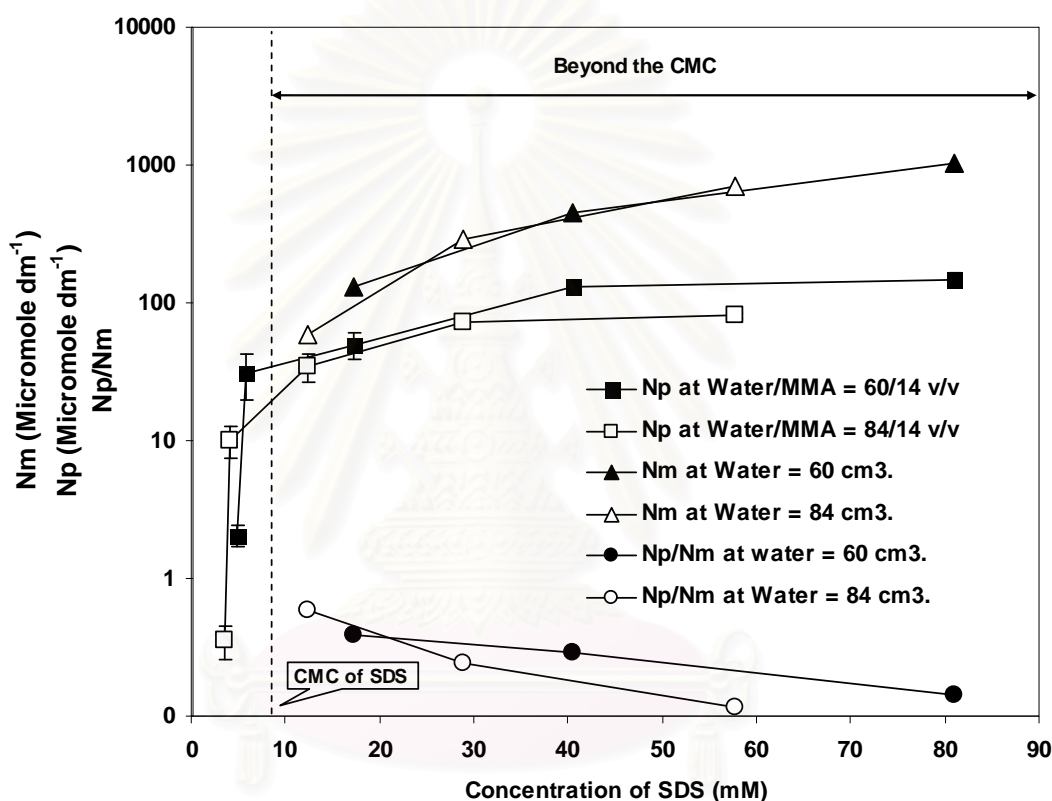
Figure 3.6 Dependence of N_p, N_m, and their fractions on the concentrations of the surfactant.

The concentration of polymer particles (N_p) and micelles (N_m) increased with an increase in the concentration of the surfactant; however, the ratio of N_p/N_m decreased with the concentration of surfactant. Figure 3.6 demonstrates that over the experimental range of [SDS] investigated, the concentration of polymer particles increased from 2.04

to 147 μM when the ratio of the water/monomer was 60/14 (v/v) and from 0.36 to 80.6 μM when the ratio of the water/monomer was 84/14 (v/v). The concentration of micelles increased from 129 to 1024 μM and from 58.9 to 698 μM when the ratios of water/monomer were 60/14 (v/v) and 84/14 (v/v), respectively at an SDS concentration above its CMC. The fraction of N_p/N_m decreased from 0.38 to 0.14 and from 0.58 to 0.12 when the ratio of water/monomer was 60/14 (v/v) and 84/14 (v/v), respectively. This phenomenon may be explained by the nucleation mechanism. Compared to APS, an initiator used in He et al's work [4-5], AIBN used in the present work is rather oil soluble and thus it is believed that a heterogeneous nucleation mechanism [73-78] prevailed in the reaction system employed in this work rather than the homogeneous nucleation mechanism which was proposed in He et al's work [5]. The solubility of AIBN is 4 x 10^{-5} g g^{-1} in H_2O [79] and the partitioning of AIBN between the monomer phase and the water phase is 115/1 [79]. Under the assumption that f (an initiator efficiency) is equal to 1, the generation rates of AIBN radicals [$(CH_3)_2(CN)C^*$] in the monomer phase and in the aqueous phase at 70°C are 1.61 x 10^{19} and 1.40 x 10^{17} dm^{-3} min^{-1}, respectively [79]. The concentration of AIBN radicals generated in the aqueous phase is two orders of magnitude smaller than that in the monomer phase. This suggests that the formation of particle nuclei in the aqueous phase should be rather limited; i.e., heterogeneous nucleation presumably predominates [79].

Considering the limiting case in which AIBN radicals generated in the micelles predominate in the particle nucleation process, we have found that N_p obtained from the AIBN-initiated polymerization should be less than that obtained from the N_m [79]. So heterogeneous nucleation is observed when the fraction of N_p/N_m was equal or less than

1. The heterogeneous nucleation mechanism is therefore believed to be the predominant particle nucleation mechanism for the high molecular weight PMMA nanoparticle produce when AIBN is employed as an initiator.

3.3.6 Tacticity of PMMA latex nanoparticles

The tacticity of PMMA affects its performance, such as the diffusivity of other materials inside it [19] and its miscibility with other polymers [80]. The ^{1}H-NMR spectrum of PMMA latex nanoparticles is presented in Figure 3.7. The tacticity of the PMMA latex nanoparticles at different concentrations of SDS and different water/monomer ratios is given in Table 3.3.
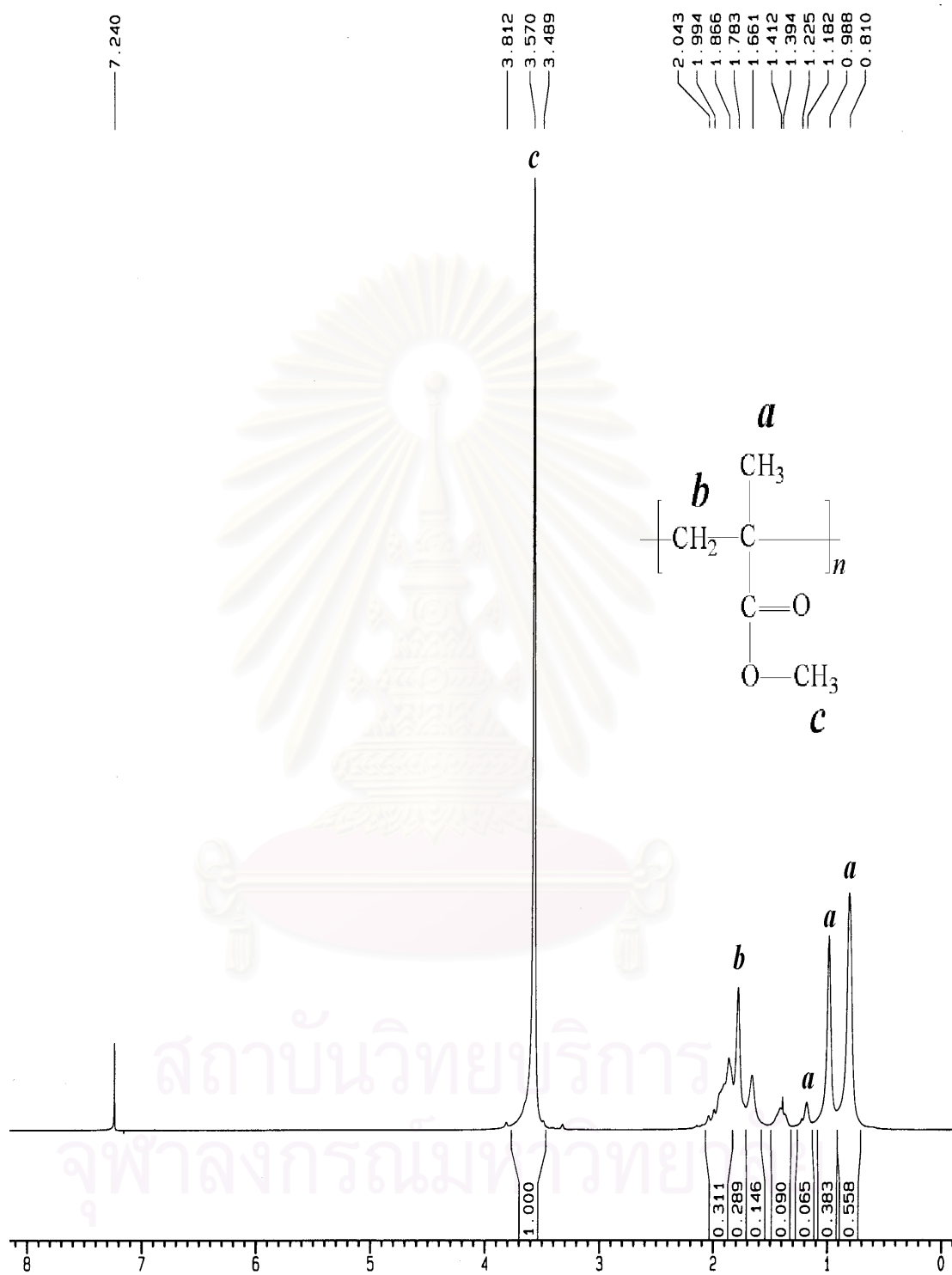
Figure 3.7 ^{1}H-NMR spectrum of PMMA latex nanoparticles (MMA 14 cm^3, SDS 0.7 g

and water 60 cm^3 polymerized at 70°C for 2.5 h.).

Table 3.3 Dependence of tacticity and glass transition temperature (Tg) of PMMA latex
nanoparticles on the concentrations of SDS, water and monomer at the reaction
time = 2.5 h. (*rr* = syndiotactic configuration, *mr* = atactic configuration,
and *mm* = isotactic configuration)

Water/MMA	[SDS] (mM)	M_w x 10^{-6}	M_n x 10^{-6}	% Tacticity			Tg (°C)
				rr	*mr*	*mm*	
60/14	4.91	2.28	1.17	56	38	6	123
60/14	5.78	3.75	1.86	57	37	6	120
60/14	17.34	2.69	1.57	54	39	7	119
60/14	40.45	1.02	6.95	55	38	6	124
60/14	80.91	1.15	7.64	56	37	7	123
84/14	3.51	2.41	1.37	55	39	7	122
84/14	4.13	3.02	1.80	54	39	8	122
84/14	12.38	2.73	1.62	53	39	7	121
84/14	28.89	1.19	7.43	56	38	7	124
84/14	57.79	1.12	0.73	53	39	8	125

The experimental results show that the tacticity of PMMA latex nanoparticles at
the triad level is almost independent of the concentrations of SDS and the
water/monomer ratio, which is advantageous for the high syndiotactic PMMA
preparation by the microemulsion polymerization as has been previously discussed [19,
44]. Possible reasons for the almost independent variation of tacticity with the
concentration of SDS and the water/monomer ratio used in the polymerizing mixture
were (1) that the primary locus of propagation was in the bulk of the particle and (2) that
the tacticity of the chain was not affected by the environment of the particle surface. As
with the differential microemulsion polymerization system previously reported, there are
no monomer droplets [5]. The reactions in the present work are believed to happen within
the micelles (heterogeneous nucleation) since an oil soluble initiator was used. At a
higher SDS concentration, there are more micelles which provide more nucleation sites in

the system. Otherwise, for the two systems with different MMA/water ratios, at a given SDS concentration, the micelle numbers are believed to be the same after the SDS concentration exceeds the CMC. Thus, according to the different MMA/water ratios in the two systems, each micelle needs to convert a slightly higher monomer amount in the system with a MMA/water = 14/60 v/v than in the system with a MMA/water = 14/84 v/v. Thus, at a given MMA/water ratio or SDS concentration, a higher SDS concentration or MMA/water ratio results in an almost constant percentage of tacticity.

The percentage of syndiotactic PMMA seems to be constant regardless of the SDS concentrations as shown in Table 3.3. A random coil of high molecular weight (1 x 10^6 g mol^{-1}) PMMA has an unperturbed root-mean-square end-to-end distance of 55 nm in the bulk [19, 44]. Therefore a few chains per particle of PMMA made by the differential microemulsion polymerization were toward the low end of the nanoscale (less than 40 nm) leading to the compact size required for more gauche conformations in the polymer chain to reduce its high potential energy in a small particle [19, 44]. Therefore, the PMMA formed in a differential microemulsion polymerization is conformationally restricted throughout the reaction.

Nevertheless, the differential microemulsion polymerization of MMA initiated by 2, 2'-azobisisobutyronitrile produces predominantly the syndiotactic PMMA containing 53-57% of syndiotactic (*rr*), 37-38% of heterotactic (*mr*), and 6-8% of isotactic (*mm*). The configuration of a PMMA chain in a microemulsion is more compact than its usual random coil conformation [19, 44]. Compared to isotactic PMMA, the syndiotactic PMMA has a net lower repulsive energy and allows the new in coming MMA molecules to easily interact with the growing polymer chains [54] since the syndiotactic

configuration of growing polymer chains has two methyl side groups being placed on different planes of the C-C backbone, which provide less of a steric hindrance effect. The low potential energy of any configuration of PMMA chains is an important property to stabilize the PMMA chains in the nanoparticle. The syndiotactic PMMA chain exhibits a lower total and intramolecular energy than the isotactic PMMA chain [54], so the syndiotactic configuration predominates over the isotactic configuration.

3.3.7 Conversion with polymerization time

The evolution of polymerization conversion (X_m), defined by Equations (3.1), with polymerization time is represented in Figure 3.8.
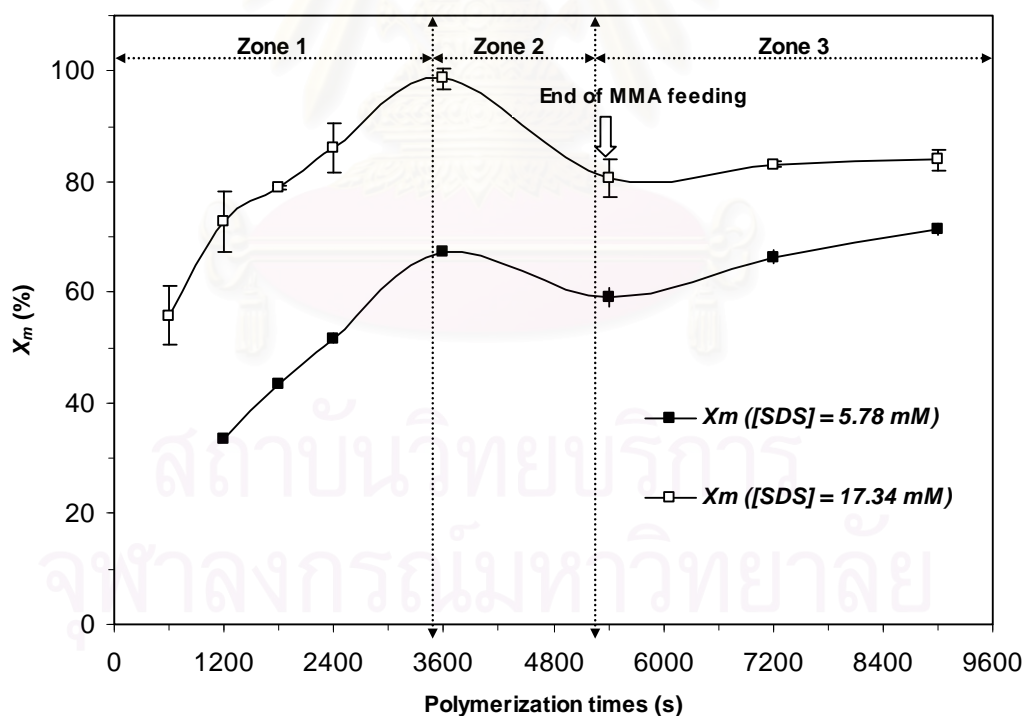
Figure 3.8 Relationship between the polymerization conversion, against with the

polymerization time of PMMA.

In the present study, an oil soluble initiator AIBN was used, which is sparsely dissolved in water. Because of the special operation procedures in the differential microemulsion polymerization, at the beginning of the polymerization the oil phase may not have a sufficient capacity for the AIBN initiator to be completely dissolved in the system and some AIBN flakes were thus observed. According to the observation, it was found that a period of 10 min was required to form an oil phase in which all of the AIBN flakes were completely dissolved. The results after 10 min of the reaction time are displayed in Figure 3.8.

According to Figure 3.8, the X_m – polymerization time curves can be distinguished into 3 zones: at polymerization times < 3600 s (denoted as Zone 1), 3600 - 5400 s (denoted as Zone 2) and > 5400 s (denoted as Zone 3). In Zone 1, the polymerization conversion rapidly increased up to a maximum value of 98.6 % for an SDS concentration of 17.3 mM, and 67.4 % for an SDS concentration of 5.78 mM at a polymerization time of 3600 s. In Zone 2, the conversion decreased to 80.7 % for an SDS concentration of 17.3 mM; and 59.10 % for an SDS concentration of 5.78 mM at the end of MMA feeding at a polymerization time of 5400 s. This trend is understandable because there are two factors which affect the polymerization conversion in an opposite manner. During the monomer addition period, on the one hand, with the addition of monomer the denominator in Equation (3.1) was increased, which decreased the calculated X_m; and on the other hand, at the same time, with the addition of the monomer, the particle population was increased and the particle size was also increased. More particles imply that the average number of radicals per particle was decreased, and the probability of the termination of the active polymer chains was decreased; thus the

polymerization conversion could be expected to increase [82]. In Zone 1, i.e. times up to 3600 s, the effect from generating more particles was possibly dominant, and the polymerization conversion increased with the addition of monomer, as shown in Figure 3.8. During Zone 2 (the period of 3600 – 5400 s), the particle population may not increase further, which could be caused by a balance between the particle population and micelle population. Thus most of the additionally added monomer molecules have to enter into the existing particles, which were larger than the newly nucleated particles, and the time needed for the monomer diffusion into the particles would decrease the polymerization conversion, as confirmed in Figure 3.8. Thus, the polymerization conversion decreased with the addition of monomer. In Zone 3, the addition of monomer had been stopped already and thus the denominator in equation (3.1) did not increase any further. However, the reaction was still going on; therefore, the polymerization conversion in Zone 3 increased.

3.3.8 Molecular weight and their PDI

The dependence of molecular weight and the PDI of the produced polymer with respect to reaction time at the two levels of SDS concentrations (5.78 and 17.34 mM) are presented in Figure 3.9.
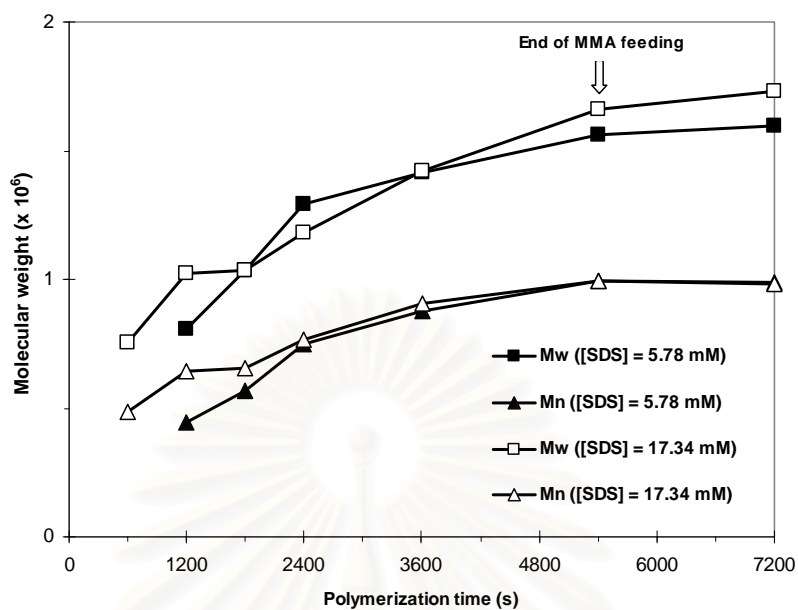
(a)
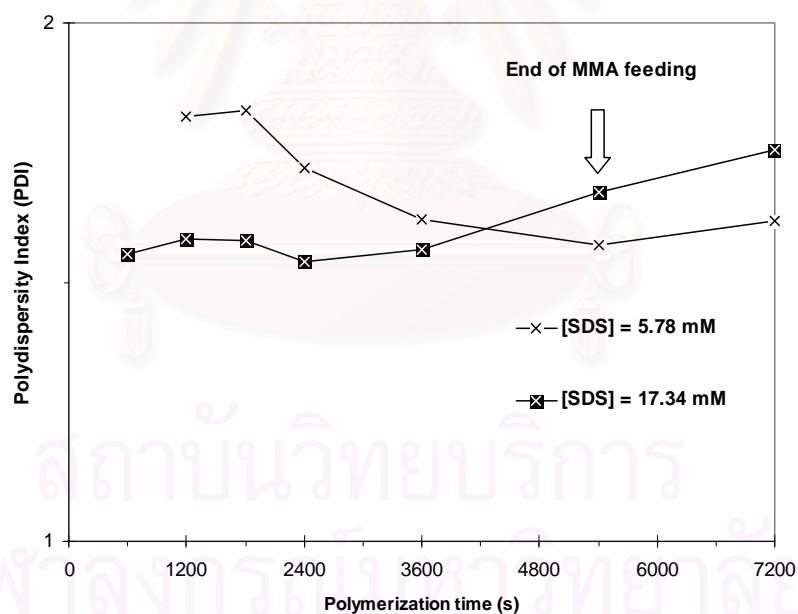
(b)

Figure 3.9 Relationship between the molecular weight and the polymerization time of

PMMA microemulsion measured by GPC-MALLS: (a) molecular weight,

(b) polydispersity index.

The molecular weights ($\overline{M}_w$ and $\overline{M}_n$ as shown in Figure 3.9a) obtained at both

levels of SDS concentration did not differ much during the early stages of polymerization

up until 7200 s (at which $\overline{M}_w$ changed from about 0.7 x 10^6 to 1.7 x 10^6 while $\overline{M}_n$

changed from about 4 x 10^5 to 9 x 10^5). Unlike the molecular weights, the PDI (shown in

Figure 3.9b) for both levels of SDS concentration are not much different (at [SDS] =

17.34 mM, PDI varied from about 1.55 to 1.75, while at [SDS] = 5.78 mM, it varied from

about 1.82 to 1.62). The nearly constant value of PDI over the whole range of

polymerization time could be attributed to the significance of particle nucleation

occurring via a heterogeneous nucleation mechanism, rather than that of a homogeneous

nucleation mechanism. The almost constant molecular weight during the polymerization

time from 3600 to 7200 s, which was possibly confined by the nano-sized particles, is an

advantage of the polymerization method investigated in this work.

3.3.9 Glass transition temperature of the resultant polymer

The glass transition temperature (Tg) of the resultant PMMA at different

concentrations of SDS and different water/monomer ratios is given in Table 3.3. The high

T_g results from the high molecular weight and the high percentage of syndiotactic

configuration [19, 71, and 81] produced by the differential microemulsion polymerization

technique. Soldera [81] found that the computed total intramolecular energy for isotactic

PMMA is higher than that of syndiotactic PMMA, but syndiotactic PMMA has higher

intermolecular energy. According to the free volume theory [57], high interactions

between the neighboring polymer chains will give a higher T_g. Therefore, the syndiotactic

dominant PMMA has a higher T_g value.

According to Table 3.4, the T_g of the synthesized PMMA is almost constant across the whole reaction period.

Table 3.4 Tacticity and glass transition temperature of PMMA latex nanoparticles with polymerization times at water/monomer ration = 60/14. (*rr* = syndiotactic configuration, *mr* = atactic configuration, and *mm* = isotactic configuration)

Polymerization	[SDS] = 5.78 mM				[SDS] = 17.34 mM			
Times (s)	% rr	% mr	% mm	Tg	% rr	% mr	% mm	Tg
600	-	-	-	-	56	38	6	112
1200	53	39	8	113	56	38	7	110
1800	56	38	6	112	56	38	6	113
2400	56	38	6	117	57	38	5	113
3600	55	39	6	118	57	37	6	111
5400	54	39	7	115	53	39	8	119
7200	56	38	7	114	56	38	6	117

The resultant PMMA nanoparticles so synthesized over a reaction time of 2.5 h as shown in Table 3.4, have a T_g range of 120 to 125ºC, which is significantly higher than the values of 105 to 107ºC generally reported [83] for the general polymerization to produce PMMA.

3.4 Summary

When differential microemulsion polymerization of MMA using AIBN, an oil soluble initiator, is employed, PMMA particles can be controllably synthesized with respect to their nanosize and molecular weight as well as polymer chain number in the particles. To produce nano PMMA particles of less than 20 nm, the reaction conditions can be much milder when using the differential microemulsion polymerization than when using the conventional emulsion or microemulsion polymerization methods. The

differential microemulsion polymerization technique was employed for synthesizing nano-sized particles of PMMA having high molecular weight of 10^6 g mol^{-1} using the AIBN oil soluble initiator. The high molecular weight PMMA latex nanoparticles have a rich syndiotactic configuration (53-57 % *rr* triads). The rate of polymerization increased with an increase in the concentration of the SDS surfactant. The maximum conversion of polymerization was observed at a polymerization time of 3600 s. The nearly constant value of PDI over the whole range of polymerization time could be attributed to the significance of particle nucleation occurring via a heterogeneous nucleation mechanism. The high molecular weight PMMA nanoparticles have spherical shape with a T_g of about 125ºC. It is very interesting to note that the polymerization conversion reaches a maximum, within a short reaction time in the presence of less surfactant and without the need of a co-surfactant and with a high monomer-to-water ratio. Thus, AIBN an oil soluble initiator is another effective initiator to polymerize PMMA latex nanoparticles via differential microemulsion polymerization.

CHAPTER 4

SYNTHESIS OF CORE/SHELL STRUCTURE OF GLYCIDYL-FUNCTIONALIZED POLY(METHYL METHACRYLATE) LATEX NANOPARTICLES VIA A TWO-STEP DIFFERENTIAL MICROEMULSION POLYMERIZATION PROCESS

4.1 Introduction

Differential microemulsion polymerization was proposed to be a possible an effective method to prepare the core/shell structure of glycidyl-functionalized PMMA latex nanoparticles having a high density of glycidyl functional groups on the surface. AIBN, an oil soluble initiator, is a selected initiator for the synthesis of the core/shell nanostructure as have been reviewed in Chapter 2.

In the previous chapter, high molecular weight syndiotactic PMMA latex nanoparticles were obtained via polymerization of MMA monomer using the differential microemulsion polymerization method with AIBN, an oil soluble initiator. Thus, the preparation of a core/shell structure of glycidyl-functionalized PMMA latex nanoparticles will be studied by the differential microemulsion polymerization via a two-step process using AIBN an oil soluble initiator.

This chapter reports on a synthesis of glycidyl-functionalized PMMA latex nanoparticles using differential microemulsion polymerization via a two-step process [6-7]. The effects of the surfactant concentration, the water content, and the percentage weight of the GMA comonomer on particle size and distribution, percentage of solid

content, glass transition temperature, copolymer composition, the percentage weight of GMA in the copolymer, glycidyl functional group on the particle surface, average-molecular weights and polydispersity index, and morphology of the glycidyl-functionalized latex nanoparticles were also investigated.

4.2 **Experimental**

4.2.1 **Materials**

Methyl methacrylate (MMA) with 10 ppm of an inhibitor (AR grade from Aldrich), glycidyl methacrylate (GMA) with 100 ppm hydroquinone monomethyl ether (97% purum grade from Aldrich), sodium dodecyl sulfate (SDS) powder (97% purity from Aldrich), azo-bis-isobutyronitrile (AIBN) (AR grade from Polysciences), methanol (practical grade), cyclohexane (AR grade from Aldrich), and tetrahydrofuran (THF) (HPLC grade from Aldrich) were used as received. De-ionized (DI) water was used as obtained from the Department of Chemical Engineering at the University of Waterloo, Ontario, Canada.

4.2.2 Preparation of glycidyl-functionalized PMMA latex nanoparticles

Glycidyl-functionalized PMMA latex nanoparticles were prepared using differential microemulsion polymerization via a two-step process and the recipes are given in Table 4.1.

Table 4.1 Polymerization Recipe.

Water (cm^3)	MMA (cm^3)	GMA (wt%)	AIBN (g)	SDS (mM)
60	14	2-8	0.08	4.9-80.9
84	14	2-8	0.08	3.5-57.8

The initiator and surfactant were mixed in a certain amount of water in a 500 cm^3 Pyrex glass reactor (Aldrich, Canada), which was equipped with a double-jacket condenser and a dropping funnel for monomer feeding. Then the system was subjected to heating at 70ºC under constant agitation (200 rpm) of a magnetic stirring bar on a stirrer/temperature hotplate incorporated with a digitally controlled temperature measuring device and constant nitrogen gas feed through a gas inlet tube. The monomer was fed very slowly by a drop-wise addition after the temperature of the system had reached 70ºC. The MMA monomer feed time was about 1.5 h. Then, the GMA comonomer was fed into the system in a similar manner for about 0.5 h after the MMA feeding was finished. When the MMA monomer and GMA comonomer feedings were completed, the reaction system was kept at the polymerization temperature (70°C) with constant agitation (200 rpm) for another 1 h in order to obtain a higher conversion of the glycidyl-functionalized PMMA latex nanoparticles.

4.2.3 Separation of glycidyl-functionalized PMMA for characterization

The resultant glycidyl-functionalized PMMA was precipitated in an excess amount of methanol before it was separated by a vacuum-filtration technique. The surfactant and initiator were washed with 250 cm^3 of warm DI water and 150 cm^3 of

methanol each time for about 10 times. The glycidyl-functionalized PMMA was then dried at ambient temperature in a fume hood for 24 h. The unreacted monomer was removed using a cold extraction method by adding 20 cm^3 of cyclohexane into the dried polymer (about 5 g) and the mixture was kept at 37-40ºC in a temperature controlled water bath for 24 h. The copolymer was then separated using a vacuum filtration system. The copolymer, after the extraction, was left at ambient temperature in the fume hood for 24 h to evaporate any absorbed cyclohexane (cyclohexane has a vapor pressure of 95 mm Hg at 20ºC) and the residual cyclohexane was further removed in an oven at 100ºC for 24 h.

4.2.4 Characterization of the glycidyl-functionalized PMMA latex nanoparticles

4.2.4.1 Molecular structure of the glycidyl-functionalized PMMA

The polymer composition of the glycidyl-functionalized PMMA was analyzed by ^{1}H-NMR spectroscopy on a Brucker 400 MHz spectrometer at room temperature using $CDCl_3$ as a solvent.

4.2.4.2 Particle size and particle size distribution

After the polymerization was completed, the number-average diameter (D_n) and the particle size distribution of the glycidyl-functionalized PMMA latex nanoparticles were measured by dynamic light scattering technique on a Nanotrac®150 (Microtrac, Montgomeryville, USA).

4.2.4.3 Percentage solid content

The resultant percentage solid content at the end of polymerization time was investigated by a gravimetric method as shown in Equations (4.1).

$$\%\text{Solid} = \frac{W_1}{W_2} \times 100\% \qquad\qquad (4.1)$$

where W_1 and W_2 are the weights of the dried polymer and the latex polymer, respectively.

4.2.4.4 Average molecular weight averages and polydispersity index

The purified glycidyl-functionalized PMMA was dissolved in THF. Average-molecular weights and the polydispersity index (PDI) were determined by gel permeation chromatography, multi-angled laser light scattering (GPC-MALLS) by injecting 50 μL of 0.05-0.11 %w/v of each copolymer solution (THF solvent, 25°C, flow rate 1 cm^3 min^{-1}) into a GPC-MALLS set up (Wyatt Technology Corporation, California, U.S.A.) equipped with an RI detector (Water 150-CV refractive index detector) and an MALLS detector (DAWN®DSP-F laser photomer). A column set was employed consisting of three 300 x 8 mm columns filled with a PL gel with an average particle size of 10 μm.

4.2.4.5 wt% of GMA in the copolymer analysis

The determination of the glycidyl functional group content on the particle surface was based on the method involving a reaction between the oxirane ring and sodium thiosulfate [8]. The reaction is shown as follows in Equation 4.2:

$$R - \overset{\overset{H}{|}}{\underset{\underset{O}{\diagdown \diagup}}{C}} CH_2 + 2Na^+ + S_2O_3^{2-} \xrightarrow{H_2O} R - \overset{\overset{H}{|}}{\underset{\underset{OH}{|}}{C}} - \overset{\overset{H_2}{|}}{C} - S_2O_3^- + 2Na^+ + OH^-$$

$$(4.2)$$
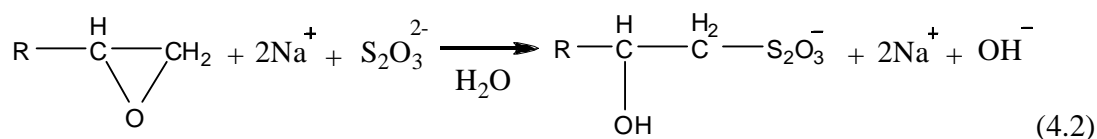
The oxirane ring was opened and converted to $RCH(OH)-CH_2-S_2O_3^-$, the release of OH^- group was followed by titration with 0.01 N HCl solution using a pH-meter. To carry out this reaction, the polymer particles (0.4 g) were mixed with 20 cm^3 of methanol (analytical grade, Merck) and 40 cm^3 of 0.1 M sodium thiosulfate ($Na_2S_2O_3$) aqueous solution (volumetric solution of Ajax Finechem) and they were continuously stirred with a magnetic stirrer bar in a controlled speed stirrer/hotplate at 200 rpm for 30 min. The released OH^- group was titrated with 0.01 N HCl solution (volumetric solution of Ajax Finechem) followed using a pH-meter (Precisa pH 900). The amount of glycidyl functional groups was calculated from the amount of hydrochloric acid needed in order to maintain neutrality. One mole of the OH^- group produced corresponds to one mole of the epoxy groups converted.

4.2.4.6 Percentage weight of GMA in the glycidyl-functionalized PMMA analysis by ^{1}H-NMR

^{1}H-NMR spectroscopy was used to determine the composition of the polymer. The assignment of the resonance peaks in the ^{1}H-NMR spectra leads to an accurate evaluation of the content of each kind of monomeric units incorporated into the polymer chains [9, 65]. Thus, the composition analysis of glycidyl methacrylate functional monomer in the glycidyl-functionalized PMMA were calculated by measuring the integrated peak areas of the three resonances of epoxide protons of the GMA unit and

methoxyl protons of the MMA monomer unit. The following expression shown in Equation (4.3) is used to determine the composition of copolymer. The ratio between the integrated peak areas of the three resonances of the GMA divided by the integrated peak areas of methoxyl protons of the MMA was defined by "A". With m_1 being the mole fraction of GMA and $1 - m_1$ that of the MMA monomer. The proton resonances of the methoxyl group in MMA at 3.570 ppm and those of the epoxide group in GMA at about 3.209, 2.822 and 2.615 ppm are clearly resolved. The GMA contains 3 epoxide protons and the MMA also contains 3 methoxyl protons as shown in Figure 4.1 and the calculations are given in Equations (4.3-4.6):

$$A = \frac{\text{Integrated peak area at 2.615-3.209 ppm}}{\text{Integrated peak area at 3.570 ppm}} \quad (4.3)$$

$$A = \frac{3m_1}{3(1-m_1)} \quad (4.4)$$

On simplification, this gives:

$$m = \frac{A}{1+A} \quad (4.5)$$

$$\%\text{wt of GMA} = \frac{m \times \text{molecular weight of GMA}}{(m \times \text{molecular weight of GMA}) + [(1-m) \times \text{molecular weight of MMA}]} \quad (4.6)$$

Therefore, the wt% of GMA in the resultant glycidyl-functionalized PMMA can be determined from Equation (4.6).

4.2.4.7 Glass transition temperature (T_g) measurement

T_g values of the glycidyl-functionalized PMMA were measured using a

NETZSCH DSC-204 F1 differential scanning calorimeter with 10 mg samples at a scan rate of 10ºC min^{-1} from 25 to 180ºC, followed by rapid cooling and heating again at the same rate. Mercury (mp = 38.8ºC), bi-benzene compound (mp = 69.2ºC), indium (mp = 156.6ºC), tin (mp = 231.9ºC), bismuth (mp = 271.4ºC) were used to calibrate the instrument. The T_g from the second heating was reported since the T_g from the first measurement may not have yet reached the thermal equilibrium state. T_g is analyzed by the midpoint method.

4.2.4.8 Morphology

Morphology of the glycidyl-functionalized PMMA latex nanoparticles was investigated by transmission electron microscopy (TEM). TEM micrographs of unstained nanoparticles were obtained with a high resolution transmission electron microscope (Philips CM20 Super Twin) operating at 100 kV. TEM micrographs of the stained nanoparticles were obtained with a transmission electron microscope (JEOL JEM-2100, Tokyo, Japan) operating at 80 kV. The latex of core/shell particles was diluted with DI water to about 0.1-0.5 wt% of the solid content before it was deposited on a TEM copper grid and stained with ruthenium tetroxide vapor from its 0.5% aqueous solution (EM grade from Electron Microscopy Science, USA).

Morphology of the glycidyl-functionalized PMMA was investigated using scanning electron microscopy (SEM). The polymer specimen was sputter coated with gold for about 3 min in a Cathodic Pulverizer Balzers SCD040 sputtering system (Balzers AG, Liechtenstein) before examination with the SEM (JEOL JSM-5410LV) at an accelerating voltage of 15 kV.

4.3 Results and Discussion

4.3.1 Molecular structure analysis of the glycidyl-functionalized PMMA

The 1H-NMR spectrum of the glycidyl-functionalized PMMA is shown in Figure 4.1. Based on the discussion of Chen and Lee [8], each pair of GMA-MMA carrying a dangling oxirane group was assumed. From Figure 4.1 found the following chemical shifts;

a: doublet at 0.809 and 0.988 ppm characterizing the CH_3 protons.

b: peaks at 1.784 and 1.866 ppm of the methylene protons of the polymer chain.

c, d, e: three peaks at 2.615, 2.822 and 3.209 ppm evidencing the epoxy-ring protons.

f, g: set of peaks between 3.653-3.810 ppm and 4.290 ppm characterizing CH_2

　　proton next to the ester functional group.

h: peak at about 3.5-3.7 ppm characterizing the $-OCH_3$ protons of MMA.
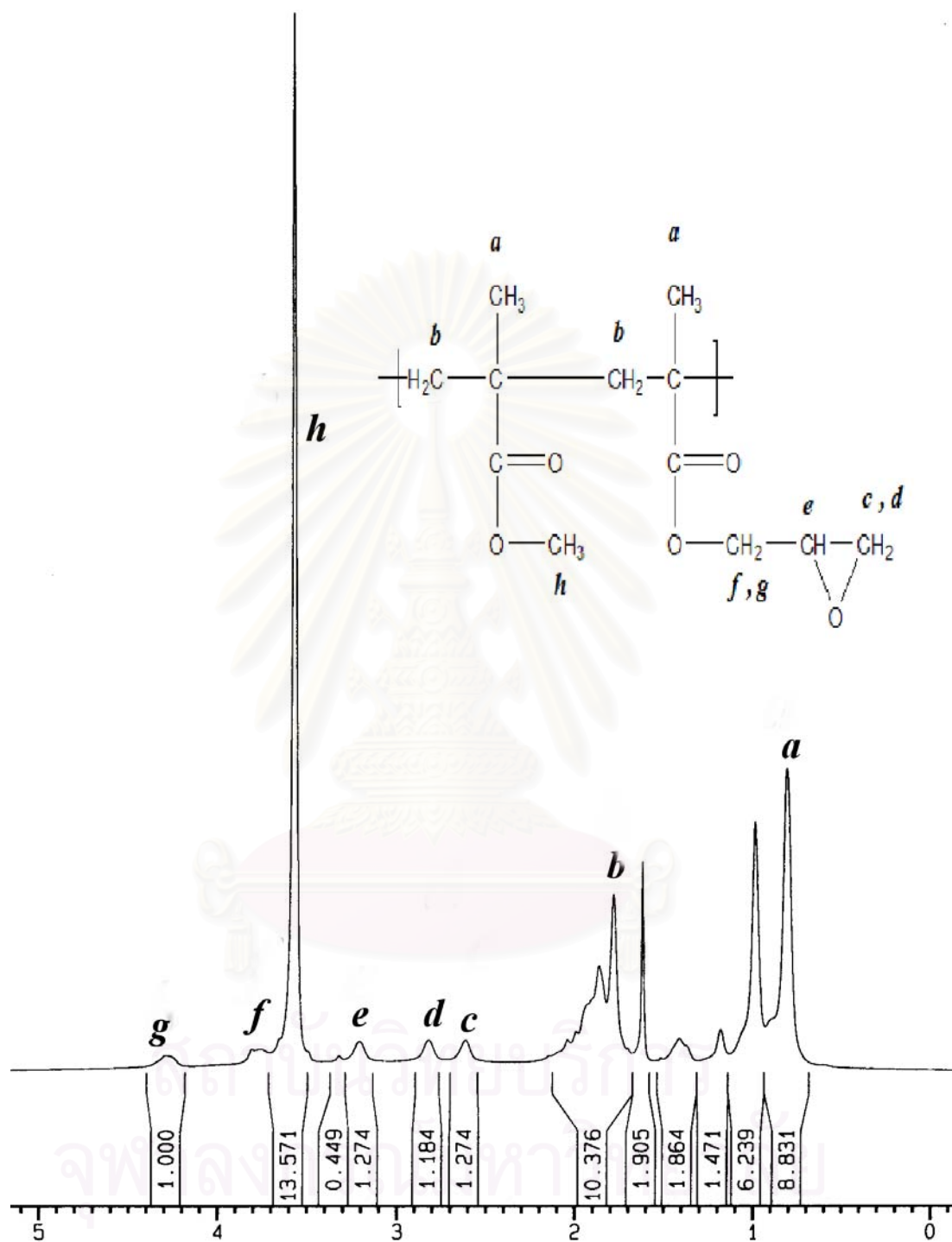
Figure 4.1 ^{1}H-NMR spectrum of glycidyl-functionalized PMMA (MMA 14 cm^3, GMA
39 wt%, AIBN 0.08 g, SDS 5.78 mM, and DI water 60 g and the
polymerization temperature at 70ºC.

The ^{1}H-NMR spectrum (Figure 4.1) shows the presence of methoxy protons (h) and of oxiranyl protons (c, d, and e). The ^{1}H-NMR spectrum exhibits two α-methyl peaks at about 0.8 and 1.0 ppm. For the corresponding homopolymers of poly(methyl methacrylate) and poly(glycidyl methacrylate), these peaks are located at different positions, and have been reported previously [9, 65]. In the case of random copolymers, these two peaks are not well separated and still have almost the same signals with the homopolymers of poly(methyl methacrylate) [9, 65]. The α-methyl peaks of the nano-seed PMMA nanoparticles found in the glycidyl-functionalized PMMA are not well separated from the α-methyl peaks of the random copolymer formed on their surface. It can be thus concluded that the random copolymers formed on the surface of nano-seed PMMA nanoparticles do not contain homopolymeric blocks of any length. This conclusion is in favor of random placement of the monomer units along the chain [8-9, and 65]. The ^{1}H-NMR spectrum (Figure 4.1) of the copolymer also exhibits only two α-methyl proton absorption peaks at 0.809 and 0.988 ppm, confirming the above statement. The synthesis of random copolymers at the surface of nano-seed PMMA nanoparticles in which the two monomer units are randomly distributed along the polymer chain is thus possible. The formation of glycidyl-functionalized PMMA latex nanoparticles using PMMA as the nano-seed eliminating from MMA first polymerizes to form nanosized particles. These PMMA nanoparticles are the nuclei for GMA to copolymerize with the unreacted MMA on them so that the core/shell structured latex nanoparticles will be observed as shown in the TEM micrograph. As mentioned above, the reactivity ratios of GMA and MMA are 1.28 and 0.75 [85], respectively, therefore, the product of r_{MMA} and r_{GMA} equals 0.96, an indication of a random copolymer. Therefore, the glycidyl-

functionalized PMMA latex nanoparticle is believed to be composed of a nano-seed of PMMA nanoparticle and the poly[(methyl methacrylate)-*ran*-(glycidyl methacrylate)] random as a shell layer on the surface of the PMMA nano-seed.

4.3.2 Particle size (Dn) of glycidyl-functionalized PMMA latex nanoparticles

Figures 4.2 and 4.3 show the effects of SDS concentration at the two levels of water content and three levels of percentage weight of GMA comonomer added on particle size of the resultant glycidyl-functionalized PMMA latex nanoparticles, respectively.
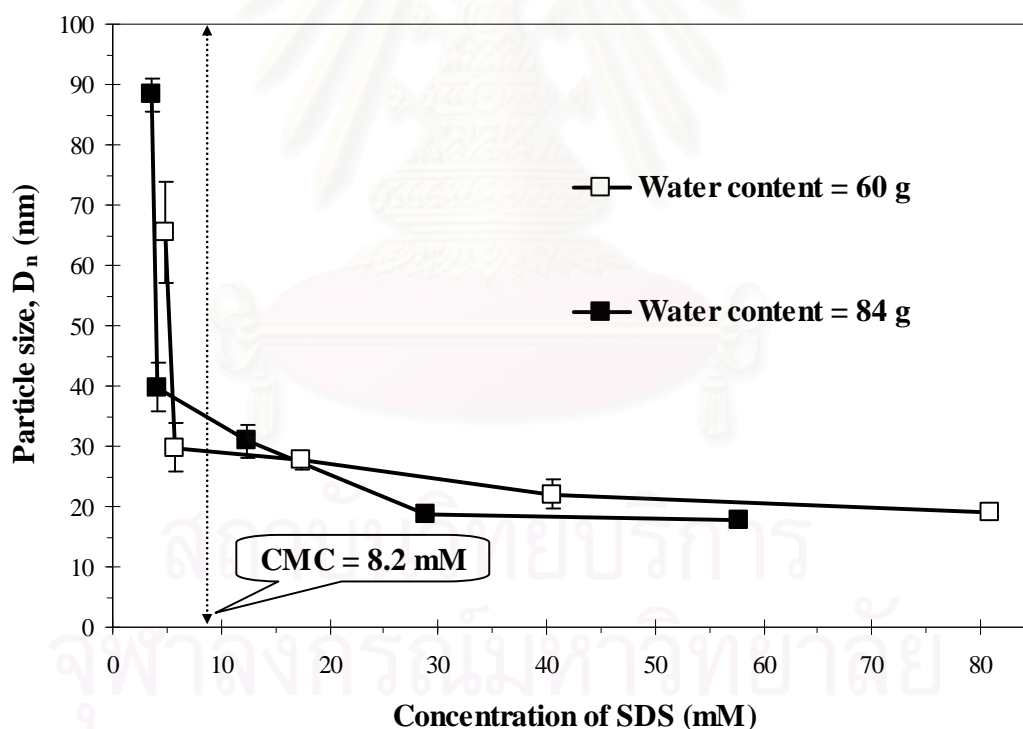
Figure 4.2 Effect of SDS concentrations on the particle size at various water contents

The results in Figure 4.2 demonstrate that the change in size of the glycidyl-functionalized PMMA latex nanoparticles with respect to the SDS concentration. The

largest particle size of the glycidyl-functionalized PMMA latex nanoparticles at 88 nm was obtained when SDS concentration was 3.85 mM. The smallest particle size of the glycidyl-functionalized PMMA latex nanoparticles at 18 nm was obtained when the SDS concentration was 57.79 mM. The polymerization system investigated in the present work gave much smaller particle size. Through the differential microemulsion technique, it is more economical and easier to control the particle size. It is thus justified to state that the differential microemulsion polymerization via a two-step process is a most promising method for synthesizing the glycidyl-functionalized PMMA latex nanoparticles using an extremely low amount of the surfactant. A large particle size of the glycidyl-functionalized PMMA latex nanoparticles at the low concentration of SDS can be explained as follows. The low concentrations of SDS provide fewer loci [16] for GMA to polymerize, so that the amount of GMA in the region of each seed is increased and the particles formed are larger. Figure 4.2 also demonstrates that the water content does not have a significant effect on the particle size of the glycidyl-functionalized PMMA latex nanoparticles because the nucleation most likely occurred within micelles of PMMA nano-seed rather than in the water phase, and thus the water content may not significantly affect the conditions inside micelles where the surfactant concentration does not have a significant effect on particle size, i.e., the surfactant amount is sufficient to stabilize the particles.
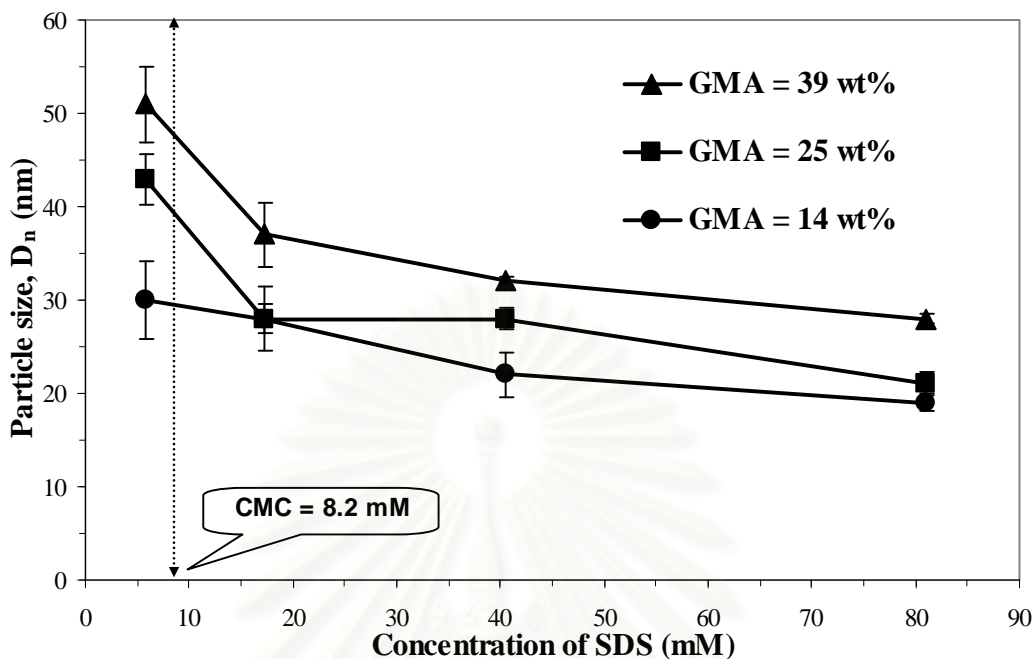
Figure 4.3 Effects of SDS concentration on particle size at various wt% of GMA added

The results in Figure 4.3 demonstrate the changes in size of the glycidyl-functionalized PMMA latex nanoparticles with respect to the percentage weight of GMA comonomer added. The largest particle size of core/shell latex nanoparticles at 51 nm was obtained when the percentage weight of GMA comonomer added was high (about 39 wt%) and SDS concentration was about 5.78 mM. The smallest particle size of the core/shell nanoparticles at 19 nm was obtained when the percentage by weight of GMA comonomer added was about 14 wt% and the concentration of SDS was about 80.91 mM. The increase in the percentage weight of GMA added can increase the percentages by weight of GMA to polymerize on each PMMA nano-seed. So a large size of the glycidyl-functionalized PMMA latex nanoparticle is obtained.

4.3.3 The percentage of solid content

Figures 4.4 and 4.5 show the effect of SDS concentration at the two levels of water content and three levels of percentage by weight of the GMA comonomer added on the percent solids content of the glycidyl-functionalized PMMA, respectively.
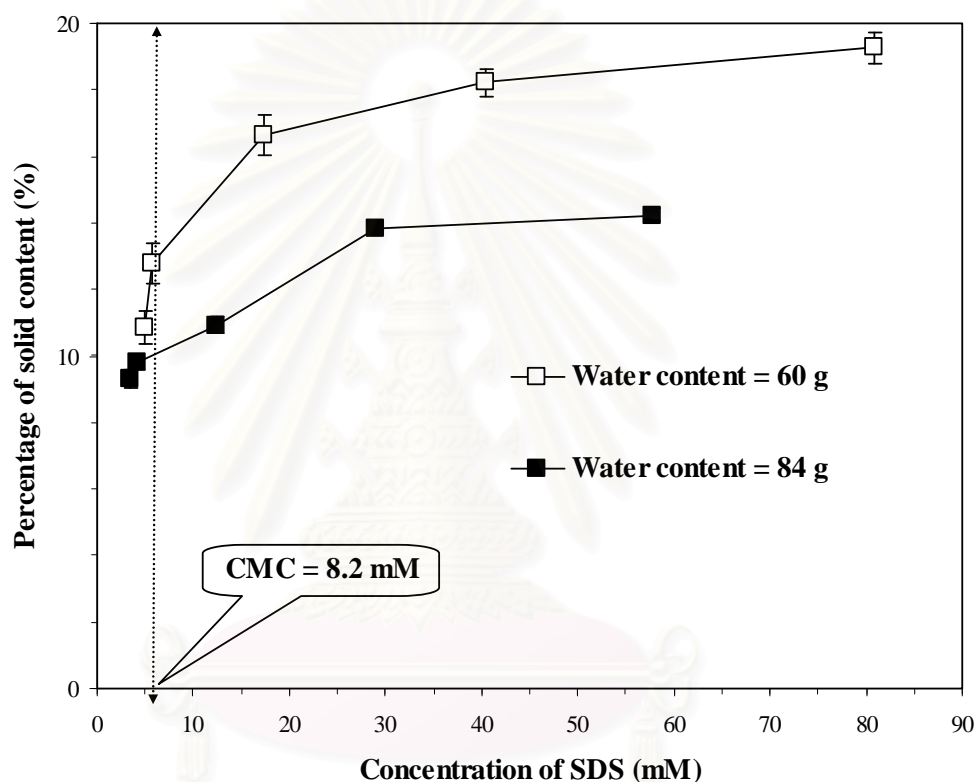
Figure 4.4 The effects of SDS concentration on percentage of solid content at various water contents.

It is seen from Figure 4.4 that with an increase in the SDS concentration, the percentage solid content was increased. In addition, with a decrease in the water content, the percentage solid content was significantly increased. The reactions in the present work are believed to happen in the PMMA nano-seed micelles. At a higher SDS concentration, there are more PMMA nano-seed micelles which provide more nuclei for

GMA to copolymerize. Thus, at a given water content, a higher SDS concentration results in a higher conversion. For the two systems with different water contents, at a given SDS concentration, the PMMA nano-seed numbers are believed to be the same after the SDS concentration exceeds the CMC as has been discussed in the previous chapter. Thus, according to the different water content in the two systems, each PMMA nano-seed needed to convert a slightly higher monomer amount in the system with 60 g water than in the system with 84 g water. However, a slightly different AIBN concentration in these two systems may offset the difference in the water content, which may be the reason that there is no significant difference in the percentage solid content (about 4 %) between the two systems. According to such an analysis, it may be deduced that the glycidyl-functionalized PMMA produced from the system with water of 60 g would have a higher molecular weight than the system with water of 84 g, which shall be indeed confirmed in the next section.
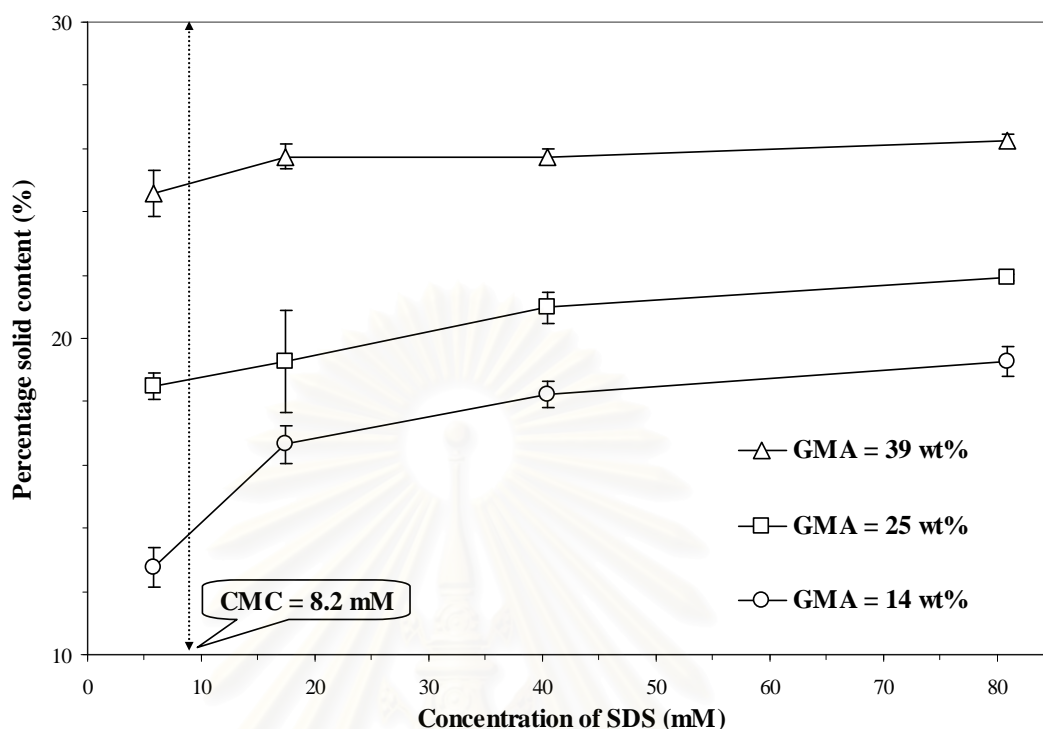
Figure 4.5 The effects of SDS concentration on the percentage solid content at various

   percentage weights of GMA monomer added.

The results in Figure 4.5 demonstrate the changes in the percentage solid content

of the glycidyl-functionalized PMMA latex nanoparticles with respect to the percentage

by weight of GMA comonomer added, i.e., the higher the GMA content, the larger the

percentage solid content which is similarly shown in the case of particle size (Dn) of

core/shell latex nanoparticles. The resultant core/shell latex nanoparticles can be

produced by an extremely low ratio of the surfactant to monomer of 1/217 and the

surfactant/water ratio as low as 1/600 when the larger particle size of about 50 nm is

acceptable. As shown in Figure 4.5, the core/shell latex nanoparticles gave a solid content

as high as 24.60% when [SDS] is 5.78 mM.

4.3.4 Average molecular weights ($\overline{M}_w$ and $\overline{M}_n$), and its polydispersity index (PDI)

The effects of SDS concentration at the two levels of the water content, and percentage weight of the added GMA comonomer on average molecular weights $(\overline{M}_w$ and $\overline{M}_n)$, and its polydispersity index (PDI) of the glycidyl-functionalized PMMA investigated are shown in Figures 4.6 and 4.7, respectively.
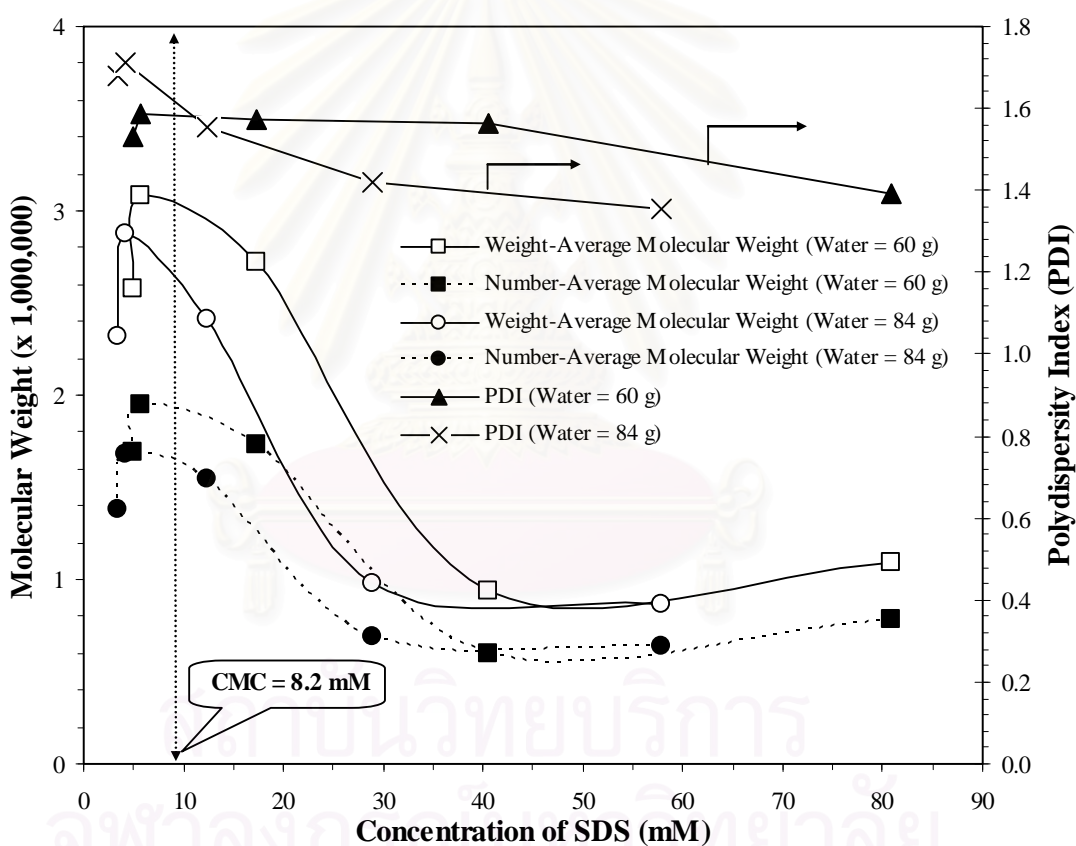
Figure 4.6 The effects of SDS concentration on molecular weight ($\overline{M}_w$ and $\overline{M}_n$) and polydispersity index (PDI) at various water contents.

Figure 4.6 indicates an interesting dependence of molecular weight on the SDS concentration. For all molecular weight curves in Figure 4.6 with an increase in the SDS concentration, the molecular weight was initially increased over a small SDS concentration range, and it was then relatively constant over a certain range of SDS concentrations. Beyond the CMC point, the molecular weights decreased steadily, and finally were maintained at another relatively constant level of about 10^6 (slightly over 10^6 for $\overline{M}_w$ and slightly below 10^6 for $\overline{M}_n$). Therefore, when increasing the SDS concentration, the molecular weight distribution changed at a constant water content and the higher SDS concentration gave the smaller PDI. The highest molecular weight and the broader polydispersity index (1.59) were obtained at a SDS concentration around the CMC (8.2 mM) of SDS. The lowest molecular weight and the narrowest polydispersity index (1.35) were accomplished at a SDS concentration far beyond the CMC. This suggests that by adjusting the SDS concentration, the molecular weights of the glycidyl-functionalized PMMA can be well controlled. It is also noted that the dependence of molecular weight of glycidyl-functionalized PMMA (Figure 4.6) on the SDS concentration has a similar trend as that for the dependence of particle size of glycidyl-functionalized PMMA latex nanoparticles on the SDS concentration (Figure 4.2) when SDS concentration was far beyond the CMC.
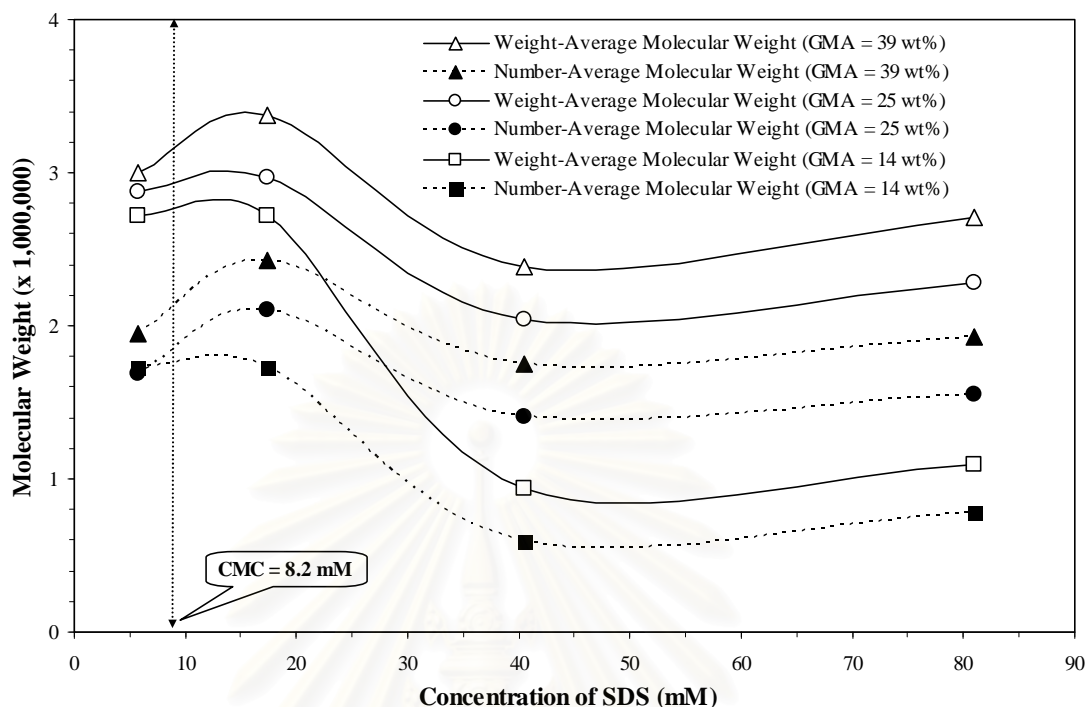
Figure 4.7 The effects of SDS concentration on molecular weight ($\overline{M}_w$ and $\overline{M}_n$) at

various GMA concentrations.

Figure 4.7 indicates the dependence of molecular weight on the percentage weight

of the GMA comonomer added. The highest molecular weights of over $3x10^6$ for $\overline{M}_w$

and over $2x10^6$ for $\overline{M}_n$ were obtained when the SDS concentration was 17.34 mM and

the added GMA comonomer was 39 wt%. As predicted in the previous section and as

shown in Figure 4.5, the molecular weights of the glycidyl-functionalized PMMA with a

higher percentage weight of the GMA comonomer added were higher than those when

the lower concentrations of the comonomer were added. This indicates that by using this

differential microemulsion polymerization method via a two-step process, the glycidyl-

functionalized PMMA latex nanoparticles so obtained are probably composed of the high

molecular weight PMMA as a nano-seed and equivalently high molecular weights of

random copolymer formed on the surface of nano-seed. However, this postulated nanostructure of core/shell latex nanoparticles needs to be confirmed via the glass transition temperature (T_g) results by DSC measurement and the morphology study carried out by TEM.

4.3.5 Morphology and glass transition temperature (T_g)

Figure 4.8 shows the TEM micrographs of the glycidyl-functionalized PMMA latex nanoparticles.

(a)

(b)

(c)

(d)
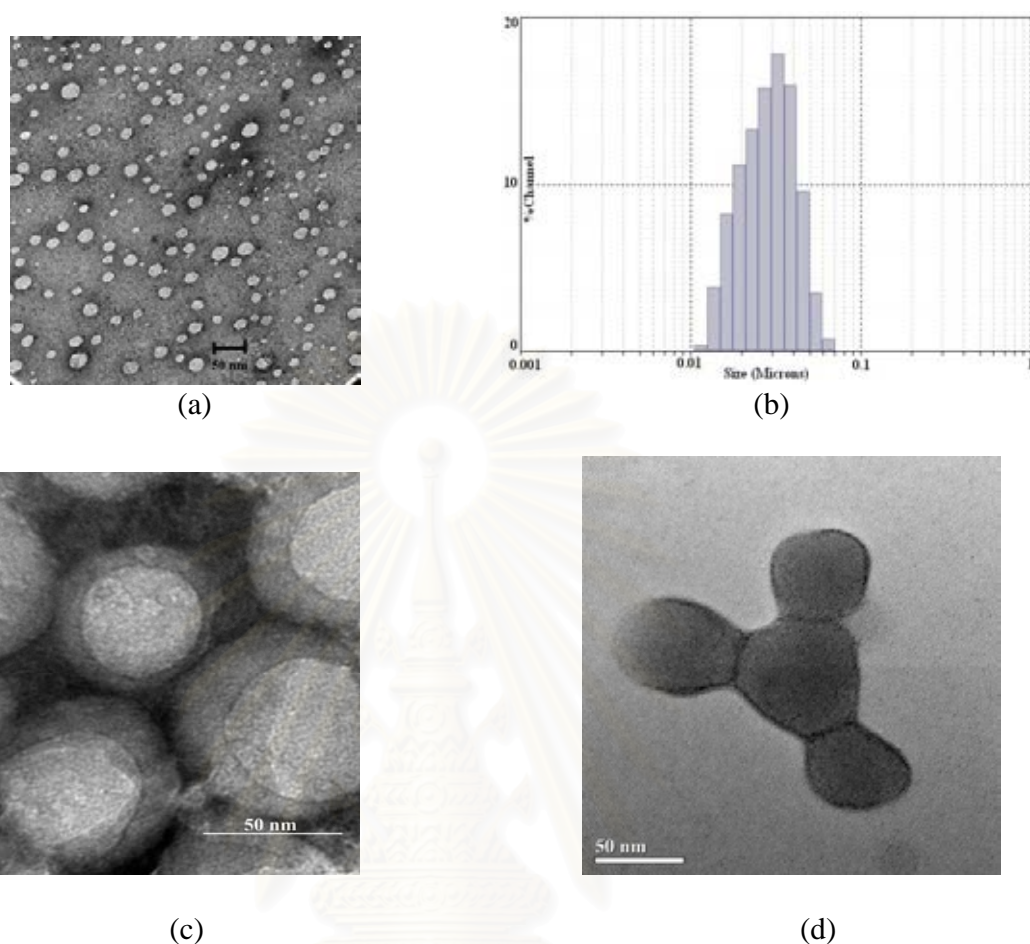
Figure 4.8 TEM Micrographs and size distribution histogram of glycidyl-functionalized PMMA latex nanoparticles: (a) micrograph of the unstained TEM glycidyl-functionalized PMMA nanoparticles (MMA 14 cm^3, GMA 14 wt%, in the presence of AIBN 0.08 g, SDS 40.45 mM, and DI water 60 g was copolymerized at 70°C); (b) the size histogram of the glycidyl-functionalized PMMA latex nanoparticles. (MMA 14 cm^3, GMA 39 wt%, in the presence of SDS 40.45 mM and water 60 g was copolymerized at 70°C); (c and d) micrographs of the stained TEM glycidyl-functionalized PMMA nanoparticles (MMA 14 cm^3, GMA 39 wt%, in the presence of AIBN 0.08 g, SDS 5.78 mM, and DI water 60 g was copolymerized at 70°C).

It is seen that the particles are spherical in shape, as shown in Figure 4.8(a). Figure 4.8(b) shows the size histogram of the glycidyl-functionalized PMMA latex nanoparticles. The glycidyl-functionalized random copolymer, part of the glycidyl-functionalized PMMA nanoparticles in Figure 4.8(c) and Figure 4.8(d) were detected by vapor staining with ruthenium tetroxide since the glycidyl functional group on GMA could interact with the ruthenium tetroxide much more easily than the methacrylate group on PMMA. The glycidyl-functionalized random copolymer section is observed as a dark circle encompassing the PMMA nano-seed, as shown in Figures 4.8(c) and Figure 4.8(d). Figure 4.8(d) shows a TEM micrograph of a sample in which surfactant and water was absorbed from the latex before staining followed by staining with RuO4. In this case (Figure 4.8(d)), some coalescence of the particles was observed, however, the glycidyl functionalization in the the shell is still clearly observed. The white areas on the stained particles in Figure 4.8(c) are the unstained PMMA covered by the surfactant. Figures 4.8(c) and Figure 4.8(d) indicate that the core/shell structure was possibly developed from the differential microemulsion polymerization via a two-step process. In addition, the high peak of the histogram which appears in Figure 4.8(b) possibly belongs to the aggregate form of the glycidyl-functionalized PMMA latex nanoparticles.

Moreover, the T_g measurement of the glycidyl-functionalized PMMA indicates the two T_g regions at about 90ºC and 125ºC as shown in Figure 4.9
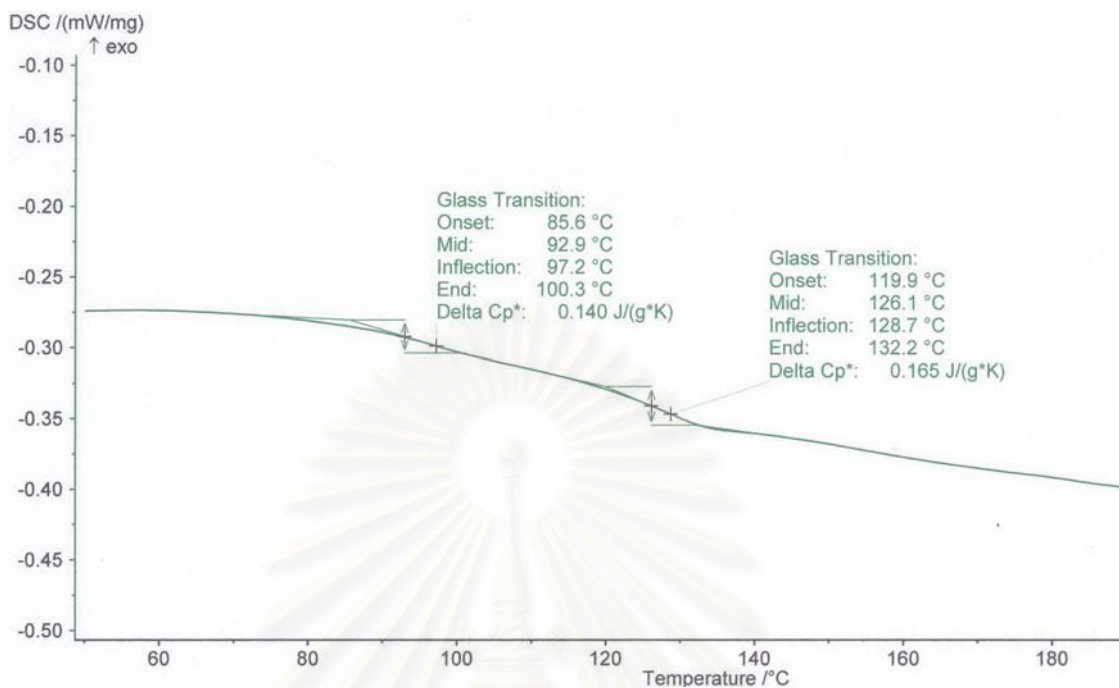
Figure 4.9 Thermogram of core/shell latex nanoparticle. (The core/shell was synthesized

by using MMA 14 cm^3, GMA 4 cm^3, in the presence of SDS 0.3 g, AIBN

0.08 g, and water 60 cm^3 was polymerized with the differential microemulsion

copolymerization).

The first T_g region at 90°C is assigned to the random copolymer between MMA

monomer and GMA comonomer. The second T_g region at 125°C is assigned to the high

molecular weight PMMA as the core particle. Poly(glycidyl methacrylate) has a T_g at

about 85ºC [86] and the high molecular PMMA has a T_g at about 125°C, the random

copolymer between MMA monomer and GMA comonomer should then have a T_g in a

range between the homopolymer of poly(glycidyl methacrylate) and high molecular

weight PMMA. The T_gs of glycidyl-functionalized PMMA support the TEM micrographs

that the glycidyl-functionalized PMMA latex nanoparticles are composed of the large

core PMMA surrounded by the thin section of the random copolymer of poly[(methyl methacrylate)-*ran*-(glycidyl methacrylate)].

4.3.6 Percentage weight of GMA analyzed by ^{1}H-NMR

Tables 4.2 and 4.3 show the effect of SDS concentration, the water content, and the percentage weight of GMA comonomer added on the percentage weight of GMA in the glycidyl-functionalized PMMA analyzed by ^{1}H-NMR spectroscopy.

Table 4.2 Effect of water contents on the wt% of GMA in the glycidyl-functionalized
PMMA at various concentrations of SDS.

Water contents (g)	[SDS] (mM)	wt% of GMA added in copolymer	wt% of GMA in copolymer by ^{1}H-NMR	wt% of glycidyl functional group by titration
60	4.91	14	14	2
60	5.78	14	12	1
60	17.34	14	7	1
60	40.45	14	7	1
60	80.91	14	5	1
84	3.51	14	11	2
84	4.13	14	11	1
84	12.38	14	10	1
84	28.89	14	7	1
84	57.79	14	5	1

The glycidyl-functionalized PMMA was synthesized by the differential microemulsion copolymerization via a two-step process at 70 ºC of MMA 14 cm^3, GMA 14 wt%, AIBN 0.08 g, varied concentrations of SDS, and various water contents.

Table 4.3 Effect of amounts of GMA monomer added on the wt% of GMA of the

glycidyl-functionalized PMMA at various concentrations of SDS.

[SDS] (mM)	wt% of GMA added in copolymer	wt% of GMA in copolymer by ^{1}H-NMR	wt% of glycidyl functional group by titration
5.78	14	12	1
	25	20	2
	39	30	2
17.34	14	7	1
	25	17	1
	39	24	1
40.45	14	7	1
	25	18	1
	39	26	1
80.91	14	5	1
	25	15	1
	39	19	1

The glycidyl-functionalized PMMA was synthesized by the differential microemulsion copolymerization via a two-step process at 70ºC by using MMA 14 cm³, AIBN 0.08 g, water 60 g, variation percentage weight of added GMA comonomer, and variation concentration of SDS.

The amount of the GMA found in the glycidyl-functionalized PMMA was related with the amount of GMA comonomer added. The effects of the water content, the concentration of SDS, and the amount of GMA comonomer added on the amount of GMA in the glycidyl-functionalized PMMA support the discussion in the preceding part regarding the percentage solid content as shown in Figures 4.2 and 4.3.

4.3.7 Glycidyl functional group analysis by titration method

The glycidyl functional group analysis by the selected titration method cannot be applied to the glycidyl-functionalized PMMA latex nanoparticles directly. So the functionality study in this section will analyze the glycidyl-functionalized PMMA. The glycidyl-functionalized PMMA was separated from the glycidyl-functionalized PMMA latex nanoparticle by the precipitation and purification processes. So the coagulation of the polymer latex nanoparticles was possibly observed. The coagulation by the aggregation and fusion of the polymer latex nanoparticles deformed the core/shell structure and probably reduced the surface functionality of the glycidyl-functionalized PMMA.

The effects of SDS concentration, the water content, and the percentage by weight of GMA comonomer added on the glycidyl functional group analysis of the glycidyl-functionalized PMMA by the titration method were presented in Tables 4.2 and 4.3. Both tables indicate that the percentage weight of the glycidyl functional group on the glycidyl-functionalized PMMA analyzed by the titration method was only 1 wt% since the glycidyl functional groups confirmed by titration were a small fraction of the surviving glycidyl groups on the glycidyl-functionalized PMMA latex nanoparticle after the precipitation and purification process. Based on the oxirane ring in the glycidyl monomer, the percentage by weight of glycidyl functional group can be used to represent the percentage by weight of the GMA comonomer in the solid. The acid titration method for glycidyl functional group analysis gave an extremely low amount compared to that analyzed by ^{1}H-NMR spectroscopy. The coagulation of the glycidyl-functionalized PMMA latex nanoparticle during the precipitation and purification are the main reasons

to conceal most of the glycidyl functional group beneath the surface of the glycidyl-functionalized PMMA; whereas the ^{1}H-NMR spectroscopy directly determined the GMA content in the glycidyl-functionalized PMMA. On the other hand, the ^{1}H-NMR spectroscopic analysis method also includes the entrapped glycidyl functional groups inside the glycidyl-functionalized PMMA since the $CDCl_3$ used to dissolve the solid copolymer is indeed a good solvent for the copolymer.

The ^{1}H-NMR spectroscopy is a good method to determine the percentage by weight of GMA in the glycidyl-functionalized PMMA but the functional analysis of the glycidyl-functionalized PMMA latex nanoparticle directly is an important issue for further investigation. Furthermore, the new precipitation method to separate the polymer nanoparticle from the polymer latex nanoparticle without the aggregation and fusion of polymer particle is also of interest and should be pursued. SEM micrographs of the glycidyl-functionalized PMMA were taken in further studies shown in Section 4.3.8.

4.3.8 SEM micrograph of glycidyl-functionalized PMMA

Figure 4.10 illustrates the SEM micrographs of the glycidyl-functionalized PMMA. It is seen that the spherical particles are not observed as shown in Figure 4.10(a) compared with the morphology of the glycidyl-functionalized PMMA latex nanoparticles in Figure 4.8(a), 4.8(c), and 4.8(d).

(a)   **(b)**
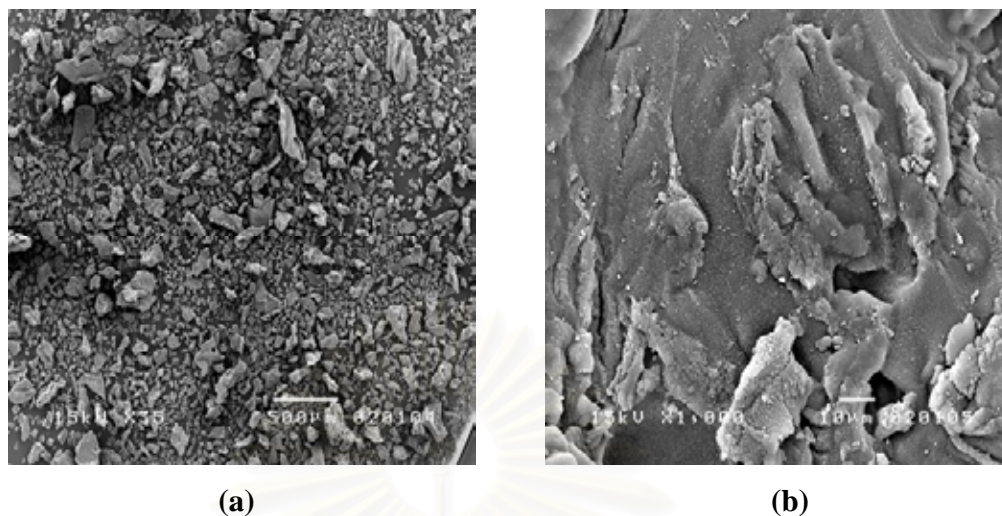
Figure 4.10 SEM Micrographs of glycidyl-functionalized PMMA: (a and b) micrographs of the glycidyl-functionalized PMMA at low and high magnification, respectively (MMA 14 cm^3, GMA 39 wt%, in the presence of AIBN 0.08 g, SDS 5.78 mM, and DI water 60 g was copolymerized at 70°C).

The coagulation of the glycidyl-functionalized PMMA latex nanoparticles is observed in Figures 4.10(a) and 4.10(b). The coagulation of the glycidyl-functionalized PMMA latex nanoparticles deformed the spherical and core/shell structure of the polymer latex nanoparticles. So the amounts of the surface functionality of the core/shell structure in the glycidyl-functionalized PMMA were not as high as expected from the core/shell structure of the glycidyl-functionalized PMMA latex nanoparticles.

4.4   Summary

The differential microemulsion polymerization technique was used to synthesize nanoparticles of glycidyl-functionalized poly(methyl methacrylate) via a two-step

process, by which the amount of sodium dodecyl sulfate (SDS) surfactant required was 1/217 of the monomer amount by weight and the surfactant/water ratio could be as low as to 1/600. These levels are extremely low in comparison to those used in a conventional microemulsion polymerization system. The glycidyl-functionalized PMMA nanoparticles are composed of nanoparticles of high molecular weight of a poly(methyl methacrylate) (PMMA) core plus with the random copolymer of poly[(methyl methacrylate)-*ran*-(glycidyl methacrylate)] as a shell layer on the surface. Particle sizes of about 50 nm were achieved. High ratios of the glycidyl methacrylate of about 5−26 wt% in the glycidyl-functionalized PMMA were achieved depending on the reaction conditions. The molecular weight of glycidyl-functionalized PMMA was in the range of about $1x10^6$ to $3x10^6$ g mol^{-1}. The percentages of solid content of glycidyl-functionalized PMMA increased when the amount of added glycidyl methacrylate was increased. The glycidyl-functionalized polymer on the surface of nano-seed PMMA nanoparticle is a random copolymer which was confirmed by ^{1}H-NMR spectroscopy; the amounts of glycidyl methacrylate comonomer on the PMMA nanoparticle were also calculated by integration of the related peaks in the NMR spectrum. The amounts of functionalization were investigated by the titration of the glycidyl functional group. The location of the glycidyl-functionalized random copolymer on the nano-seed PMMA nanoparticles was confirmed by staining with RuO_4 and viewed using a TEM technique. The glycidyl-functionalized PMMA has two regions of T_g at 90ºC and 125ºC from which the first region T_g of glycidyl-functionalized PMMA was indicated to poly[(methyl methacrylate)-*ran*-(glycidyl methacrylate)] and the second region T_g was for PMMA. A core/shell structure of the glycidyl-functionalized PMMA latex nanoparticles was observed.

CHAPTER 5

CONCLUSIONS AND RECOMMENDATIONS

5.1 Conclusions

5.1.1 The differential microemulsion polymerization technique was employed for synthesizing nano-sized particles of PMMA having high molecular weight of 10^6 g mol^{-1} using the AIBN oil soluble initiator. Using the differential microemulsion polymerization, PMMA particles can be well controllably synthesized with respect to their nanosize, high molecular weight as well as a few polymer chains in the particle. To produce nano PMMA particles of less than 20 nm, the reaction conditions can be much milder when the differential microemulsion polymerization was used instead of the conventional emulsion or microemulsion polymerization methods. The high molecular weight PMMA latex nanoparticles have a rich syndiotactic configuration (53-57 % *rr* triads). The rate of polymerization increased with an increase in the concentration of the SDS surfactant. The nearly constant value of PDI over the whole range of polymerization time could be attributed to the significance of particle nucleation occurring via a heterogeneous nucleation mechanism. The high molecular weight PMMA nanoparticles have spherical shape with a T_g of about 125ºC. It is very interesting to note that the conversion reaches a maximum within a short reaction time in the presence of lower amounts of SDS surfactant and without the need of a co-surfactant and with a high monomer-to-water ratio.

5.1.2 AIBN oil soluble initiator is an effective initiator for the differential microemulsion polymerization to prepare the high performance PMMA nanoparticles.

5.1.3 The glycidyl-functionalized PMMA latex nanoparticles having the PMMA nanoparticle surrounded by the poly[(methyl methacrylate)-*ran*-(glycidyl methacrylate)] are synthesized by differential microemulsion polymerization via a two-step process. The nanosized particles with a narrow size distribution and high molecular weight are synthesized at a very mild reaction condition. Poly(methyl methacrylate) with very high molecular weights of over 10^6 g mol^{-1} is the core particle (nano-seed) and is encompassed by the poly[(methyl methacrylate)-*ran*-(glycidyl methacrylate)]. The two T_g values of the glycidyl-functionalized PMMA at 90°C for poly[(methyl methacrylate)-*ran*-(glycidyl methacrylate)] and at 125°C for poly(methyl methacrylate) support the nanoparticle morphologies revealed by TEM. The mild reaction conditions were used to synthesize the nanoparticles at a low ratio of surfactant (SDS) to water of 1:600 and surfactant-to-monomers ratio of 1:217 at 70°C. A particle size of 50 nm at this condition is acceptable. The amount of GMA in the glycidyl-functionalized PMMA is in a range of 5-26% weight depending on the reaction condition but only about 1 wt% of glycidyl functionality can survive on the glycidyl-functionalized PMMA since a coagulation of the glycidyl-functionalized PMMA latex nanoparticles during the precipitation and purification processes occurs as was observed by SEM. So most of the glycidyl functional groups were concealed beneath the surface of the glycidyl-functionalized PMMA. The differential microemulsion polymerization via a two-step process is definitely a good and easy technique to use for the synthesis of nanoparticle-sized polymers especially for the core/shell morphology.

5.1.4 The differential microemulsion polymerization via a two-step process by using AIBN oil soluble initiator is a suitable process to produce the core/shell structure of glycidyl-functionalized PMMA latex nanoparticles. The functional group of functionalized polymer is located on the surface of the polymer latex nanoparticles. The coagulation of the glycidyl-functionalized PMMA latex nanoparticles is a major problem which accounts for the low amount of glycidyl-functional groups at the surface of the clean and dry solid PMMA particle.

5.2 Recommendations

5.2.1   Further investigations of the polymerization mechanism, a heterogeneous nucleation mechanism, when the oil soluble initiator is applied instead of the water soluble initiator in the differential microemulsion polymerization will provide a better understanding of this technique. An appropriate model possibly could be created to compare with the experimental results.

5.2.2   Investigation of a suitable application of the nanosized PMMA particles in biotechnology area should be pursued such as protein separation.

5.2.3   Investigation into details of copolymerization between MMA and GMA on the surface nanoparticles can highlight the location of GMA in PMMA nanoparticles. The copolymerization mechanism could possibly be investigated by high-performance chromatography (HPLC).

5.2.4   Investigation of a freeze dried process for the nanoparticles latex polymer should be carried out to maintain their spherical shape and immobilize the surface functionalized nanoparticles.

REFERENCES

[1]   Kawaguchi, H., Functional Polymer Microspheres. Progress in Polymer Science 25
      (2000): 1171-1210.

[2]   Pichot, C., Surface-Functionalized Latexes for Biotechnological Applications.
      Current Opinion in Colloid & Interface Science 9 (2004): 213-221.

[3]   Pavel, F.M., Microemulsion Polymerization. Journal of Dispersion Science and
      Technology 25 (2004): 1-16.

[4]   He, G., Pan, Q., and Rempel, G. L., Synthesis of Poly(methyl methacrylate)
      Nanosize Particles by Differential Microemulsion Polymerization.
      Macromolecular Rapid Communications 24 (2003): 585-588.

[5]   He, G., Pan, Q., and Rempel, G. L., Modeling of Differential Microemulsion
      Polymerization for Synthesizing Nanosized Poly(methyl methacrylate)
      Particles. Industrial Engineering and Chemistry Research 46 (2007): 1682-
      1689.

[6]   He, G., Pan, Q., and Rempel, G. L., Differential Microemulsion Polymerization of
      Styrene: A Mathematical Kinetic Model. Journal of Applied Polymer Science
      105 (2007): 2129-2137.

[7] He, G., and Pan, Q., Synthesis of Polystyrene and Polystyrene/Poly(methyl methacrylate) Nanoparticles. <u>Macromolecular Rapid Communications</u> 25 (2004): 1545-1548.

[8] Chen, C.-H., and Lee, W.-C., Preparation of Methyl Methacrylate and Glycidyl Methacrylate Copolymerized Nonporous Particles. <u>Journal of Polymer Science: Part A: Polymer Chemistry</u> 37 (1999): 1457-1463.

[9] Ergozhin, E. E., Bektenov, N. A., and Chopabaeva, N. N. NMR Study of the Structure of Polymers Based on 2,3-Epoxypropyl Methacrylate. <u>Russian Journal of Applied Chemistry</u> 77 (2004): 813-816.

[10] Capek, I., Radical Polymerization of Polar Unsaturated Monomers in Direct Microemulsion Systems. <u>Advances in Colloid and Interface Science</u> 80 (1999): 85-149.

[11] Capek, I., Microemulsion Polymerization of Styrene in The Presence of Anionic Emulsifier. <u>Advances in Colloid and Interface Science</u> 82 (1999): 253-273.

[12] Stoffer, J.O. and Bone, T., Polymerization in Water-in-Oil Microemulsion Systems, <u>Journal of Polymer Science: Polymer Chemistry Edition</u> 18 (1980): 2641-2648.

[13] Roy, S. and Devi, S., Mechanism of Microemulsion Polymerization of Methyl Methacrylate: Experimental Evidence. <u>Journal of Applied Polymer Science</u> 62 (1996): 1509-1516.

[14] Gan, L. M., Chews, C. H., Hg, S. C., and Loh, S. E., Polymerization of Methyl Methacrylate in Ternary Systems: Emulsion and Microemulsion. <u>Langmuir</u> 9 (1993): 2799-2803.

[15] Rodriguez-Guadarrama, L. A., Mendizabal, E., Puig, J. E., and Kaler, E. W., Polymerization of Methyl Methacrylate in 3-Component Cationic Microemulsion. <u>Journal of Applied Polymer Science</u> 48 (1993): 775-786.

[16] Gan, L. M., Lee, K. C., Chew, C. H., Tok, E. S., and NG, S. C., Growth of Poly(methyl methacrylate) Particles in Three-Component Cationic Microemulsions. <u>Journal of Polymer Science: Part A: Polymer Chemistry</u> 33 (1995): 1161-1168.

[17] Ming, W. H., Jones, F. N., and Fu, S. K., Synthesis of Nanosize Poly(methyl methacrylate) Microlatexes with High Polymer Content by A Modified Microemulsion Polymerization. <u>Polymer Bulletin</u> 40 (1998): 749-756.

[18] Ming, W. H., Jones, F. N., and Fu, S. K., High Solids-Content Nanosize Polymer Latexes Made by Microemulsion Polymerization. <u>Macromolecular Chemistry</u>

and Physics 199 (1998): 1075-1079.

[19] Pilcher, S. C., and Ford, W. T., Structure and Properties of Poly(methyl methacrylate) Latexes Formed in Microemulsions. Macromolecules 31 (1998): 3454-3460.

[20] Upson, D.A., Reactive Functional Latex Polymers. Journal of Polymer Science: Polymer Symposium 72 (1985): 45–54.

[21] Pichot, C., Charleux, B., Charreyre, M. T., and Revilla, J., Recent Developments in The Design of Functionalized Polymeric Microspheres. Macromolecular Symposia 88 (1994): 71–87.

[22] Pichot, C., Delair, T., and Elaissari, A., Polymer Colloids for Biomedical and Pharmaceutical Applications. In J. M. Asua (ed.), Polymeric Dispersions: Principles and Applications, pp. 515-539. Dordrecht: Kluwer Academic, 1997.

[23] Blackley, D. C., Preparation of Carboxylated Latices by Emulsion Polymerization. In G. W. Poehlein, R. H. Goodwill, and J. W. Goodwin (eds), Science and Technology of Polymer Colloids, pp. 203-219. Nijhoff: The Hague, 1983.

[24] Pichot, C., Recent Developments in The Functionalization of Latex Particles.

Macromolecular Symposia 35/36 (1990): 327–347.

[25] Pichot, C., Functional Polymer Latexes. Polymer for Advanced Technologies 6 (1995): 427–434.

[26] Pokhriyal, N. K., Sanghvi, P. G., Shah, D. O., and Devi, S., Kinetics and Behavior of Copolymerization in Emulsion and Microemulsion Systems. Langmuir 16 (2000): 5864-5870.

[27] Reddy, G. V. R., Babu, Y. P. P., and Reddy, N. S. R., Microemulsion and Conventional Emulsion Copolymerizations of Methyl Methacrylate with Acrylonitrile. Journal of Applied Polymer Science 85 (2002): 1503-1510.

[28] Reddy, G. V. R., Kumar, C. R., and Sriram, R., Microemulsion Copolymerization of Methyl Methacrylate with Acrylonitrile. Journal of Applied Polymer Science 94 (2004): 739-747.

[29] Xu, P., Zhong, W., Wang, H., Tong, R., and Du, Q., On The Copolymerization of Acrylates in The Modified Microemulsion Process. Colloid Polymer Science 282 (2004): 1409-1414.

[30] Gu, S.-J., Wang, Y.-P., and Zhang, F.-A., Study on Acrylic Emulsion with Core/Shell Structure containing High Hydroxyl Content. Journal of

Macromolecular Science, Part A: Pure and Applied Chemistry 42 (2005): 771-781.

[31] Li, P., Zhu, J., Sunintaboon, P., and Harris, F. W., Preparation of Latexes with Poly(Methyl Methacrylate) Cores and Hydrophilic Polymer Shells containing Amino Groups. Journal of Dispersion Science and Technology 24(2003): 607-613.

[32] Černáková, L., Chrástová, V., and Volfová, P., Nanosized Polystyrene/Poly(Butyl Acrylate) Core/Shell Latex Nanoparticles Functionalized with Acrylamides. Journal of Macromolecular Science, Part A: Pure and Applied Chemistry 42 (2005): 427-439.

[33] Zhang, Y., Guo, T., Hao, G., Song, M., and Zhang, B., Novel Nanosized Polymer Latexes Prepared by A Core/Shell Microemulsion Polymerization: Preparation and Characterization. International Journal of Polymeric Materials 54 (2005): 279-291.

[34] Xu, Z., Lu, G., Cheng, S., and Li, J. Study on Copolymer Emulsion Containing an Epoxy Group. Journal of Applied Polymer Science 56 (1995): 575-580.

[35] Chen, S., and Lee S., Seeded Latex Polymerizations: Studies on The Particle Growth Mechanism of Latex Particles. Polymer (33) 1992: 1437-1444.

[36] Chainey, M., Wilkinson, M., and Hearn J., Preparation of Overcoated Polymer Latices by A "Shot-Growth" Technique. <u>Industrial & Engineering Chemistry Product Design and Development</u> (21) 1982: 171-176.

[37] Sheu, H., El-Aasser, M., and Vanderhoff, J., Phase Separation in Polystyrene Latex Interpenetrating Polymer Networks. <u>Journal of Polymer Science Part A: Polymer Chemistry</u> (28) 1990: 629-651.

[38] Zurkova, E., Bouchal, K., Zdenkova, D., Pelzbauer, Z., Svec, F., and Kalal, J., Preparation of Monodisperse Reactive Styrene-Glycidyl Methacrylate Latexes by The Emulsifier-Free Dispersion Copolymerization Technique. <u>Journal of Polymer Science: Polymer Chemistry</u> (21) 1983: 2949-2960.

[39] Sumi, Y., Shiroya, T., Fujimoto, K., Wada, T., Handa, H., and Kawaguchi, H., Application of Cationic Latex Particles for Protein Separation. <u>Colloids and Surfaces B: Biointerfaces</u> (2) 1994: 419-427.

[40] Elaissari, A., Cros, P., Pichot, C., Laurent, V., and Mandrand, B., Adsorption of Oligonucleotides onto Negatively and Positively Charged Latex Particles. <u>Colloids and Surfaces A: Physicochemical and Engineering Aspects</u> (83) 1994: 25-31.

[41] Okubo, M., and Takahashi, M., Production of Submicron-Size Monodisperse

Polymer Particles having Aldehyde Groups by The Seeded Aldol Condensation Polymerization of Glutaraldehyde (II). <u>Colloid & Polymer Science</u> (271) 1993: 422-426.

[42] Tsuruta T, Hayashi T, Kataoka K, Ishihara K, and Kimura Y, <u>Biomedical Applications of Polymeric Materials</u>. Boca Raton, FL: CRC, 1993.

[43] Daniels, E, Sudol, E, and El-Aasser, M. <u>Polymer Latexes: Preparation, Characterization and Applications</u>. Washington, DC: American Chemical Society, 1992.

[44] Elaissari, A., <u>Colloidal Polymers</u>. New York: Marcel Dekker, 2003.

[45] Gilbert, R., <u>Emulsion Polymerization: A Mechanistic Approach</u>. London: Academic Press, 1995.

[46] Fitch, R., <u>Polymer Colloids: A Comprehensive Introduction</u>. London: Academic Press, 1997.

[47] Preston, W., Some Correlating Principles of Detergent Action. <u>Journal of Physical Colloid Chemistry</u> (52) 1948: 84-97.

[48] Kumar, A., and Gupta, R., <u>Fundamental of Polymer Engineering</u>. 2nd ed. New York:

Marcel Dekker, 2003.

[49]   Odian, G., <u>Principles of Polymerization</u>. 3rd ed. New York: John Wiley & Sons, 1991.

[50]   Nomura, M., Tobita, H., and Suzuki, K., Emulsion Polymerization: Kinetic and Mechanistic Aspects. <u>Advances in Polymer Science</u> 175 (2005): 1-128.

[51]   Guillaume, J., Pichot, C., and Guillot, J., Emulsifier-Free Emulsion Copolymerization of Styrene and Butyl Acrylate. III. Kinetic Studies in The Presence of A Surface Active Comonomer, The Sodium Acrylamido Undecanoate. <u>Journal of Polymer Science Part A: Polymer Chemistry</u> (28) 1990: 137–152.

[52]   Emelie, B., Pichot, C., and Guillot, J., Characterization of The Surface Morphology in Carboxylated Methyl Methacrylate-Butyl Acrylate Emulsion Copolymers. <u>Die Makromolekulare Chemie</u> (189) 1988: 1879–1891.

[53]   Delair, T., Meunier, F., Elaissari, A., Charles, M., and Pichot, C., Amino-Containing Cationic Latex-Oligodeoxyribonucleotide Conjugates: Application to Diagnostic Test Sensitivity Enhancement. <u>Colloids and Surfaces A: Physicochemical and Engineering Aspects</u> (153) 1999: 341–353.

[54] Okubo, M., Kamei, S., Tosaki, Y., Fukunaga, K., and Matsumoto, T., Covalent Immobilization of Trypsin onto Poly(2-hydroxyethyl methacrylate)/Polystyrene Composite Microspheres by Cyanogen Bromide Method and Its Enzymatic Activity. Colloid & Polymer Science (265) 1987: 957–964.

[55] Okubo, M., Ikegami, K., and Yamamoto, Y., Preparation of Micron-Size Monodisperse Polymer Microspheres having Chloromethyl Group. Colloid & Polymer Science (267) 1989: 193–200.

[56] Guillaume, J., Pichot, C., and Guillot, J., Emulsifier-Free Emulsion Copolymerization of Styrene and Butyl Acrylate. II. Kinetic Studies in The Presence of Ionogenic Comonomers. Journal of Polymer Science Part A: Polymer Chemistry (26) 1988: 1937–1959.

[57] Hofman-Caris, C., Polymers at The Surface of Oxide Nanoparticles. New Journal of Chemistry (18) 1994: 1087–1096.

[58] Oyama, H., Sprycha, R., Xie, Y., Partch, R., and Matijevic, E., Coating of Uniform Inorganic Particles with Polymers. 1. Journal of Colloid and Interface Science (160) 1993: 298–303.

[59] Sprycha, R.; Oyama, H.T.; Zelenev, A.; Matijevic, E. Characterization of Polymer

Coated Silica Particles by Microelectrophoresis. <u>Colloid & Polymer Science</u> (273) 1995: 693–700.

[60] Partch, R., Gangolli, S., Matijevic, E., Cai, W., and Arajs, S., Conducting Polymer Composites. I. Surface-Induced Polymerization of Pyrrole on Iron (iii) and Cerium (iv) Oxide Particles. <u>Journal of Colloid and Interface Science</u> (144) 1991: 27–35.

[61] Ottewill, R., Schofield, A., Waters, J., and Williams, N., Preparation of Core/Shell Polymer Colloid Particles by Encapsulation. <u>Colloid & Polymer Science</u> (275) 1997: 274–283.

[62] Hergeth, W., Steinau, U.J, Bittrich, H., Schmutzler, K., and Wartewig, S., Submicron Particles with Thin Polymer Shells. <u>Progress in Colloid and Polymer Science</u> (85) 1991: 82-90.

[63] Paul, S., and Ranby, B. Studies of Methyl Methacrylate-Glycidyl Methacrylate Copolymers: Copolymerization to Low Molecular Weights and Modification by Ring-Opening Reaction of Epoxy Side Groups. <u>Journal of Polymer Science: Polymer Chemistry</u> 14 (1976): 2449-2461.

[64] Kartasheva, Z. S., and Kasaikini, O. T., Decomposition Kinetics of Free Radical Initiators in Micellar Solutions. <u>Russian Chemical bulletin</u> 43 (1994): 1657-

1662.

[65] Hild, G., Lamps, J. P., and Rempp, P., Synthesis and Characterization of Anionic 2,
3-Epoxypropyl Methacrylate Polymers and of Related Random and Block
Copolymers with Methyl Methacrylate. Polymer 34 (1993): 2875-2882.

[66] Antonietti, M., Polymerization in Microemulsions – A New Approach to Ultrafine,
Highly Functionalized Polymer Dispersions. Macromolecular Chemistry and
Physics 196 (1995): 441-466.

[67] Couvreur, P., and Puisieux, F., Nano- and Microparticles for The Delivery of
Polypeptides and Proteins. Advanced Drug Delivery Reviews 10 (1993): 141-
162.

[68] Salata, O. V., Applications of Nanoparticles in Biology and Medicine. Journal of
Nanobiotechnology 2 (2004): 3-7.

[69] Cumbal, L., Greenleaf, J., Leun, D., and SenGupta, A. K., Polymer Supported

Inorganic Nanoparticles: Characterization and Environmental Applications.

Reactive & Functional Polymers 54 (2003): 167-180.

[70] Caruso, F., Colloids and Colloidal Assemblies. Weinheim: Wiley-VCH

Verlag GmbH & Co. KGaA, 2004.

[71] Jiang, W., Yang, W., Zeng, X. and Fu, S., Structure and Properties of Poly(methyl

methacrylate) Particle Prepared by A Modified Microemulsion

Polymerization. Journal of Polymer Science: Part A: Polymer Chemistry 42

(2004) 733-741.

[72] Chen, C. –S., and Lin, C. –H., Particle Nucleation Loci in Emulsion Polymerization

of Methyl Methacrylate. Polymer 41 (2000) 4473-4481.

[73] Gardon, J. L., Emulsion Polymerization. I. Recalculation and Extension of The

Smith-Ewart Theory. Journal of Polymer Science: Polymer Chemistry Edition

6 (1968), 623.

[74] Gardon, J. L., Emulsion Polymerization. II. Review of Experimental Data in The Context of The Revised Smith-Ewart Theory. <u>Journal of Polymer Science: Polymer Chemistry Edition</u> 6 (1968), 643.

[75] Sajjadi, S., Particle Formation under Monomer-Starved Conditions in The Semibatch Emulsion Polymerisation of Styrene. Part II. Mathematical Modeling. <u>Polymer</u> 44 (2003), 223.

[76] Hansn, F. K., and Ugelstad, J., Particle Nucleation in Emulsion Polymerization. IV. Nucleation in Monomder Droplets. <u>Journal of Polymer Science: Polymer Chemistry Edition</u> 17 (1979), 3069-3082.

[77] Alduncin, J. A., Forcada, J., and Asua, J. M., Miniemulsion Polymerization Using Oil-Soluble Initiators. <u>Macromolecules</u> 27 (1994), 2256-2261.

[78] Nomura, M., Ikoma, J., and Fujita, K., Kinetics and Mechanisms of Emulsion Polymerization Initiated by Oil-Soluble Initiators. IV. Kinetic Modeling of

Unseeded Emulsion Polymerization of Styrene Initiated by 2,2-
Azobisisobutyronitrile. Journal of Polymer Science Part A: Polymer
Chemistry 31 (1993), 2103-2113.

[79] Chern, C.-S., and Tang, H.-S., Microemulsion Polymerization Kinetics and
Mechanisms. Journal of Applied Polymer Science 97 (2005), 2005-2013.

[80] Vorenkamp, E. J., Brinke, G. T., Meijer, J. G., Jager, H., and Challa, G., Influence
of The Tacticity of Poly(methyl methacrylate) on The Miscibility with
Poly(vinyl chloride). Polymer 26 (1985): 1725-1732.

[81] Soldera, A., Energetic Analysis of The Two PMMA Chain Tacticities and PMA
Through Molecular Dynamics Simulations. Polymer 43 (2002): 4269-4275.

[82] He, G. Synthesis and Characterization of Nano-Sized Polymer Particles
using Differential Microemulsion Polymerization. Doctor of Philosophy's
Thesis, Department of Chemical Engineering, Faculty of Engineering,
University of Waterloo, 2006.

[83] Brydson, J. A., <u>Plastics Materials</u>. 7th ed. Oxford: Butterworth-Heinemann, 1999.

[84] Sperling, L. H., <u>Introduction to Physical Polymer Science</u>, 4th ed. New Jersey: Wiley-Interscience, 2006.

[85] Brandrup, J., and Immergut, E. H. Polymer Handbook, 3rd ed. New York: Wiley-Interscience, 1989.

[86] Safa, K. D., and Nasirtabrizi, M. H. Ring Opening Reactions of Glycidyl Methacrylate Copolymers to Introduce Bulky Organosilicon Side Chain Substituents. <u>Polymer Bulletin</u> 57 (2006): 293-304.

APPENDICES

APPENDIX A

A1. Calculations of %solid and %conversion (X_m) of PMMA nanoparticles

A1.1　% Solid　　=　$\dfrac{\text{Weights of dried polymers}}{\text{Weights of emulsion polymers}}$ x 100%

A1.2　% Conversion (X_m)　=　$\dfrac{\text{\% Solid}}{\text{wt.\% of MMA feed in reactor}}$ x 100%

A1.3　wt. % of MMA feed in reactor

　　=　$\dfrac{\text{Volume of MMA (cm}^3\text{) x Density of MMA (g cm}^{-3}\text{)}}{\text{Weights of water (g)}}$ x 100%

A1.4　Density of MMA　　=　　0.936　g cm^{-3}

A2. Calculation of %solid of the glycidyl-functionalized PMMA

A2.1　% Solid　　=　$\dfrac{\text{Weights of dried copolymers}}{\text{Weights of emulsion copolymers}}$ x 100%

ต้นฉบับไม่มีหน้านี้
NO THIS PAGE IN ORIGINAL

APPENDIX B

SYNTHESIS AND ANALYSIS OF FUNCTIONAL CORE/SHELL
POLYMERIC NANOPARTICLES BY
A DIFFERENTIAL MICROEMULSION COPOLYMERIZATION
VIA A FULL FACTORIAL EXPERIMENTAL DESIGN

B1.   Introduction

Recently, functional-polymeric nanoparticles have attracted enormous interest because of their unique properties, compatibility with various biomolecules, and capable of forming the covalent bond with some biomolecules. Among the various functional polymeric materials, glycidyl-functional polymeric materials are especially interesting because of their excellent properties, such as good adhesion with various substrates and easy modification to many kinds of functional groups by simple chemical reactions [1-3].

Polymeric nanoparticles are successfully prepared by microemulsion polymerization method [4-10]. The microemulsion method required a higher amount of surfactant compared with conventional emulsion polymerization, which is concerned with a post-treatment to remove the surfactant after the end of polymerization which has a high impact with the polymer being used as a biomedical material. A modified microemulsion polymerization and a differential microemulsion polymerization were developed to minimize the amount of surfactant, increase the polymer content, and decrease the particle size diameter [11-12]. The differential microemulsion polymerization can produce the smaller diameter particles and utilize the amount of surfactant fewer than other methods. Although these two polymerization methods are not quite different, the modified microemulsion

polymerization can be classified as a semi-continuous process while the differential microemulsion polymerization classified as a continuous process if the monomer feeding process is considered.

Microemulsion copolymerization has been studied extensively, such as a copolymerization between 2-ethylhexyl acrylate and acrylonitrile monomers [13], another type between methyl methacrylate and acrylonitrile monomers [14-15], and so on. As already shown in the above mentioned literature, the microemulsion copolymerizations could be carried out inside the microemulsion droplets and be a continuous process as the conventional emulsion polymerization.

Xu et al. [15] has introduced the copolymerization of acrylate monomers in the modified microemulsion process. They found that the particle sizes of the copolymer microlatex did not change distinctly with the monomer composition. An estimation of the emulsifier coverage on the microlatex particles indicated that the process switched from a traditional microemulsion to a normal seeded emulsion polymerization which polymerized very fast after monomer dropping had begun. Therefore, a longer monomer dropping time is needed to produce microlatex with a narrow particle size dispersion. Besides, the modified microemulsion polymerization needs less emulsifier to produce stable microlatex. This behavior is related to the mechanism of a normal seeded emulsion polymerization during monomer dropping. However, the surfactant/monomer weight ratio was still constant at 1:10 being similar to the conventional modified microemulsion polymerization process.

He et al. [16] synthesized polystyrene nanosized particles by a differential microemulsion polymerization process using a small amount of poly(methyl methacrylate)(PMMA) as a seed. Sodium dodecyl sulfate (SDS) and ammonium persulfate (APS) were used as the surfactant and initiator, respectively. The

differential microemulsion polymerization is more effective not only in decreasing the particle size of polystyrene but also in decreasing the amount of surfactant required. The size of the polystyrene particles was significantly decreased and particles smaller than 20 nm were achieved at an SDS/(styrene+MMA) weight ratio of 0.043.

The copolymer of glycidyl methacrylate (GMA) with methyl methacrylate (MMA) has been prepared using a batch dispersion polymerization [17]. In addition, GMA copolymers have been synthesized using a semi-batch dispersion by adding GMA monomer into the polymerization reaction after the first monomer has been polymerized [18]. From those techniques, GMA copolymer so obtained had core-shell morphology by that GMA becomes an important component of the shell layer.

A systematic study on the differential microemulsion polymerization to decide appropriate polymerization conditions that can produce polymer with predetermined properties is of greater industrial importance. The statistical method will be very useful to design the experimental conditions to achieve this goal [19-21]. As such, a 2^k factorial design is a proper tool for determining the relationship of any parameter understudy [22-23].

In this work, a differential microemulsion copolymerization of MMA and GMA to achieved a core-shell copolymer of poly(GMA-*ran*-MMA) shall be synthesized. The effects of monomer/comonomer ratios, amounts of surfactant and water contents on the percentage of conversion of core/shell nanoparticles were studied. A full factorial design of 2^3 experiments is used in planning the studies. The effects of the three process variables for the differential microemulsion polymerization, namely the MMA/GMA ratio, amount of the surfactant and water contents on the percentages of conversion were investigated. Besides, the particle size

and particle size distribution, molecular weight and polydispersity index of the copolymer were also measured.

B2. Experimental

B2.1 Materials

Commercial methyl methacrylate (MMA) was obtained from the Thai MMA Co., Ltd. (Rayong, Thailand) and used without further purification. Commercial grade of glycidyl methacrylate (GMA) supplied by Dow Chemical Co., Ltd., was used as a comonomer without any purification. Azo-bis-isobutyronitrile (AIBN) was obtained from Siam Chemical Industry Co., Ltd. and sodium dodecyl sulfate (SDS) from Cognis (Thailand) Co, Ltd. was used as received. High quality deionized water obtained from the FabriNet Co., Ltd., was used in all experiments.

B2.2 Synthesis of Core/Shell Copolymeric Nanoparticles by Differential Microemulsion Polymerization Technique

The core/shell copolymeric nanoparticles consisting of poly(methyl methacrylate) core particle and poly(glycidyl methacrylate) shell particle were accomplished by the differential microemulsion polymerization of MMA and GMA using AIBN as an initiator and SDS as a surfactant in a four-necked flat-bottomed flask of 250 cm^3 equipped with a condenser, two dropping funnels, a nitrogen inlet capillary tube, a magnetic bar immersed in a water bath. The stirrer speed was 200 rpm, the reaction temperature was 75ºC., monomers feeding time was 2 h (MMA feeding time about 1.5 hour and GMA feeding time about 0.5 hour), and the reaction time was one hour. The sequence of monomer feeding was to prepare PMMA first and then prepare the copolymer of PGMA-*ran*-PMMA. The basic experimental procedures were as follows: The deionized water, initiator and SDS emulsifier were

charged into a 250-cm^3 glass reactor. The reactor was immersed in a water bath having the reaction temperature of 75ºC. The reaction was stirred at 200 rpm by an elliptical shape magnetic bar at all time. After the reaction temperature had reached 75 ºC, MMA monomer (14 cm^3) was dropped into the reaction at a constant rate for 1½ h. Then GMA monomer (2 cm^3 or 4 cm^3) was dropped into the reaction mixture within 30 minutes. The reaction proceeded in another 1 hr at 75 ºC under the constant reaction temperature and stirrer speed.

The poly[(methyl methacrylate)-*ran*-(glycidyl methacrylate)] particles were obtained by precipitating the microemulsion polymers in methanol and being filtrated out by a vacuum filtration technique, washing out the precipitates by excess methanol and deionized water to eliminate the SDS emulsifier and AIBN oil-soluble initiator, and finally dried out in a vacuum oven at 40ºC for 24 h.

Table B1 Recipe for differential microemulsion copolymerization of

MMA/GMA copolymers

Materials	Amount
MMA, cm^3	14
GMA	*Variable*
AIBN, g	0.08
SDS	*Variable*
Water	*Variable*

Table B2 A 2^3 Factorial design

Run	Variables		
	GMA	SDS	Water
1	-	+	-
2	+	-	-
3	+	-	+
4	+	+	-
5	-	-	-
6	-	-	+
7	-	+	+
8	+	+	+

+ means a high level, - means a low level.

Table B3 Variable identification.

Variables	**-** (low level)	**+** (high level)
GMA, cm^3	2	4
SDS, g	0.7	1.4
Water, cm^3	60	84

B2.3   Characterization of the Copolymers

B2.3.1 The solid content and the percentage conversion

The solid content (%Solid) and percentage of conversion (% conversion) of the copolymer microemulsions were determined by the weight difference as shown in Equations (B1) and (B2)

$$\%\text{Solid} = (W_1 / W_2) \times 100\% \qquad (B1)$$

$$\%\text{Conversion} = (\%\text{Solid} / W_3) \times 100\% \qquad (B2)$$

Where W_1, W_2, and W_3 were the weights of dried copolymer, copolymer microemulsions, and percent weight of total monomers in charge, respectively. The dried copolymer was a pure copolymer after removing the initiator, surfactant, and residual monomer by washing with excess methanol and DI water.

B2.3.2 Particle size and particle size distribution

Particle size and particle size distribution were determined by means of dynamic light scattering technique in a Zetasizer nano ZS of Malvern Instrument equipped with a He-Ne laser source at wavelength 633 nm and the purified DI water was used as a dispersing medium. The microemulsion copolymer was diluted to 1 %w/v before analysis.

B2.3.3 Molecular weights and theirs polydispersity index (PDI)

The weight and number average molecular weights ($\overline{M_w}$ and $\overline{M_n}$) as well as the polydispersity index (PDI) were determined by gel permeation chromatography (GPC) in a Water 150-CV equipped with a column set of PLgel 10 μm mixed B (2 columns) having a molecular weight resolving range of 500-10,000,000 at a flow rate 1.0 cm^3 min^{-1} at 30°C and tetrahydrofuran was used as an eluent. A Calibration curve was constructed using the standard polystyrene having a molecular weight range of 4,490 to 1,112,000 g mol^{-1}. The dried copolymer was dissolved in tetrahydrofuran at a concentration of 0.3 %w v^{-1} and then filtered with nylon membrane (pore size 0.45 μm) before injection.

B2.3.4 Morphology of the core/shell nanoparticles

Morphology of the core/shell copolymeric nanoparticles was investigated by transmission electron microscopy. The copolymer emulsion was diluted to 1%, v v^{-1}, then one drop of this diluted emulsion was dropped on a copper grid, negatively stained by phosphor tungstic acid and dried at room temperature. Another dried copolymer was stained with OsO_4 vapor at room temperature for 60 min and was then carefully dispersed in an epoxy matrix, cured at room temperature, and microtomed to obtain ultrathin specimens. Both the negatively stained samples on the copper grid and ultra-thin cross-sectioned specimens were observed by a transmission electron microscope (TEM, Joel JEM-200CX).

B3.   Results and Discussion

The statistical analysis in this work was performed by Program Minitab version 13.20. All of the calculated statistical values were also obtained by calculation of the program. In addition, the confidential level of all experiments was set at 95%. The heterogeneous nucleation mechanism was believed to predominantly control both of PMMA core polymerization and core/shell copolymerization. The summary of all data was shown in Tables B4 and B5.

Table B4. Summarized data of PMMA core nanoparticles

Run	2^3 Full Factorial Experiment						Response	Observe				
	[GMA] (cm^3)	[SDS] (g)	[Water] (cm^3)	Design Level			% Conversion	$\overline{M}_n$ x 10^{-6}	$\overline{M}_w$ x 10^{-6}	PDI	Size (nm.)	PSD
				[GMA]	[SDS]	[Water]						
1	-	1.4	60	none	+	-	83.77	0.24	0.63	2.70	24.76	0.249
2	-	0.7	60	none	-	-	79.61	0.28	0.78	2.80	41.40	0.448
3	-	0.7	84	none	-	+	83.55	0.23	0.69	2.90	32.16	0.267
4	-	1.4	60	none	+	-	83.77	0.24	0.63	2.70	24.76	0.249
5	-	0.7	60	none	-	-	79.61	0.28	0.78	2.80	41.40	0.448
6	-	0.7	84	none	-	+	83.55	0.23	0.69	2.90	32.16	0.267
7	-	1.4	84	none	+	+	89.16	0.23	0.57	2.50	30.07	0.379
8	-	1.4	84	none	+	+	89.16	0.23	0.57	2.50	30.07	0.379

(PDI = polydispersity index of molecular weights and PSD = particle size distribution)

Table B5. Summary data of core/shell nanoparticles

Run	2³ Full Factorial Experiment						Response	Observe				
	[GMA] (cm³)	[SDS] (g)	[Water] (cm³)	Design Level			% Conversion	$\overline{M_n}$ x 10⁻⁶	$\overline{M_w}$ x 10⁻⁶	PDI	Size (nm.)	PSD
				[GMA]	[SDS]	[Water]						
1	2	1.4	60	-	+	-	92.59	0.20	1.50	7.60	25.69	0.264
2	4	0.7	60	+	-	-	89.53	0.15	0.49	3.30	29.83	0.276
3	4	0.7	84	+	-	+	90.67	0.19	0.56	2.90	27.67	0.250
4	4	1.4	60	+	+	-	88.51	0.20	0.60	3.10	38.33	0.439
5	2	0.7	60	-	-	-	92.24	0.21	2.20	10.40	25.40	0.280
6	2	0.7	84	-	-	+	98.42	0.18	0.61	3.40	29.49	0.268
7	2	1.4	84	-	+	+	99.55	0.17	0.78	4.50	38.65	0.415
8	4	1.4	84	+	+	+	92.02	0.19	0.79	4.20	24.79	0.270

(PDI = polydispersity index of molecular weights and PSD = particle size distribution)

The summarized data in Tables B4 and B5 indicate that the percentages of conversion of the core/shell nanoparticles increased as expected when the shell layer was formed by the copolymerization. So the $\overline{M_w}$ of the core/shell nanoparticle was increased as well as the percentage of conversion. The $\overline{M_n}$ of the core/shell nanoparticles decreased since the GMA oligomers from the homopolymerization in the aqueous phase was probably precipitated and left the micelles before further chain growing and/or chain termination could take place. So PDI of the core/shell nanoparticles was increased. The particle size and particle size distribution of the core/shell nanoparticles were almost in the same range with the PMMA core particles since the copolymerization was possibly dominated by the reaction between the fed GMA and swollen MMA in polymer micelles and then a few amount of comonomer was not affected by the particle size and size distribution.

B3.1   Statistical analysis

B3.1.1 PMMA core nanoparticles

In Table B6, the statistical analysis values of the percentages of conversion of the resultant PMMA core nanoparticles indicated that the percentages of conversation were significantly affected by [SDS], [water], and their interaction.

Table B6. Factorial fitted results of the %conversion of PMMA core nanoparticles
by Minitab

Term	Effect	Coef	SE Coef	T	P
Constant		84.0250	0.03021	2781.58	0.000
[GMA]	0.0000	0.0000	0.03021	0.00	1.000
[SDS]	4.8833	2.4417	0.03021	80.83	0.000
[Water]	4.6633	2.3317	0.03021	77.19	0.000
[GMA]*[[SDS]	0.0000	0.0000	0.03021	0.00	1.000
[GMA]*[Water]	0.0000	0.0000	0.03021	0.00	1.000
[SDS]*[Water]	0.7233	0.3617	0.03021	11.97	0.000
[GMA]*[SDS]*[Water]	0.0000	0.0000	0.03021	0.00	1.000

$S = 0.147986$ R-Sq = 99.87%   R-Sq (adj) = 99.82%

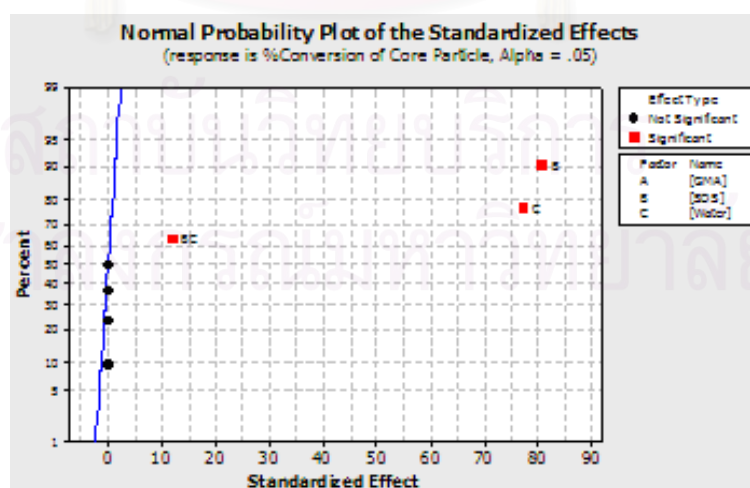| Source	DF	Seq SS	Adj SS	Adj MS	F	P
Main Effects	3	273.562	274.562	91.1872	4163.80	0.000
2-Way Interactions	3	3.139	3.139	1.0464	47.78	0.000
3-Way Interactions	1	0.000	0	0.0000	*	*
Residual Error	16	0.350	0.35	0.0219		
Pure Error	16	0.350	0.35	0.0219		
Total	23	277.051				

Figure B1. Normal probability plot of the standardized effects for PMMA core
nanoparticles.

The SDS micelles were the important nucleation site in the heterogeneous nucleation mechanism, since the high SDS content provided the high amount of micelles. Then the percentages of conversion were dependent on the amount of SDS micelles. The effect of the water content was related to the aggregation of polymer nanoparticles during polymerization when the fewer amounts of water were used because they could lead to the high chance of micelles aggregation. We can conclude that the percentages of conversion are also dependent upon the water content. In addition, the interaction between the amounts of SDS and water could be attributed by the stability of polymer micelles. Therefore, the interaction between SDS and water contents is also the important factor on the percentages of conversion. Figure B1 indicates the positive effects of the contents of SDS and water, and their interaction on the percentages of conversion of resultant PMMA core nanoparticles.

The SDS, an anionic surfactant, usually stabilizes the monomer droplets through a micelle formation and subsequently leads to stable polymer micelles. As differential microemulsion polymerization proceeds, polymer micelles are always swollen with its monomer. Increasing the number of monomer-swollen polymer micelles, as the polymerization proceeds, can increase the percentage of monomer conversion, i.e., the higher the SDS concentration, the greater the monomer conversion.

When increasing the amount of water charged to the system, a higher percentage of conversion of monomer was observed because chain transfer from the PMMA growing chains to the MMA monomer was a major termination step rather than a normal combination of the two PMMA growing chains to become a larger PMMA chain. Thus, a higher amount of MMA monomer was consumed. The second

role of water is to dilute the ingredient of polymerization system and reduce the polymerization reaction and a smaller chance of polymer micelle aggregation. As mentioned in the factorial design experiment, the interaction effect of SDS and water content increased the percentage of monomer conversion, a synergistic effect between the SDS and water could be attributed by the stability of polymer micelles in the presence of SDS, which could reduce the micelle aggregation to reduce and/or inhibit chain termination by combination.

B3.1.2 Core/shell nanoparticles.

In Table B7, the statistical analysis of the percentages of the resultant core/shell nanoparticles indicates that the percentages of conversation are significantly affected by the contents of SDS, water, GMA, and their interactions (the 2- and 3-way interactions).

Based on the values of T and p statistic and Figure B2, all variables studied affected the percentages of conversion of core/shell nanoparticles since the random copolymer between MMA and GMA was possibly copolymerized at the surface of PMMA core nanoparticles inside the SDS micelles. In addition, the water content had some relation with the aggregation of polymer micelles. The parameters of SDS and water, and their 2-way interaction gave the positive effect on percentage of conversion, while GMA and its 2-way interaction with SDS and water gave the negative interaction. It is very interesting that the 3-way interaction among the GMA, SDS and water provided the weakly positive result. It is anticipated that the effect of SDS and water overwhelms the strongly negative effect of GMA.

Table B7. Factorial fit resulted of the %conversion of core/shell nanoparticles from Minitab.

Term	Effect	Coef	SE Coef	T	P
Constant		92.941	0.03449	2694.69	0.000
[GMA]	-5.517	-2.758	0.03449	-79.97	0.000
[SDS]	0.453	0.227	0.03449	6.57	0.000
[Water]	4.447	2.223	0.03449	64.46	0.000
[GMA][[SDS]*	-0.292	-0.146	0.03449	-4.23	0.001
[GMA][Water]*	-2.118	-1.059	0.03449	-30.71	0.000
[SDS][Water]*	0.785	0.393	0.03449	11.38	0.000
[GMA][SDS]*[Water]*	0.400	0.200	0.03449	5.80	0.000

S = 0.168967   R-Sq = 99.86%   R-Sq (adj) = 99.80%

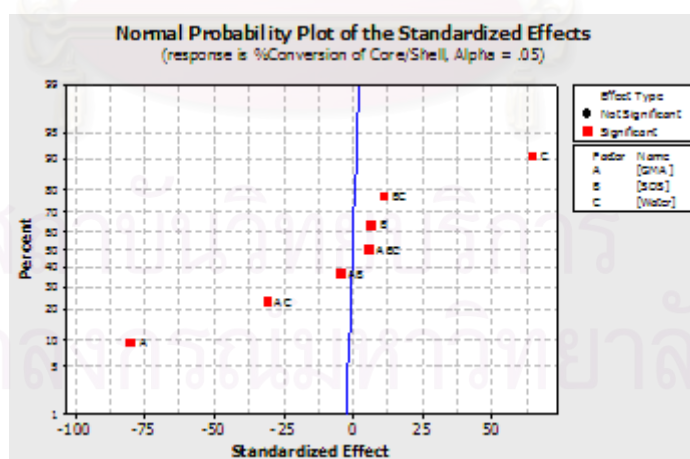| Source	DF	Seq SS	Adj SS	Adj MS	F	P
Main Effects	3	302.472	302.472	100.8240	3531.49	0.000
2-Way Interactions	3	31.132	31.132	10.3770	363.48	0.000
3-Way Interactions	1	0.960	0.96	0.9600	33.63	0.000
Residual Error	16	0.457	0.457	0.0290		
Pure Error	16	0.457	0.457	0.0290		
Total	23	335.020				

Figure B2. Normal probability plot of the standardized effects and residual plot for percent conversion of percent conversion for core/shell particle copolymerization

GMA is a better water soluble monomer (its solubility in water = 50 g dm^{-3} at 25°C) than MMA (its solubility in water = 15 g dm^{-3}) and thus GMA can polymerize more in the aqueous phase via free radicals generated from the chain termination by chain transfer to monomer or from the free radical of AIBN left in the system. However, the homopolymerization of GMA in the emulsion system was not as good as discussed elsewhere [24]. In addition, the PMMA core nanoparticles were nucleated inside the surfactant micelles then the precipitation of GMA oligomers on PMMA core nanoparticles could be affected by the SDS micelle around the particles. Therefore, GMA could be possibly copolymerized with MMA droplets swollen in the polymer micelles and/or an active chain end of the polymer micelles to form a shell layer of a random copolymer between MMA and GMA [17, 25]. Moreover, the effect of water content probably came from the extent of aqueous phase polymerization of GMA as mentioned above. Under the polymerizations carried out in the differential microemulsion polymerization, the GMA content, interaction between GMA and water, and GMA and SDS gave a negative effect. The extent of negative effect was larger in the interaction between GMA and water than that of GMA and SDS.

B3.2   Morphology study

As shown in Figure B3, The PMMA core nanoparticle (a) and the core/shell nanoparticles (b) have a spherical shape. In addition, the high concentration of polymer sample was a cause of the aggregation of polymer nanoparticles presented in both micrographs.
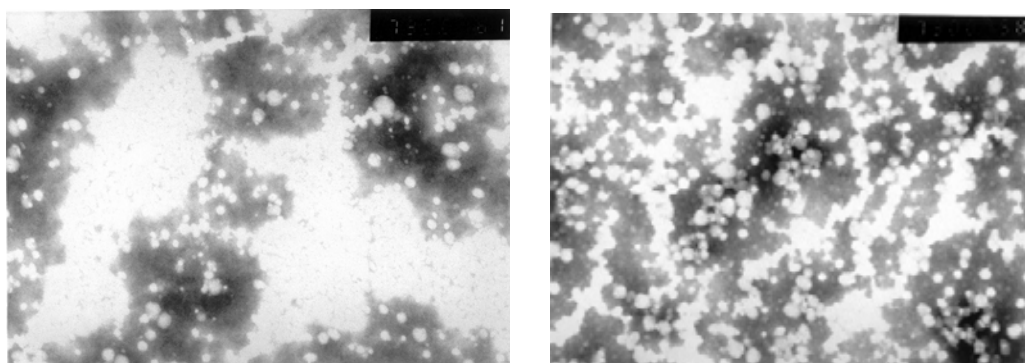
(a)   **(b)**

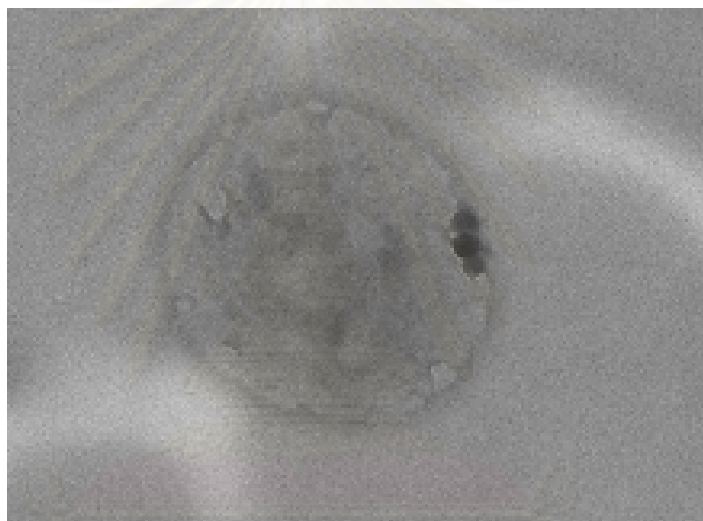Figure B3. Transmission electron micrograph: (a) PMMA core particle, and (b) core/shell nanoparticles

Figure B4. Transmission electron micrograph of cross-sectioned surface of the dried

core/shell particle in run 6

The TEM shown in Figure B4 indicates that the core/shell particle was composed of the PMMA at the core particle. The random copolymer of poly(GMA-*ran*-MMA) at shell layer was observed by a thin dark line surround the nanoparticle since the glycidyl functional group on the surface of core/shell nanoparticles could react with Osmium tetroxide staining agent better than PMMA core nanoparticles.

B4. Conclusions

Functionalized core/shell nanoparticles of MMA/GMA copolymer could be polymerized by the differential microemulsion polymerization. The core/shell nanoparticles have a high percentage conversion, high molecular weight, low surfactant usage (a weight ratio of SDS/monomer is 1:24), small particle size (25-30 nm). The statistical analysis indicated that SDS, water, and their interaction have a positive effect on the percentage of conversion of PMMA core nanoparticles. On the other hand, the GMA, interaction between GMA*SDS, and interaction between GMA*water have a negative effect on the percentage of conversion of core/shell nanoparticles.

B5 Acknowledgements

B6 References

1. Kawaguchi, H., Functional Polymer Microspheres. Progress in Polymer Sciences 25 (2000): 1171-1210.

2. Pichot, C., Surface-Functionalized Latexes for Biotechnological Applications. Current Opinion in Colloid & Interface Science 9 (2004): 213-221.

3. Pavel, F.M., Microemulsion Polymerization. Journal of Dispersion Science and Technology 25 (2004): 1-16.

4. Rodriguez-Guadarrama, L. A., Mendizabal, E., Puig, J. E., and Kaler, E. W., Polymerization of Methyl Methacrylate in 3-Component Cationic Microemulsion. Journal of Applied Polymer Science 48 (1993): 775-786.

5.   Gan, L. M., Lee, K. C., Chew, C. H., Tok, E. S., and NG, S. C., Growth of Poly(methyl methacrylate) Particles in Three-Component Cationic Microemulsions. Journal of Polymer Science: Part A: Polymer Chemistry 33 (1995): 1161-1168.

6.   Ming, W. H., Jones, F. N., and Fu, S. K., Synthesis of Nanosize Poly(methyl methacrylate) Microlatexes with High Polymer Content by a Modified Microemulsion Polymerization. Polymer Bulletin 40 (1998): 749-756.

7.   Ming, W. H., Jones, F. N., and Fu, S. K., High Solids-Content Nanosize Polymer Latexes Made by Microemulsion Polymerization. Macromolecular Chemistry and Physics 199 (1998): 1075-1079.

8.   Pilcher, S. C., and Ford, W. T., Structure and Properties of Poly(methyl methacrylate) Latexes formed in Microemulsions. Macromolecules 31 (1998): 3454-3460.

9.   Upson, D.A., Reactive Functional Latex Polymers. Journal of Polymer Science: Polymer Symposium 72 (1985): 45–54.

10. Pichot, C., Charleux, B., Charreyre, M. T., and Revilla, J., Recent Developments in the Design of Functionalized Polymeric Microspheres. Macromolecular Symposia 88 (1994): 71–87.

11. Pichot, C., Delair, T., and Elaissari, A., Polymer Colloids for Biomedical and Pharmaceutical Applications. In J. M. Asua (ed.), Polymeric Dispersions: Principles and Applications, pp. 515-539. Dordrecht: Kluwer Academic, 1997.

12. Blackley, D. C., Preparation of Carboxylated Latices by Emulsion Polymerization. In G. W. Poehlein, R. H. Goodwill, and J. W. Goodwin (eds), Science and Technology of Polymer Colloids, pp. 203-219. Nijhoff: The Hague, 1983.

13. Reddy, G. V. R., Babu, Y. P. P., and Reddy, N. S. R., Microemulsion and Conventional Emulsion Copolymerizations of Methyl Methacrylate with Acrylonitrile. Journal of Applied Polymer Science 85 (2002): 1503-1510.

14. Reddy, G. V. R., Kumar, C. R., and Sriram, R., Microemulsion Copolymerization of Methyl Methacrylate with Acrylonitrile. Journal of Applied Polymer Science 94 (2004): 739-747.

15. Xu, P., Zhong, W., Wang, H., Tong, R., and Du, Q., On the Copolymerization of Acrylates in the Modified Microemulsion process. Colloid Polymer Science 282 (2004): 1409-1414.

16. He, G., Pan, Q., and Rempel, G. L., Differential Microemulsion Polymerization of Styrene: A Mathematical Kinetic Model. Journal of Applied Polymer Science 105 (2007): 2129-2137.

17. He, G., and Pan, Q., Synthesis of Polystyrene and Polystyrene/Poly(methyl methacrylate) Nanoparticles. Macromolecular Rapid Communications 25 (2004): 1545-1548.

18. Guillaume, J., Pichot, C., and Guillot, J., Emulsifier-free emulsion copolymerization of styrene and butyl acrylate. III. Kinetic Studies in the Presence of a Surface Active Comonomer, the Sodium Acrylamido Undecanoate. Journal of Polymer Science Part A: Polymer Chemistry (28) 1990: 137–152.

19. Emelie, B., Pichot, C., and Guillot, J., Characterization of the Surface Morphology in Carboxylated Methyl Methacrylate-Butyl Acrylate Emulsion Copolymers. Die Makromolekulare Chemie (189) 1988: 1879–1891.

20. Delair, T., Meunier, F., Elaissari, A., Charles, M., and Pichot, C., Amino-Containing Cationic Latex-oligodeoxyribonucleotide Conjugates: Application to Diagnostic Test Sensitivity Enhancement. Colloids and Surfaces A: Physicochemical and Engineering Aspects (153) 1999: 341–353.

21. Okubo, M., Kamei, S., Tosaki, Y., Fukunaga, K., and Matsumoto, T., Covalent Immobilization of Ttrypsin onto Poly(2-hydroxyethyl methacrylate)/Polystyrene Composite Microspheres by Cyanogen Bromide Method and Its Enzymatic Activity. Colloid & Polymer Science (265) 1987: 957–964.

22. Okubo, M., Ikegami, K., and Yamamoto, Y., Preparation of Micron-size Monodisperse Polymer Microspheres Having Chloromethyl Group. Colloid & Polymer Science (267) 1989: 193–200.

23. Guillaume, J., Pichot, C., and Guillot, J., Emulsifier-free Emulsion Copolymerization of Styrene and Butyl Acrylate. II. Kinetic Studies in the Presence of Ionogenic Comonomers. Journal of Polymer Science Part A: Polymer Chemistry (28) 1990: 137–152.

24. G., *Principles of Polymerization*. 3rd ed. New York: John Wiley & Sons, 1991.

25. Kumar, A., and Gupta, R., <u>Fundamental of Polymer Engineering</u>. 2nd ed. New York: Marcel Dekker, 2003.
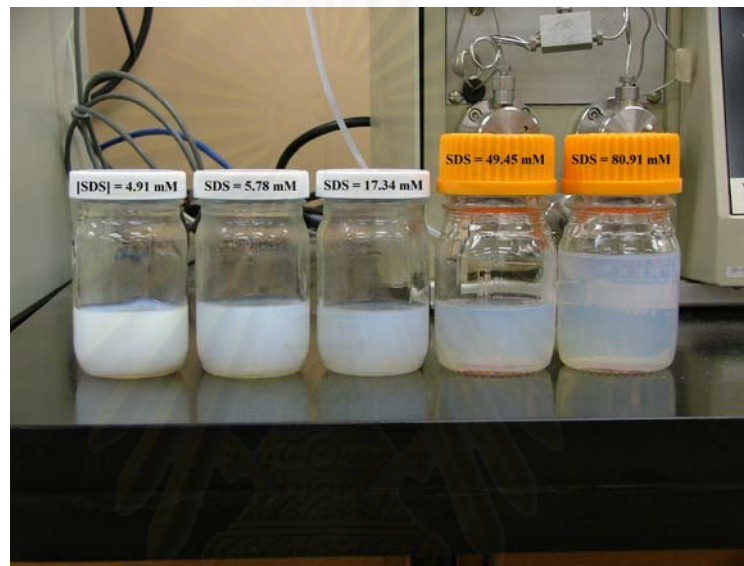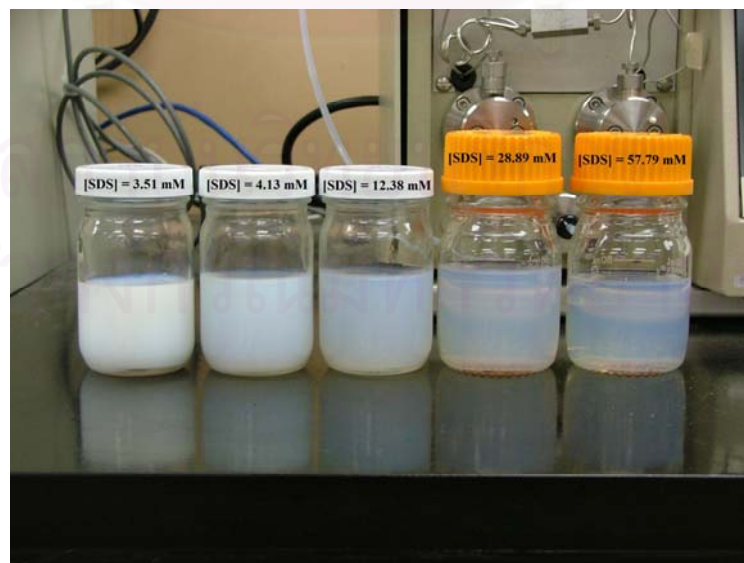
APPENDIX C

Photographs of glycidyl-functionalized PMMA latex nanoparticle samples.

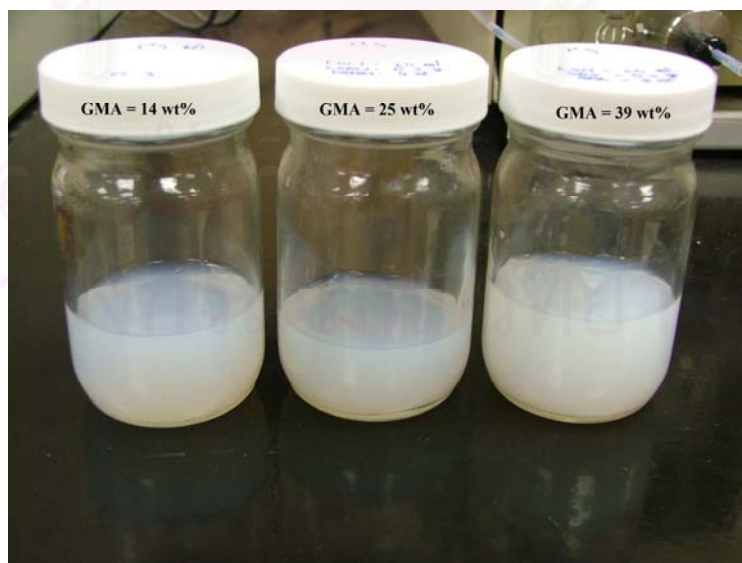**C1. Vary [SDS], water = 60 g, and GMA = 14 wt%**

C2. Vary [SDS], water = 84 g, and GMA = 14 wt%

C3. Vary GMA, water = 60 g, and [SDS] = 5.78 mM

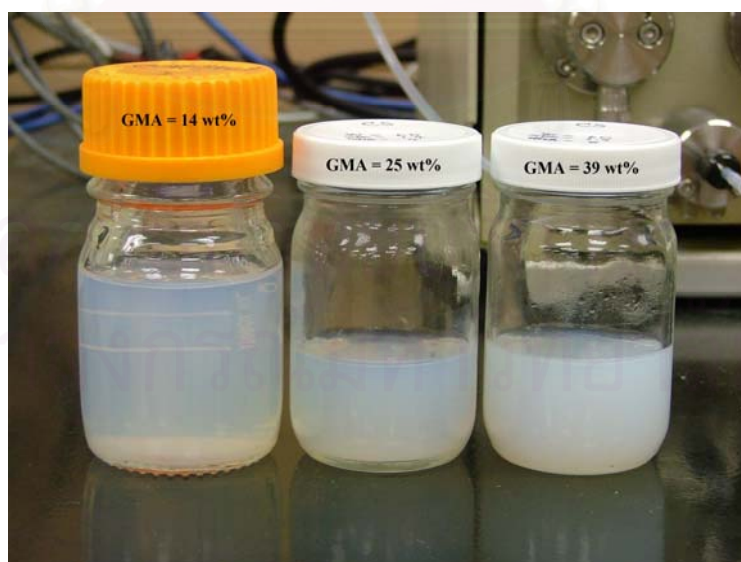
C4. Vary GMA, water = 60 g, and [SDS] = 17.34 mM

C5. Vary GMA, water = 60 g, and [SDS] = 49.45 mM

C6. Vary GMA, water = 60 g, and [SDS] = 80.91 mM

VITAE

Mr. Chaiwat Norakankorn was born in Bangkok, Thailand on May 3, 1975. He received his Bachelor degree of Science from Field Polymer and Textile, Department of Materials Science, Faculty of Science, Chulalongkorn University in May 1998. He continuous studied on Field of Applied Polymer Science and Textile Technology, Department of Materials Science, Faculty of Science, Chulalongkorn University and received his Master of Science in May 2000. His master thesis got a financial support from Shell Contennial Education Fund in April 2000. A literature from his thesis was published in a local science research journal and another literatures was published in journal of applied polymer science. For the next three years he pursued a career in materials engineer, working on a new business development, new production transfer from USA & Canada, qualification process of optical communication product, auditing suppliers, customer service, failure analysis on both of optical communication devices and hard disk drive devices, process improvement and development for optical communication device, sourcing (raw materials), and R&D in the Fabrinet, Co., Ltd., Patumthani, Thailand. In November 2003 entered the Graduate School at Chulalongkorn University.